REMARKS

Amendments to the Claims

The Applicants respectfully ask the Examiner to replace all prior versions and listings of claims in the present application with the listing of claims currently provided. Claims 35-37, 39, 40, 43-47, 49-52, 54-61, 64, 65, 68-72, 79, 82-84, 90-94 and 96-99 were amended, Claim 62 was canceled and Claims 101-123 are new.

Amendment support for Claims 35-37, 60, 61, 79, 83, 84 and 103 can be found throughout the present specification, *e.g.*, at pg. 28, ¶ 1; pg. 46, ¶ 1; and Table 1.

Amendment support for Claims 43-47, 68-72, 90-94, 101, 102, 106, 107, 115 and 116 can be found throughout the present specification, *e.g.*, at pg. 13, ¶ 3; pg. 14, ¶ 1; pg. 17, ¶ 2; pg. 94, ¶ 4 through pg. 95,, ¶ 1; and pg. 104, ¶ 4 through pg. 107, ¶ 1.

Amendment support for Claims 54-59, 108-114 and 120-123 can be found throughout the present specification, *e.g.* at pg. 10, ¶ 3 through pg. 11, ¶ 1; and pg. 19, ¶ 2.

Amendment support for Claims 104, 105 can be found throughout the present specification, *e.g.* at pg. 88, ¶ 2.

Amendment support for Claims 117-119 can be found throughout the present specification, *e.g.* at pg. pg. 83, ¶ 2.

Rejection Pursuant to 35 U.S.C. § 101 Obviousness-type Double Patenting

The Examiner has provisionally rejected Claims 35, 36, 38, 39, 41, 42, 44, 45, 47, 48 and 53 as allegedly being unpatentable over Claims 61-63, 67, 71-74 of U.S. Patent Application 10/261,161, Fernandez-Salas, E. et al., *Cell-based FRET Assays for Clostridial Toxins* under the judicially created doctrine of obviousness-type double patenting under 35 U.S.C. § 101. The Applicants respectfully traversed.

According to the MPEP § 804, obviousness-type double patenting rejection is intended to prevent improper patent term extension of a first patent by prohibiting the issuing of claims in a second patent that are not patentably distinct from the claims in a first patent.

The Applicants respectfully submit that the present patent application has a filing date of August 28, 2001, whereas the 10/261,161 patent application cited by the Examiner has a later filing date of February 27, 2002. The present application is considered the first patent in this case because it has the earlier filing date. Thus, the 10/261,161 patent application cannot be used as an obviousness-type double patenting reference against the present application.

Therefore, the Applicants respectfully submit that this rejection is unsupported and request withdrawal of the 35 U.S.C. § 101 obviousness-type double patenting rejection for Claims 35, 36, 38, 39, 41, 42, 44, 45, 47, 48 and 53.

Rejection Pursuant to 35 U.S.C. § 112, ¶ 2 Definiteness

The Examiner has rejected Claims 68-72 and 90-94 as allegedly being indefinite under 35 U.S.C. § 112, ¶ 2 arguing that these claims fail to particularly point out and distinctly claim the subject matter of the claimed invention. Specifically, the Examiner contends that dependent Claims 68-72 lack clear antecedent basis to independent Claim 60 and Claims 90-94 lack clear antecedent basis to independent Claim 79 because the acceptor is not particularly defined and the steps of the dependent claims lack clear antecedent basis in the independent claim. The Applicants respectfully ask for reconsideration under 37 C.F.R. § 1.111.

The Applicants submit that amended Claim 68-72, 79 have proper antecedent basis from Claim 60 and amended Claim 90-94 have proper antecedent basis from Claim 79. Therefore, the Applicants respectfully request withdrawal of the 35 U.S.C. § 112, ¶ 2 indefinite rejection for Claims 68-72 and 90-94.

Rejection Pursuant to 35 U.S.C. § 112, ¶ 1 Written Description

The Examiner has rejected Claims 35, 36 and 38-59 as allegedly being indefinite under 35 U.S.C. § 112, ¶ 1 indicating that the claims contain subject matter that was not described in the specification in such a way as to reasonably convey to one skilled in the relevant art that the inventors had possession of the claimed invention at the time the application was filed. Specifically, the Examiner contends that the specification supports recognition sequences from a specific residue range, but not substrate lengths of 19, 20, 21, 22, 69 or 72. The Examiner also alleges that the specification fails to describe any FRET pair that provides energy transfer using peptides of 69 and 72 amino acids in length. The Applicants respectfully ask for reconsideration under 37 C.F.R. § 1.111.

Written description support for various BoNT/A substrate lengths can be found throughout the present specification. As a non-limiting example, substrate length ranges from at most 20 residues, at most 40 residues, at most 50 residues, at most 100 residues, at most 150 residues, at most 200 residues, at most 250 residues, at most 300 residues, at most 350 residues or at most 400 residues are disclosed at, *e.g.*, pg. 10, ¶ 3; and pg. 19, ¶ 2. As another non-limiting example, substrate lengths of 16, 19, 20, 21, 22, 23 and 24 amino acids can be found in Example 1.

Additionally, a BoNT/A substrate of the present application comprise a BoNT/A recognition sequence. Thus, recognition sequence lengths of 13, 15, 16, 17, 18, 70 and 73 as disclosed, *e.g.*, at pg. 37, ¶ 3 indicate a BoNT/A substrate of at least these lengths. Further disclosure indicates that a BoNT/A recognition sequence can comprising a S1, a S2, a S3 and/or a S4 α-helical motif, *e.g.*, at pg. 25, ¶ 3; pg. 30, ¶ 1 through pg. 31, ¶ 1; pg. 37, ¶ 2 through pg. 44, ¶ 1 and FIG. 4A. Thus, a BoNT/A recognition sequence comprising a S1 α-helical motif can have a length, such as, *e.g.*, 180-206 amino acids; a BoNT/A recognition sequence comprising a S2 α-helical motif can have a length, such as, *e.g.*, 166-206 amino acids; a BoNT/A recognition sequence comprising a S3 α-helical motif can have a length, such as, *e.g.*, 152-206 amino acids; and a BoNT/A recognition sequence comprising a S4 α-helical motif can have a length, such as, *e.g.*, 56-206 amino acids. Again, since a BoNT/A substrate comprises a BoNT/A recognition sequence, a BoNT/A substrate must be of at

least these lengths. Thus, the Applicants respectfully submit that there is adequate written description support for the substrate lengths claimed.

Written description support for various FRET pairs useful for the BoNT/A substrates disclosed in the present specification can be found throughout the present specification, *e.g.*, at pg. 71, ¶ 3 through pg. 84, ¶ 2, Table 6 and Table 7. Additional FRET pairs were indicated in Haugland, Handbook of Fluorescent Probes and Research Chemicals 6th Edition, Molecular Probes, Inc., Eugene, Oregon, 1996, which was incorporated by reference in the present specification.

The Applicants submit that amended Claims 35, 36 and 38-59 have proper written description support. Therefore, the Applicants respectfully request withdrawal of the 35 U.S.C. § 112, ¶ 1 written description rejection for Claims 35, 36 and 38-59.

Rejection Pursuant to 35 U.S.C. §102 (e) Anticipation

The Examiner has rejected Claims 60, 61, 63-68 and 74-78 as allegedly anticipated under 35 U.S.C. §102(e) by James J. Schmidt and Robert G. Stafford, *High Throughput Assays for the Proteolytic Activities of Clostridium Neurotoxins*, U.S. Patent 6,762,280 (priority filing date Sep. 25, 2000), hereafter the "Schmidt I patent.". Specifically, the Examiner contends that the Schmidt I patent discloses a modified botulinum or tetanus toxin comprising three non-native cleavage sites and one disulfide bond cleavage site, cleavage sites being selected for cleavage in tissues and/or affected cells where toxicity is desired and undesired. The Applicants respectfully traverse this rejection and ask for reconsideration under 37 C.F.R. §1.111.

According to MPEP 21331, for a reference to anticipated a pending claim, that reference must either expressly or inherently teach each and every element of the pending claim.

Independent Claim 60 recites, in part, "a BoNT/A recognition sequence comprising a BoNT/A P_5-P_4-P_3-P_2-P_1-P_1'-P_2'-P_3'-P_4'-P_5' cleavage site region including a BoNT/A P_1-P_1' cleavage site, said BoNT/A cleavage site intervening between said donor fluorophore and said acceptor; wherein either said donor fluorophore or said acceptor is not positioned within

said BoNT/A cleavage site region." The Schmidt I patent does not anticipate Claim 60 because the peptide substrates disclosed in the Schmidt I patent contain both the donor and quencher within the BoNT/A cleavage site region.

Claims 61, 63-68 and 74-78 are all dependent on Claim 60, and as such, are also directed toward a BoNT/A substrate where the donor fluorophore or the acceptor is not positioned within the BoNT/A cleavage site region. Thus, the Schmidt I patent does not read on these claims for the reasons given above for Claim 60.

Therefore, the Applicants respectfully submit that the pending claims are not anticipated by the Schmidt I patent and respectfully request withdrawal of the 35 U.S.C. §102(e) anticipation rejection for Claims 60, 61, 63-68 and 74-78.

Rejection Pursuant to 35 U.S.C. § 103(a) Obviousness

I. Obviousness rejections over Schmidt I in view of Clegg

The Examiner has rejected Claims 69, 70 and 73 as allegedly being obvious under 35 U.S.C. § 103(a) over James J. Schmidt and Robert G. Stafford, *High Throughput Assays for the Proteolytic Activities of Clostridium Neurotoxins*, U.S. Patent 6,762,280 (priority filing date Sep. 25, 2000), hereafter the "Schmidt I patent" in view of Robert M. Clegg, *Fluorescence Resonance Energy Transfer*, 6(1) Curr. Opin. Biotech. 103-110 (1995), hereafter the "Clegg reference."

The Examiner contends that it would have been *prima facie* obvious to a person of ordinary skill in the art at the time the invention was made to combine the teaching of these references and come up with a method of determining clostridial toxin activity as presently claimed in Claims 69, 70 and 73. Specifically, the Examiner argues that it would have been obvious to modify the quench-release assay disclosed in the Schmidt I patent to measure donor emissions at multiple time points because the Clegg reference teaches that FRET assays with double-labeled fluorescent molecules can achieve this continuous

measurement in order to arrive at the presently claimed invention. The Applicants respectfully ask for reconsideration under 37 C.F.R. § 1.111.

Schmidt I and Clegg combination changes the principle of operation of Schmidt I.

According to MPEP §2143.01, if a proposed modification or combination of the prior art would change the principle of operation of the prior art invention being modified, then the teachings of the references are not sufficient to render the claims *prima facie* obvious. The Applicants respectfully submit that it would not be obvious for one of ordinary skill in the art to combine the cited references because combining the Schmidt I patent with the Clegg reference as suggested by the Examiner would change the principle of operation of the quench-release assay disclosed in the Schmidt I patent.

The Schmidt I patent relies on a quenching assay where the fluorescence of a donor is prevented by a quencher, see, *e.g.*, col. 4, lines 14-17; col 5, lines 9-15; and col 6, lines 54-59. Enzyme activity is measured as an increase in fluorescence because cleavage of the toxin substrate results in the separation of the donor from the quencher. This separation leads to the unquenching of the donor and a corresponding increase in donor in fluorescence, see, *e.g.*, col. 5, lines 8-15; and col. 6, lines 54-62. The quenching-based assays disclosed in the Schmidt I patent rely on the principle of operation called radiating (contact) quenching. One of the hallmarks of the operative principle of radiating quenching is the close proximity of the donor and quencher, a distance calculated by the Stern-Volmer equation, see, *e.g.*, Chapter 8 Quenching of Fluorescence, pg. 239, col. 2, Sections 8.2 and 8.3 in Principles of Fluorescence Spectroscopy (Ed. Joseph R. Lakowicz, Kluwer Academic/Plenum Publisher, 2nd Ed.1999), hereafter the "Lakowicz reference." This is because in radiating quenching, the quenching effect occurs by the physical contact of the electron orbits of the donor and quencher molecules, see, *e.g.*, the Lakowicz reference, pg. 237, col. 1, ¶2.

That the peptide substrates disclosed in the Schmidt I patent rely on radiating quenching is evident through the design of the peptide substrates. Close proximity of the donor and quencher is essential to achieve radiating quenching because this type of quenching relies on the physical interaction of the electron orbits of the donor and the quencher. The

Schmidt I patent teaches the close placement of the donor and quencher molecules of all disclosed peptides. For example, the Schmidt I patent discloses two 17 amino acid substrates with a BoNT/A cleavage site, two 35 amino acid substrates with a BoNT/B cleavage site, and three 39 amino acid substrates containing BoNT/ D and BoNT/F cleavage sites, see, *e.g.*, col 5, line 20 through col. 6, line 53. However, despite the large peptide sizes, the distance of the donor from the quencher for each substrate is between two and five amino acids.

Furthermore, the close proximity requirement discussed above necessitates that the donor and quencher be located within the P_5-P_5' cleavage site region of the substrate. Because this cleavage site region interacts with the catalytic site of the toxin, extensive mutagenesis work was conducted in order to identify which amino acids could be altered and still retain the ability to be cleaved by the toxin. For example, amino acid substitutions surrounding the BoNT/A cleavage site were tested using at least 56 different peptides, see, *e.g.*, James J. Schmidt and Karen A. Bostian, *Assays for the Proteolytic Activities of Serotype A from Clostridium botulinum*, U.S. Patent 5,965,699 (Oct. 12, 1999), hereafter the Schmidt II patent. Substitution of an original amino acid with a different amino acid or an amino acid analog within the P_5-P_5' cleavage site more time than not resulted in an ineffective substrate because the resulting peptide substrate was inefficiently cleavage. This work revealed that only certain amino acids within the P_5-P_5' cleavage site region could be altered, see *e.g.*, col. 5 through col 11; and Table I of the '699 patent and Table F, pg. 82, of the present specification. This work lead to the two BoNT/A substrates disclosed in the Schmidt I patent and to the conclusion that modifications to the disclosed substrates are not straightforward because of complex and stringent limitations placed on the location of the donor and quencher moieties when using a radiating principle of operation, see, *e.g.*, col. 7, lines 1-12. Nowhere does the Schmidt I patent teach, suggest or motivate one skilled in the art to place a donor or quencher outside of the P_5-P_5' cleavage site region.

The Clegg reference discusses the general utility of fluorescence resonance energy transfer (FRET). FRET is a non-radiating-based principle. In this principle, energy is transferred from one molecule to another by intermolecular long-range dipole-dipole coupling, see, *e.g.*, the Clegg reference at pg. 103, col. 2, ¶1, lines 1-5; see also, the Lakowicz reference,

Chapter 13 Energy Transfer, pg. 367, col. 1, ¶1. In this principle of operation, energy transfer depends on the extent of spectral overlap of the donor emissions spectrum and the acceptors absorption spectrum, and not on the physical contact of electron orbits of the molecules. The optimal spectral overlap distance is calculated using the Förster equation and not the Stern-Volmer equation. In fact, the Clegg reference itself contrasts the radiating and non-radiating principles of operation, see, *e.g.*, pg. 106, col. 1, ¶3, lines 1-15.

Adding an acceptor fluorophore to a Schmidt I peptide would change the principle of operation from a quench-release assay based on a radiating principle of operation to a resonance energy transfer assay based on a non-radiating principle of operation. Thus, the Applicants respectfully submit that a *prima facie* case of obviousness cannot be made because combining the Schmidt I patent with the Clegg reference as suggested by the Examiner would change the principle of operation of the quench-release assay disclosed in the Schmidt I patent.

Schmidt I teaches away from the claimed invention.

According to MPEP §2143.03, to establish *prima facie* obviousness of a claimed invention, all the claim limitations must be taught or suggested by the prior art. The Applicants respectfully submit that it would not be obvious to combine the cited references because the Schmidt I patent teaches away from using an acceptor fluorophore.

First, the Clostridial toxin substrate of dependent Claim 69, 70 and 73 recite, in part, "wherein said acceptor is a fluorophore." However, the Schmidt I patent teaches the use of non-fluorescent quenchers. The Schmidt I patent discloses peptide substrates for BoNT/A, BoNT/B, BoNT/ D and BoNT/F useful for quench release assays, see, *e.g.*, col. 5, line 8 through col 6, line 53. For example, the Schmidt I patent states, "The following are examples of FRET substrates for the proteolytic activities of clostridial toxins. Each contains a fluorescent group (fluorophore) on one side of the cleavage site, and a molecule that quenches that fluorescence on the other side of the cleavage site." See, col. 5, lines 8-12. In support of this statement, every peptide substrate disclosed in the Schmidt I patent contained the non-fluorescent quencher N(epsilon)-(2,4-dinitrophenyl)-lysine, see SEQ ID NO: 1, SEQ ID NO: 2, SEQ ID NO: 3, SEQ ID NO: 4, SEQ ID NO: 5, SEQ ID NO: 6 and

SEQ ID NO: 7. In addition, the Schmidt I only discloses donor-quencher pairs at col 6, line 63-67. Thus, the Schmidt I patent teaches away from the use of acceptor fluorophores or donor-acceptor fluorophore pairs with its peptide substrates as suggested by the Examiner.

Second, the Clostridial toxin substrate of dependent Claim 69, 70 and 73 incorporate by reference the limitations of independent Claim 60. Claim 60 recites, in part, "wherein either said donor fluorophore or said acceptor is not positioned within said BoNT/A cleavage site region as discussed above." As discussed above, the Schmidt I patent teaches that the donor and quencher can only be separated by 2-5 amino acids and that the placement of both the donor and quencher can only be located at certain positions within the P_5-P_5' cleavage site region of the substrate. Thus, the Schmidt I patent teaches away from the placement of a donor or quencher outside of the P_5-P_5' cleavage site region as suggested by the Examiner.

The Clegg reference is silent regarding the teachings of the Schmidt I patent discussed above. Therefore, this reference does not provide any teaching, suggestion or motivation for one skilled in the art to act contrary to the teachings of the Schmidt I patent.

Thus, the Schmidt I patent teaches that an acceptor must be a non-fluorescent quenching molecule and must be located within certain positions of the P_5-P_5' cleavage site region. Therefore, the Applicants respectfully submit that a prima *facie case* of obviousness cannot be made because the Schmidt I patent teaches away from an acceptor that is a fluorophore positioned outside of the P_5-P_5' cleavage site region as presently claimed.

Conclusion

For the reasons stated above, the Applicants respectfully submit that the assertion of obviousness is unsupported by the Schmidt I patent and the Clegg reference because these references would change the principle of operation of the assay taught by the Schmidt I patent, and the modifications required to produce the presently claimed invention are expressly taught away by the Schmidt I patent. Therefore, the Applicants respectfully

request withdrawal of the 35 U.S.C. § 103(a) obviousness rejection for Claims 69, 70 and 73.

II. Obviousness rejections over Schmidt I in view of Siegel

The Examiner has rejected Claim 72 as allegedly being obvious under 35 U.S.C. § 103(a) over the Schmidt I patent in view of Richard M. Siegel et al., *Measurement of Molecular Interactions in Living Cells by Fluorescence Resonance Energy Transfer Between Variants of the Green Fluorescent Protein*, 2000(38) Sci STKE PL1. (2000), hereafter the "Siegel reference."

The Examiner contends that it would have been *prima facie* obvious to a person of ordinary skill in the art at the time the invention was made to combine the teaching of these references and come up with a method of determining clostridial toxin activity as presently claimed in Claim 72. Specifically, the Examiner argues that it would have been obvious to modify the quench-release assay disclosed in the Schmidt I patent to measure donor excited state lifetimes because the Siegel reference teaches that FRET assays with double-labeled fluorescent molecules can achieve this excited state lifetime measurement in order to arrive at the presently claimed invention. The Applicants respectfully ask for reconsideration under 37 C.F.R. § 1.111.

Schmidt I and Siegel combination changes the principle of operation of Schmidt I.

The Siegel reference discusses the use of FRET. As outlined above, FRET uses a non-radiating principle of operation, and as such suffers from the same defect as the Clegg reference discussed above. Adding an acceptor fluorophore to a Schmidt I peptide would change the principle of operation from a quench release assay based on a radiating principle of operation to a resonance energy transfer assay based on a non-radiating principle of operation. Thus, the Applicants respectfully submit that a *prima facie* case of obviousness cannot be made because combining the Schmidt I patent with the Siegel reference as suggested by the Examiner would change the principle of operation of the quench-release assay disclosed in the Schmidt I patent.

Schmidt I teaches away from the claimed invention.

As discussed above, the Schmidt I patent teaches that an acceptor must be a non-fluorescent quenching molecule and must be located within certain positions of the P_5-P_5' cleavage site region. Thus, the Schmidt I patent teaches away from the use of the fluorescent molecules and the Siegel reference does not provide any teaching, suggestion or motivation for one skilled in the art to act contrary to the teachings of the Schmidt I patent. Thus, the Applicants respectfully submit that a *prima facie* case of obviousness cannot be made because this reference teaches away from the presently claimed invention.

Schmidt I and Siegel combination makes Schmidt I unsatisfactory for its intended use.

According to MPEP §2143.01, if proposed modification would render the prior art invention being modified unsatisfactory for its intended purpose, then there is no suggestion or motivation to make the proposed modification. The Applicants respectfully submit that it would not be obvious for one of ordinary skill in the art to combine the cited references because combining the Schmidt I patent with the Siegel reference would render the quench-release assay disclosed in the Schmidt I patent as inoperable for its intended use.

The Schmidt I patent discloses peptide substrates useful for quench release assays. As discussed above, the Schmidt I patent teaches that these peptides require the donor and quencher be separated by no more than 2 to 5 amino acids and that this placement must be at certain positions within the P_5-P_5' cleavage site region of the substrate.

The Siegel reference discloses the use of spectral variants of green fluorescent protein as donor and acceptor proteins for measuring FRET interactions, see, *e.g.*, pg. 1, col. 1, ¶ 1, lines 7-13. Each of these fluorescent proteins is approximately 238 amino acids in length and approximately 27 kDa, see, *e.g.*, Nupam P. Mahajan et al., *Novel Mutant Green Fluorescent Protein Protease Substrates Reveal the Activation of Specific Caspases During Apoptosis*, 6(6) Chem. Biol. 401-409 (1999) at pg. 402, col. 1, ¶ 1, lines 1-2.

The placement of an approximately 238 amino acid fluorescent protein taught by Siegel reference into the P_5-P_5' cleavage site region positions identified in the Schmidt I patent, as suggested by the Examiner, would result in an inoperable peptide substrate. First, work has shown that a BoNT/A peptide substrate requires a length of 16 amino acid peptide before appreciable cleavage can be seen, see, *e.g.*, the '699 patent at col. 14, lines 10-49. Substitution of a fluorescent protein into the sites identified by the Schmidt I patent would divide the 16 amino acid peptide region necessary for cleavage into two inoperable fragments, thereby making such a substrate unsuitable for the activity assay disclosed in Schmidt I. Second, placement of the fluorescent proteins in a manner required to maintain continuity of the 16 amino acid peptide necessary for functionality is contrary to the radiating quenching teachings of Schmidt I, discussed above, which require that the donor and quencher be separated by 2-5 amino acids.

Thus, combining the Schmidt I patent, the Mahajan reference and Anderson publication with the Clegg reference would result in an inoperable substrate because combining a fluorescent protein with the Schmidt I peptide substrates would result in an uncleavable substrate or be contrary to the radiating quenching teachings of the Schmidt I patent. Therefore, the Applicants respectfully submit that a *prima facie* case of obviousness cannot be made because combining the Siegel reference with the Schmidt I patent as suggested by the Examiner would result in an inoperable substrate.

Conclusion

For the reasons stated above, the Applicants respectfully submit that the assertion of obviousness is unsupported by the Schmidt I patent and the Siegel reference because these references would result in an inoperable quench-release assay as disclosed in the Schmidt I patent, would change the principle of operation of the quench release assay as taught by Schmidt I, and the modifications required to produce the presently claimed invention are expressly taught away by the Schmidt I patent. Therefore, the Applicants respectfully request withdrawal of the 35 U.S.C. § 103(a) obviousness rejection for Claim 72.

III. Obviousness rejections over Schmidt I in view of Auwerx

The Examiner has rejected Claim 72 as allegedly being obvious under 35 U.S.C. § 103(a) over the Schmidt I patent in view of Johan Auwerx et al., *Cofactor-based Screening Method for Nuclear Receptor Modulators and Related Modulators*, U.S. Patent Publication 2003/0104975 (priority filing date Jun. 14, 2001), hereafter the "Auwerx publication."

The Examiner contends that it would have been *prima facie* obvious to a person of ordinary skill in the art at the time the invention was made to combine the teaching of these references and come up with a method of determining clostridial toxin activity as presently claimed in Claim 72. Specifically, the Examiner argues that it would have been obvious to modify the quench-release assay disclosed in the Schmidt I patent to measure donor and acceptor parameters because the Auwerx publication teaches conventional means of measuring FRET in order to arrive at the presently claimed invention. The Applicants respectfully ask for reconsideration under 37 C.F.R. § 1.111.

The Auwerx publication discusses the general utility of FRET, see, *e.g.*, ¶ 279. As outlined above, FRET uses a non-radiating principle of operation, and as such suffers from the same defect as the Clegg and Siegel references discussed above. Adding an acceptor fluorophore to a Schmidt I peptide would change the principle of operation from a quench release assay based on a radiating principle of operation to a resonance energy transfer assay based on a non-radiating principle of operation. In addition, combining the Schmidt I patent, the Mahajan reference and the Clegg reference with the Auwerx publication would result in an inoperable substrate, as discussed above, because combining a fluorescent protein with the Schmidt I peptide substrates would result in an uncleavable substrate or be contrary to the radiating quenching teachings of the Schmidt I patent. Furthermore, as discussed above, the Schmidt I patent teaches that an acceptor must be a non-fluorescent quenching molecule and must be located within certain positions of the P_5-P_5' cleavage site region. Thus, the Schmidt I patent teaches away from the use of fluorescent molecules located outside the P_5-P_5' cleavage site region and the Auwerx publication does not provide any teaching, suggestion or motivation for one skilled in the art to act contrary to the teachings of the Schmidt I patent.

Thus, the Applicants respectfully submit that a *prima facie* case of obviousness cannot be made because combining the cited references as suggested by the Examiner would change the principle of operation of the quench release assay as taught by the Schmidt I patent, would result in an inoperable quench-release assay as disclosed in the Schmidt I patent, and the suggested modifications required to produce the presently claimed invention are expressly taught away by the Schmidt I patent. Therefore, the Applicants respectfully request withdrawal of the 35 U.S.C. § 103(a) obviousness rejection for Claim 72.

IV. Obviousness rejections over Schmidt II in view of Mahajan and Clegg

The Examiner has rejected Claims 60, 61, 63-70, 73-78, 79-83, 85-92 and 95-100 as allegedly being obvious under 35 U.S.C. § 103(a) over James J. Schmidt and Karen A. Bostian, *Assays for the Proteolytic Activities of Serotype A from Clostridium botulinum*, U.S. Patent 5,965,699 (Oct. 12, 1999), hereafter the Schmidt II patent, in view of Nupam P. Mahajan et al., *Novel Mutant Green Fluorescent Protein Protease Substrates Reveal the Activation of Specific Caspases During Apoptosis*, 6(6) Chem. Biol. 401-409 (1999), hereafter the "Mahajan reference" and the Clegg reference.

The Examiner contends that it would have been *prima facie* obvious to a person of ordinary skill in the art at the time the invention was made to combine the teaching of these references and come up with a method of determining clostridial toxin activity as presently claimed in Claims 60, 61, 63-70, 73-78, 79-83, 85-92 and 95-100. Specifically, the Examiner argues that it would have been obvious to substitute the caspase recognition sequence from the FRET substrate taught in the Mahajan reference with the BoNT/A recognition sequence taught in the Schmidt II patent in order to arrive at the presently claimed invention because this proposed assay would be an alternative to the fluorescamine detection assay disclosed in the Schmidt II patent because it would reduce the number of assay steps by omitting the independent addition of fluorescamine. The Applicants respectfully ask for reconsideration under 37 C.F.R. § 1.111.

Schmidt II teaches away from the claimed invention.

According to MPEP §2143.03, to establish *prima facie* obviousness of a claimed invention, all the claim limitations must be taught or suggested by the prior art. The Applicants respectfully submit that it would not be obvious to combine the cited references because the Schmidt II patent teaches away from using an acceptor fluorophore.

The Schmidt II patent discloses fluorescamine detection assay. The Schmidt II patent specifically teaches that fluorescent reagents are problematic, see, *e.g.*, col. 3, lines 55-61 and states that fluroescamine is used as the detection reagent because it is not fluorescent, see, *e.g.*, col. 4, lines 12-14.

Both the Mahajan and Clegg references discuss the use of fluorescent proteins and are silent regarding the use of non-fluorescent fluroescamine teachings of the Schmidt II patent discussed above. Therefore, these references do not provide any teaching, suggestion or motivation for one skilled in the art to act contrary to the teachings of the Schmidt II patent.

It would not have been obvious then, to combine the peptide substrates of Schmidt II patent with the fluorescent molecules disclosed in the Majahan reference as suggested by the Examiner because the Schmidt II patent teaches that an acceptor cannot be fluorescent molecule. Thus, the Applicants respectfully submit that a prima *facie case* of obviousness cannot be made because the Schmidt II patent teaches away from an acceptor that is a fluorescent molecule as presently claimed.

Schmidt II and Mahajan combination makes Schmidt II unsatisfactory for its intended use.

According to MPEP §2143.01, if proposed modification would render the prior art invention being modified unsatisfactory for its intended purpose, then there is no suggestion or motivation to make the proposed modification. The Applicants respectfully submit that it would not be obvious for one of ordinary skill in the art to combine the cited references because combining the Schmidt II patent with the Clegg reference would render the fluroescamine detection assay disclosed in the Schmidt II patent as inoperable for its intended use.

The Schmidt II patent discloses fluroescamine detection assay. The assay is based on the principle of operation that cleavage of a peptide by a protease results in the production of a free amino group, see, *e.g.*, col. 3, lines 25-34. These newly produced amino groups are detected by adding fluroescamine, a non-fluorescent molecule that reacts with free amino groups to produce a fluorescent compound, see, *e.g.*, col. 4, lines 12-15. Thus, fluroescamine is essential to detect whether or not a peptide substrate was cleaved.

Both the Mahajan and Clegg references discuss the use of fluorescent proteins and are silent regarding the use of non-fluorescent fluroescamine teachings of the Schmidt II patent discussed above. Therefore, these references do not provide any teaching, suggestion or motivation for one skilled in the art to act contrary to the teachings of the Schmidt II patent.

It would not have been obvious to combine the peptide substrates of Schmidt II patent with the fluorescent molecules disclosed in the Majahan reference in order to eliminate the fluroescamine addition step because the Schmidt II patent teaches that fluroescamine addition is necessary to detect the cleavage of the substrate. Elimination of the fluroescamine addition step would render the fluroescamine detection assay disclosed in the Schmidt II patent inoperable. Thus, the Applicants respectfully submit that a prima *facie case* of obviousness cannot be made because combining the Schmidt II patent with the Clegg reference as suggested by the Examiner would result in an inoperable assay..

Schmidt II, Mahajan and Clegg combination changes the principle of operation of Schmidt II.

According to MPEP §2143.01, if a proposed modification or combination of the prior art would change the principle of operation of the prior art invention being modified, then the teachings of the references are not sufficient to render the claims *prima facie* obvious. The Applicants respectfully submit that it would not be obvious for one of ordinary skill in the art to combine the cited references because combining the Schmidt II patent with the Mahajan and Clegg references as suggested by the Examiner would change the principle of operation of the fluorescamine detection assay disclosed in the Schmidt II patent.

As discussed above, the principle of operation for the fluorescamine detection assay disclosed in the Schmidt II patent requires the reaction of the non-fluorescent molecule fluorescamine with the free amino groups of a cleavage product produced upon cleavage with a protease, see, *e.g.*, col. 3, lines 25-34.

The Mahajan and Clegg references discuss the use of FRET. As outlined above, FRET uses a non-radiating principle of operation. In this principle of operation, energy is transferred from one molecule to another by intermolecular long-range dipole-dipole coupling, see, *e.g.*, the Clegg reference at pg. 103, col. 2, ¶1, lines 1-5; see also, the Lakowicz reference, Chapter 13 Energy Transfer, pg. 367, col. 1, ¶1.

Adding an acceptor fluorophore to a Schmidt II peptide would change the principle of operation from a fluorescamine detection assay based on the reactive ability of a fluorescamine with free amino groups to a resonance energy transfer assay based on a non-radiating principle of operation. Thus, the Applicants respectfully submit that a *prima facie* case of obviousness cannot be made because combining the Schmidt II patent with the Mahajan and Clegg references as suggested by the Examiner would change the principle of operation of the fluorescamine detection assay as disclosed in the Schmidt II patent.

Conclusion

For the reasons stated above, the Applicants respectfully submit that the assertion of obviousness is unsupported by the Schmidt II patent, the Mahajan reference and the Clegg reference because these references would result in an inoperable fluorescamine detection assay as disclosed in the Schmidt II patent, would change the principle of operation of the fluorescamine detection assay as taught by Schmidt II, and the modifications required to produce the presently claimed invention are expressly taught away by the Schmidt II patent. Therefore, the Applicants respectfully request withdrawal of the 35 U.S.C. § 103(a) obviousness rejection for Claims 60, 61, 63-70, 73-78, 79-83, 85-92 and 95-100.

V. Obviousness rejections over Schmidt II in view of Mahajan, Clegg and Siegel.

The Examiner has rejected Claims 72 and 94 as allegedly being obvious under 35 U.S.C. § 103(a) over the Schmidt II patent, in view of the Mahajan reference, the Clegg reference and the Siegel reference.

The Examiner contends that it would have been *prima facie* obvious to a person of ordinary skill in the art at the time the invention was made to combine the teaching of these references and come up with a method of determining clostridial toxin activity as presently claimed in Claims 72 and 94. Specifically, the Examiner argues that it would have been obvious to modify the fluorescamine detection assay as disclosed in the Schmidt II patent to measure donor excited state lifetimes because the Siegel reference teaches that FRET assays with double-labeled fluorescent molecules can achieve this excited state lifetime measurement in order to arrive at the presently claimed invention. The Applicants respectfully ask for reconsideration under 37 C.F.R. § 1.111.

The Siegel reference discloses the use of spectral variants of green fluorescent protein as donor and acceptor proteins for measuring FRET interactions, see, *e.g.*, pg. 1, col. 1, ¶ 1, lines 7-13. As outlined above, FRET uses a non-radiating principle of operation, and as such suffers from the same defect as the Mahajan and Clegg references discussed above. Adding an acceptor fluorophore to a Schmidt II peptide would change the principle of operation from a fluorescamine detection assay based on the reactive ability of a fluorescamine with free amino groups to a resonance energy transfer assay based on a non-radiating principle of operation. In addition, combining the Schmidt II patent, the Mahajan reference and the Clegg reference with the Siegel reference would result in an inoperable substrate, as discussed above, because the elimination of the fluorescamine addition step would render the fluorescamine detection assay inoperable. Furthermore, as discussed above, the Schmidt II patent teaches that the non-fluorescent molecule fluorescamine must be used in the disclosed assays. Thus, the Schmidt II patent teaches away from the use of fluorescent molecules and the Siegel reference does not provide any teaching, suggestion or motivation for one skilled in the art to act contrary to the teachings of the Schmidt II patent.

Thus, the Applicants respectfully submit that a *prima facie* case of obviousness cannot be made because combining the cited references as suggested by the Examiner would change

the principle of operation of the fluorescamine detection assay as taught by the Schmidt II patent, would result in an inoperable fluorescamine detection assay as disclosed in the Schmidt II patent, and the suggested modifications required to produce the presently claimed invention are expressly taught away by the Schmidt II patent. Therefore, the Applicants respectfully request withdrawal of the 35 U.S.C. § 103(a) obviousness rejection for Claims 72 and 94.

VI. Obviousness rejections over Schmidt II in view of Mahajan, Clegg and Auwerx

The Examiner has rejected Claims 72 and 94 as allegedly being obvious under 35 U.S.C. § 103(a) over the Schmidt II patent, in view of the Mahajan reference, the Clegg reference and the Auwerx reference. The Applicants respectfully ask for reconsideration under 37 C.F.R. § 1.111.

The Examiner contends that it would have been *prima facie* obvious to a person of ordinary skill in the art at the time the invention was made to combine the teaching of these references and come up with a method of determining clostridial toxin activity as presently claimed in Claim 72 and 94. Specifically, the Examiner argues that it would have been obvious to modify the fluorescamine detection assay as disclosed in the Schmidt II patent to measure donor and acceptor parameters because the Auwerx publication teaches conventional means of measuring FRET in order to arrive at the presently claimed invention. The Applicants respectfully ask for reconsideration under 37 C.F.R. § 1.111.

The Auwerx publication discusses the general utility of FRET, see, *e.g.*, ¶ 279. As outlined above, FRET uses a non-radiating principle of operation, and as such suffers from the same defect as the Mahajan, Clegg and Siegel references discussed above. Adding an acceptor fluorophore to a Schmidt II peptide would change the principle of operation from a fluorescamine detection assay based on the reactive ability of a fluorescamine with free amino groups to a resonance energy transfer assay based on a non-radiating principle of operation. In addition, combining the Schmidt II patent, the Mahajan reference and the Clegg reference with the Auwerx publication would result in an inoperable substrate, as discussed above, because the elimination of the fluorescamine addition step would render the fluorescamine detection assay inoperable. Furthermore, as discussed above, the

Schmidt II patent teaches that the non-fluorescent molecule fluorescamine must be used in the disclosed assays. Thus, the Schmidt II patent teaches away from the use of fluorescent molecules and the Auwerx publication does not provide any teaching, suggestion or motivation for one skilled in the art to act contrary to the teachings of the Schmidt II patent.

Thus, the Applicants respectfully submit that a *prima facie* case of obviousness cannot be made because combining the cited references as suggested by the Examiner would change the principle of operation of the fluorescamine detection assay as taught by the Schmidt II patent, would result in an inoperable fluorescamine detection assay as disclosed in the Schmidt II patent, and the suggested modifications required to produce the presently claimed invention are expressly taught away by the Schmidt II patent. Therefore, the Applicants respectfully request withdrawal of the 35 U.S.C. § 103(a) obviousness rejection for Claims 72 and 94.

CONCLUSION

For the above reasons the Applicants respectfully submit that the claims are in condition for allowance, and the Applicants respectfully urge the Examiner to issue a Notice to that effect. Should there be any questions, the Examiner is invited to call the undersigned agent. Please use Deposit Account 01-0885 for the payment of any extension of time fees under 37 C.F.R. § 1.136 or any other fees due in connection with the current response.

Respectfully submitted,

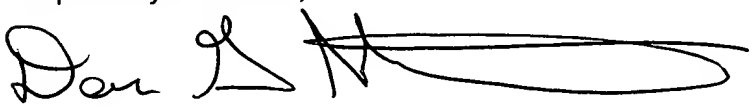

Dean G. Stathakis, Ph.D.
Registration No. 54,465
Agent of Record

ALLERGAN
LEGAL DEPARTMENT
2525 Dupont Drive
Irvine, California 92612-1599
Tel: 714/246-6521
Fax: 714/246-4249

Principles of Fluorescence Spectroscopy
(Ed. Joseph R. Lakowicz,
Kluwer Academic/Plenum Publisher, 2nd Ed.1999)

8

Quenching of Fluorescence

Fluorescence quenching refers to any process which decreases the fluorescence intensity of a sample. A variety of molecular interactions can result in quenching. These include excited-state reactions, molecular rearrangements, energy transfer, ground-state complex formation, and collisional quenching. In this chapter we will be concerned primarily with quenching resulting from collisional encounters between the fluorophore and quencher, which is called collisional or dynamic quenching. Static quenching is a frequent complicating factor in the analysis of quenching data, but it can also be a valuable source of information about binding between the fluorescent sample and the quencher. In addition to the processes described above, apparent quenching can occur due to the optical properties of the sample. For example, high optical densities or turbidity can result in decreased fluorescence intensities. This is a trivial type of quenching which contains little molecular information. Throughout this chapter, we will assume that such trivial effects are not the cause of the observed decreases in fluorescence intensity.

Fluorescence quenching has been widely studied both as a fundamental phenomenon and as a source of information about biochemical systems. The biochemical applications of quenching are due to the intrinsic role of molecular interactions in quenching phenomena. Both static and dynamic quenching require molecular contact between the fluorophore and quencher. In the case of collisional quenching, the quencher must diffuse to the fluorophore during the lifetime of the excited state. Upon contact, the fluorophore returns to the ground state, without emission of a photon. In general, quenching occurs without any permanent change in the molecules, that is, without a photochemical reaction. In the case of static quenching, a complex is formed between the fluorophore and the quencher, and this complex is nonfluorescent. For either static or dynamic quenching to occur, the fluorophore and quencher must be in contact. The requirement of molecular contact results in the numerous applications of quenching. For example, quenching measurements can reveal the accessibility of fluorophores to quenchers. Consider a fluorophore bound either to a protein or to a membrane. If the protein or membrane is impermeable to the quencher, and the fluorophore is located in the interior of the macromolecule, then neither collisional nor static quenching can occur. For this reason, quenching studies can be used to reveal the localization of fluorophores in proteins and membranes and the permeabilities of protons and membranes to quenchers. Additionally, the rate of collisional quenching can be used to determine the diffusion coefficient of the quencher.

It is important to recognize that the phenomenon of collisional quenching results in the expansion of the volume and distance within the solution, which affects the experimental observables. The root-mean-square distance $[\sqrt{(\overline{\Delta x^2})}]$ over which a quencher can diffuse during the lifetime of the excited state (τ) is given by $\sqrt{(\overline{\Delta x^2})} = \sqrt{(2D\tau)}$, where D is the diffusion coefficient. Consider an oxygen molecule in water at 25 °C. Its diffusion coefficient is 2.5×10^{-5} cm^2/s. During a typical fluorescence lifetime of 4 ns, the oxygen molecule can diffuse 44 Å. If the lifetime is longer, diffusion over still larger distances can be observed. For example, for lifetimes of 20 and 100 ns the average distances for oxygen diffusion are 100 Å and 224 Å, respectively. With the introduction of longer-lived probes with microsecond lifetimes (Chapter 20), diffusion over still larger distances can be observed. Hence, fluorescence quenching can reveal the diffusion of quenchers over moderately large distances which are comparable to the sizes of proteins and membranes. This situation is different from that for solvent relaxation. Spectral shifts resulting from reorientation of the solvent molecules are due primarily to the solvent shell immediately adjacent to the fluorophore.

8.1. QUENCHERS OF FLUORESCENCE

A wide variety of substances act as quenchers of fluorescence. One of the best-known collisional quenchers is molecular oxygen,[1] which quenches almost all known fluorophores. Depending upon the sample under investigation, it is frequently necessary to remove dissolved oxygen to obtain reliable measurements of the fluorescence yields or lifetimes. The mechanism by which oxygen quenches fluorescence has been the subject of debate. The most likely mechanism is that the paramagnetic oxygen causes the fluorophore to undergo intersystem crossing to the triplet state. In fluid solutions the long-lived triplets are completely quenched, so that phosphorescence is not observed. Aromatic and aliphatic amines are also efficient quenchers of most unsubstituted aromatic hydrocarbons. For example, anthracene fluorescence is effectively quenched by diethylaniline.[2] In this instance the mechanism of quenching is the formation of an excited charge-transfer complex. The excited-state fluorophore accepts an electron from the amine. In nonpolar solvents, fluorescence from the excited charge-transfer complex (exciplex)

Table 8.1. Quenchers of Fluorescence

Quencher(s)	Typical fluorophore(s)[a]	Reference(s)
Acrylamide	Tryptophan	5–7, 79
Amines	Anthracene, perylene	2, 80–85
Amines	Carbazole	86
Amine anesthetics	Perylene, anthroyloxy probes	87,88
Bromate	—	89
Bromobenzene	Many fluorophores	90
Carboxy groups	Indole	91
Chloride	Quinolinium, SPQ	92–95
Chlorinated compounds	Indoles and carbazoles	96–99
Cobalt (Co^{2+})	NBD, PPO, perylene (energy transfer for some probes)	100–105
Copper (Cu^{2+})	Anthroyloctanoic acid	106
Dimethylformamide	Indole	107
Disulfides	Tyrosine	108
Ethers	9-Arylxanthyl cations	109
Halogens	Anthracene, naphthalene, carbazole	110–125
Halogen anesthetics	Pyrene, tryptophan	126,127
Hydrogen peroxide	Tryptophan	128
Imidazole, histidine	Tryptophan	129
Iodide	Antracene	130–133
Methylmercuric chloride	Carbazole, pyrene	134,135
Nickel (Ni^{2+})	Perylene	136,137
Nitromethane and nitro compounds	Polycyclic aromatic hydrocarbons	138–144
Nitroxides	Naphthalene, Tb^{3+}, anthroyloxy probes	63,145–148
NO (nitric oxide)	Naphthalene, pyrene	149–151
Olefins	Cyanonaphthalene, 2,3-dimethylnaphthalene, pyrene	152–157
Oxygen	Most fluorophores	158–166
Peroxides	Dimethylnaphthalene	167
Picolinium nicotinamide	Tryptophan	168
Pyridine	Carbazole	169
Quinones	Aromatic hydrocarbons, chlorophyll	170,171
Silver (Ag^{+})	Perylene	172
Succinimide	Tryptophan	173,174
Thallium (Tl^{+})	Naphthylaminesulfonic acid	175
Thiocyanate	Anthracene, 5,6-benzoquinoline	176,177
Trifluoroacetamide	Tryptophan	35
Xenon		178

[a]Abbreviations: NBD, 7-Nitrobenz-2-oxa-1,3-diazol-4-yl; PPO, 2,5-diphenyl-1,3,4-oxadiazole; SPQ, 6-methoxy-*N*-(3-sulfopropyl) quinoline.

is frequently observed, and one may regard this process as an excited-state reaction rather than quenching. In polar solvents the exciplex emission is often quenched, so that the fluorophore–amine interaction appears to be that of simple quenching. While it is now known that there is a modest through-space component to almost all quenching reactions, this component is short-range (< 2 Å), so that molecular contact is a requirement for quenching.

Another type of quenching is due to heavy atoms such as iodine and bromine. Halogenated compounds such as trichloroethanol and bromobenzene also act as collisional quenchers. Quenching by the larger halogens such as bromine and iodine may be a result of intersystem crossing to an excited triplet state, promoted by spin–orbit coupling of the excited (singlet) fluorophore and the halogen.[3] Since emission from the triplet state is slow, the triplet emission is highly quenched by other processes. The quenching mechanism is probably different for chlorine-containing substances. Indole, carbazole, and their derivatives are uniquely sensitive to quenching by chlorinated hydrocarbons and by electron scavengers such as protons, histidine, cysteine, NO_3^-, fumarate, Cu^{2+}, Pb^{2+}, Cd^{2+}, and Mn^{2+}.[4] Quenching by these substances probably involves donation of an electron from the fluorophore to the quencher. Additionally, indole and tryptophan and its derivatives are quenched by acrylamide, succinimide, dichloroacetamide, dimethylformamide, pyridinium hydrochloride, imidazolium hydrochloride, methionine, Eu^{3+}, Ag^+, and Cs^+. Quenchers of protein fluorescence have been summarized in several insightful reviews.[5–7] Hence, a variety of quenchers are available for studies of protein fluorescence, especially to determine the surface accessibility of tryptophan residues and the permeation of proteins by the quenchers.

Additional quenchers include purines, pyrimidines, *N*-methylnicotinamide, and *N*-alkylpyridinium and -picolinium salts.[8,9] For example, the fluorescence of both FAD and NADH is quenched by the adenine moiety; flavin fluorescence is quenched by both static and dynamic processes,[10] whereas the quenching of dihydronicotinamide appears to be primarily dynamic.[11] These aromatic substances appear to quench by formation of charge-transfer complexes. Depending upon the precise structure involved, the ground-state complex can be reasonably stable. As a result, both static and dynamic quenching are frequently observed. A variety of other quenchers are known. These are summarized in Table 8.1, which is intended to be an overview and not a complete list. Known collisional quenchers include hydrogen peroxide, nitric oxide (NO), nitroxides, BrO_4^-, and even some olefins.

Because of the variety of substances which act as quenchers, one can frequently identify fluorophore–quencher combinations for a desired purpose. It is important to note that not all fluorophores are quenched by all the substances listed above. This fact occasionally allows selective quenching of a given fluorophore. The occurrence of quenching depends upon the mechanism, which in turn depends upon the chemical properties of the individual molecules. Detailed analysis of the mechanism of quenching is complex. In this chapter we will be concerned primarily with the type of quenching, that is, whether quenching is diffusive or static in nature. Later in this chapter, we describe biochemical applications of quenching.

8.2. THEORY OF COLLISIONAL QUENCHING

Collisional quenching of fluorescence is described by the Stern–Volmer equation,

$$\frac{F_0}{F} = 1 + k_q\tau_0[Q] = 1 + K_D[Q] \qquad [8.1]$$

In this equation, F_0 and F are the fluorescence intensities in the absence and presence of quencher, respectively, k_q is the bimolecular quenching constant, τ_0 is the lifetime of the fluorophore in the absence of quencher, and [Q] is the concentration of quencher. The Stern–Volmer quenching constant is given by $k_q\tau_0$. If the quenching is known to be dynamic, the Stern–Volmer constant will be represented by K_D. Otherwise, this constant will be described as K_{SV}.

Quenching data are usually presented as plots of F_0/F versus [Q]. This is because F_0/F is expected to be linearly dependent upon the concentration of quencher. A plot of F_0/F versus [Q] yields an intercept of 1 on the *y*-axis and a slope equal to K_D (Figure 8.1). Intuitively, it is useful to note that K_D^{-1} is the quencher concentration at which $F_0/F = 2$, or 50% of the intensity is quenched. A linear Stern–Volmer plot is generally indicative of a single class of fluorophores, all equally accessible to quencher. If two fluorophore populations are present, and one class is not accessible to quencher, then the Stern–Volmer plots deviate from linearity toward the *x*-axis. This result is frequently found for the quenching of tryptophan fluorescence in proteins by polar or charged quenchers. These molecules do not readily penetrate the hydrophobic interior of proteins, and only those tryptophan residues on the surface of the protein are quenched.

It is important to recognize that observation of a linear Stern–Volmer plot does not prove that collisional quench-

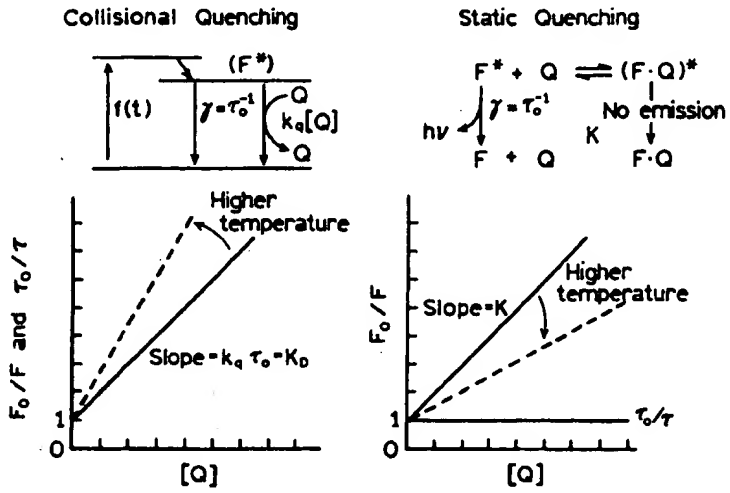

Figure 8.1. Comparison of dynamic (collisional) and static quenching.

ing of fluorescence has occurred. In Section 8.3 we will see that static quenching also results in linear Stern–Volmer plots. Static and dynamic quenching can be distinguished by their differing dependence on temperature and viscosity, or preferably by lifetime measurements. Higher temperatures result in faster diffusion and hence larger amounts of collisional quenching. Higher temperatures will typically result in the dissociation of weakly bound complexes, and hence smaller amounts of static quenching.

8.2.A. Derivation of the Stern–Volmer Equation

The Stern–Volmer equation can be derived by consideration of the fluorescence intensities observed in the absence and presence of quencher. The fluorescence intensity observed for a fluorophore is proportional to its concentration in the excited state [F*]. Under continuous illumination, a constant population of excited fluorophores is established, and therefore $d[F^*]/dt = 0$. In the absence of quencher, the differential equation describing [F*] is

$$\frac{d[F^*]}{dt} = f(t) - \gamma[F^*]_0 = 0 \qquad [8.2]$$

and in the presence of quencher,

$$\frac{d[F^*]}{dt} = f(t) - (\gamma + k_q[Q])[F^*] = 0 \qquad [8.3]$$

where $f(t)$ is the constant excitation function, and $\gamma = \tau_0^{-1}$ is the decay rate of the fluorophore in the absence of quencher. In the absence of quenching, the excited-state population decays with a rate $\gamma = (\Gamma + k_{nr})$, where Γ is the radiative decay rate and k_{nr} is the nonradiative decay rate. In the presence of quencher, there is an additional decay rate, $k_q[Q]$. With continuous excitation, the excited-state population is constant, so the derivative can be easily eliminated from these equations. Division of Eq. [8.3] by Eq. [8.2] yields

$$\frac{F_0}{F} = \frac{\gamma + k_q[Q]}{\gamma} = 1 + k_q\tau_0[Q] \qquad [8.4]$$

which is the Stern–Volmer equation.

This equation may also be obtained by considering the fraction of excited fluorophores, relative to the total, which decay by emission. This fraction (F/F_0) is given by the ratio of the decay rate in the absence of quencher (γ) to the total decay rate in the presence of quencher ($\gamma + k_q[Q]$),

$$\frac{F}{F_0} = \frac{\gamma}{\gamma + k_q[Q]} = \frac{1}{1 + K_D[Q]} \qquad [8.5]$$

which is again the Stern–Volmer equation. Since collisional quenching is a rate process which depopulates the excited state, the lifetimes in the absence (τ_0) and presence (τ) of quencher are given by

$$\tau_0 = \gamma^{-1} \qquad [8.6]$$

$$\tau = (\gamma + k_q[Q])^{-1} \qquad [8.7]$$

and therefore

$$\frac{\tau_0}{\tau} = 1 + k_q\tau_0[Q] \qquad [8.8]$$

This equation illustrates an important characteristic of collisional quenching, which is an equivalent decrease in fluorescence intensity and in lifetime (Figure 8.1, left); that is, for collisional quenching,

$$\frac{F_0}{F} = \frac{\tau_0}{\tau} \qquad [8.9]$$

The decrease in lifetime occurs because quenching is an additional rate process that depopulates the excited state. The decrease in yield occurs because quenching depopulates the excited state without fluorescence emission. Static quenching does not decrease the lifetime because only the fluorescent molecules are observed, and the uncomplexed fluorophores have the unquenched lifetime τ_0.

8.2.B. Interpretation of the Bimolecular Quenching Constant

A frequently encountered value is the bimolecular quenching constant (k_q), which can reflect the efficiency of quenching or the accessibility of the fluorophores to the quencher. As shown below, diffusion-controlled quenching typically results in values of k_q near 1×10^{10} M^{-1} s^{-1}. Smaller values of k_q can result from steric shielding of the fluorophore, and larger apparent values of k_q usually indicate some type of binding interaction.

The meaning of the bimolecular quenching constant can be understood in terms of the frequency of collisions between freely diffusing molecules. The collisional frequency (Z) of a fluorophore with a quencher is given by

$$Z = k_0[Q] \qquad [8.10]$$

where k_0 is the diffusion-controlled bimolecular rate constant. This constant may be calculated using the Smoluchowski equation,

$$k_0 = \frac{4\pi RDN}{1000} = \frac{4\pi N}{1000}(R_f + R_q)(D_f + D_q) \qquad [8.11]$$

where R is the collision radius, D is the sum of the diffusion coefficients of the fluorophore (D_f) and quencher (D_q), and N is Avogadro's number. The collision radius is generally assumed to be the sum of the molecular radii of the fluorophore (R_f) and quencher (R_q). This equation describes the diffusive flux of a molecule with a diffusion coefficient D through the surface of a sphere of radius R. The factor of 1000 is necessary to keep the units correct when the concentration is expressed in terms of molarity. The term $N/1000$ converts molarity to molecules per cubic centimeter.

The collisional frequency is related to the bimolecular quenching constant by the quenching efficiency f_Q,

$$k_q = f_Q k_0 \qquad [8.12]$$

For example, if $f_Q = 0.5$, then 50% of the collisional encounters are effective in quenching, and one expects k_q to be one-half of k_0. Since k_0 can be estimated with moderate precision, the observed value of k_q can be used to judge the efficiency of quenching. Quenchers like oxygen, acrylamide, and I^- generally have efficiencies near unity, but the quenching efficiency of succinimide depends on the solvent. The efficiency is generally less with the lighter halogens. The quenching efficiency of amines depends upon the reduction potential of the fluorophores being quenched, as may be expected for a charge-transfer reaction.

The efficiency of quenching can be calculated from the observed value of k_q, if the diffusion coefficients and molecular radii are known. The radii can be obtained from molecular models, or from the molecular weights and densities of the substances in question. Diffusion coefficients may be obtained from the Stokes–Einstein equation,

$$D = kT/6\pi\eta R \qquad [8.13]$$

where k is the Boltzmann constant, η is the solvent viscosity, and R is the molecular radius. Frequently, the Stokes–Einstein equation underestimates the diffusion coefficients of small molecules. For example, quenching efficiencies of 2–3 were calculated for oxygen quenching of fluorophores dissolved in various alcohols.[12] These impossibly large efficiencies were obtained because the diffusion coefficient of oxygen in organic solvents is severalfold larger than predicted by Eq. [8.13]. This equation describes the diffusion of molecules that are larger than the solvent molecules, which is clearly not the case for oxygen in ethanol. As an alternative method, diffusion coefficients can be obtained from nomograms based upon physical properties of the system.[13] Once the diffusion coefficients are known, the bimolecular quenching constant for $f_Q = 1$ can be predicted using the Smoluchowski equation (Eq. [8.11]).

It is instructive to consider typical values for k_q and the concentrations of quencher required for significant quenching. For example, consider the quenching of tryptophan by oxygen.[14] At 25 °C the diffusion coefficient of oxygen in water is 2.5×10^{-5} cm^2/s and that of tryptophan is 0.66×10^{-5} cm^2/s. Assuming a collision radius of 5 Å, substitution into Eq. [8.11] yields $k_0 = 1.2 \times 10^{10}$ M^{-1} s^{-1}. The observed value of the oxygen Stern–Volmer quenching constant was 32.5 M^{-1}. Since the unquenched lifetime

of tryptophan is 2.7 ns, $k_q = 1.2 \times 10^{10}\ M^{-1}\ s^{-1}$ which is in excellent agreement with the predicted value. This indicates that essentially every collision of oxygen with tryptophan is effective in quenching, that is, $f_Q = 1.0$. A bimolecular quenching constant near $1 \times 10^{10}\ M^{-1}\ s^{-1}$ may be considered as the largest possible value in aqueous solution. For quenchers other than oxygen, smaller diffusion-limited quenching constants are expected because the diffusion coefficients of the quenchers are smaller. For example, the efficiency of acrylamide quenching of tryptophan fluorescence is also near unity,[15] but $k_q = 5.9 \times 10^9\ M^{-1}\ s^{-1}$. This somewhat smaller value of k_q is a result of the smaller diffusion coefficient of acrylamide relative to that of oxygen. Frequently, data are obtained for fluorophores which are bound to macromolecules. In this case, the fluorophore is not diffusing as rapidly. Also, the quenchers can probably only approach the fluorophores from a particular direction. In such cases, the maximum bimolecular quenching constant is expected to be about 50% of the diffusion-controlled value.[16]

8.3. THEORY OF STATIC QUENCHING

In the previous section we described quenching that resulted from diffusive encounters between the fluorophore and quencher during the lifetime of the excited state. This is a time-dependent process. Quenching can also occur as a result of the formation of a nonfluorescent complex between the fluorophore and quencher. When this complex absorbs light, it immediately returns to the ground state without emission of a photon (Figure 8.1).

The dependence of the fluorescence intensity upon quencher concentration for static quenching is easily derived by consideration of the association constant for complex formation. This constant is given by

$$K_S = \frac{[F - Q]}{[F][Q]} \qquad [8.14]$$

where [F–Q] is the concentration of the complex, [F] is the concentration of uncomplexed fluorophore, and [Q] is the concentration of quencher. If the complexed species is nonfluorescent, then the fraction of the fluorescence that remains, F/F_0, is given by the fraction of the total fluorophores that are not complexed, $f = F/F_0$. Recalling that the total concentration of fluorophore, $[F]_0$, is given by

$$[F]_0 = [F] + [F - Q] \qquad [8.15]$$

substitution into Eq. [8.14] yields

$$K_S = \frac{[F]_0 - [F]}{[F][Q]} = \frac{[F_0]}{[F][Q]} - \frac{1}{[Q]} \qquad [8.16]$$

We can substitute fluorescence intensities for the fluorophore concentrations, and rearrangement of Eq. [8.16] yields

$$\frac{F_0}{F} = 1 + K_S[Q] \qquad [8.17]$$

Note that the dependence of F_0/F on [Q] is linear and is identical to that observed for dynamic quenching except that the quenching constant is now the association constant. Unless additional information is provided, fluorescence quenching data obtained by intensity measurements alone can be explained by either a dynamic or a static process. As will be shown below, the magnitude of K_S can sometimes be used to demonstrate that dynamic quenching cannot account for the decrease in intensity. The measurement of fluorescence lifetimes is the most definitive method to distinguish static and dynamic quenching. Static quenching removes a fraction of the fluorophores from observation. The complexed fluorophores are nonfluorescent, and the only observed fluorescence is from the uncomplexed fluorophores. The uncomplexed fraction is unperturbed, and hence the lifetime is τ_0. Therefore, for static quenching $\tau_0/\tau = 1$ (Figure 8.1, right). In contrast, for dynamic quenching, $\tau_0/\tau = F_0/F$.

Besides measurement of fluorescence lifetimes, static and dynamic quenching can often be distinguished on the basis of other considerations. Dynamic quenching depends upon diffusion. Since higher temperatures result in larger diffusion coefficients, the bimolecular quenching constants are expected to increase with increasing temperature (Figure 8.1). More specifically, k_q is expected to be proportional to T/η since diffusion coefficients are proportional to this ratio (Eq. [8.13]). In contrast, increased temperature is likely to result in decreased stability of complexes, and thus lower values of the static quenching constants.

One additional method to distinguish static and dynamic quenching is by careful examination of the absorption spectra of the fluorophore. Collisional quenching only affects the excited states of the fluorophores, and thus no changes in the absorption spectra are expected. In contrast, ground-state complex formation will frequently result in perturbation of the absorption spectrum of the fluorophore. In fact, a more complete form of Eq. [8.17] would include the possibility of different extinction coefficients for the free and complexed forms of the fluorophore.

8.4. COMBINED DYNAMIC AND STATIC QUENCHING

In many instances the fluorophore can be quenched both by collisions and by complex formation with the same quencher. The characteristic feature of the Stern–Volmer plots in such circumstances is an upward curvature, concave toward the *y*-axis (Figure 8.2). Then the fractional fluorescence remaining (F/F_0) is given by the product of the fraction not complexed (f) and the fraction not quenched by collisional encounters. Hence,

$$\frac{F}{F_0} = f\frac{\gamma}{\gamma + k_q[Q]} \qquad [8.18]$$

In the previous section we found that $f^{-1} = 1 + K_S[Q]$. Inversion of Eq. [8.18] and rearrangement of the last term on the right yields

$$\frac{F_0}{F} = (1 + K_D[Q])(1 + K_S[Q]) \qquad [8.19]$$

This modified form of the Stern–Volmer equation is second-order in [Q], which accounts for the upward curvature observed when both static and dynamic quenching occur for the same fluorophore.

The dynamic portion of the observed quenching can be determined by lifetime measurements. That is, $\tau_0/\tau = 1 + K_D[Q]$. If lifetime measurements are not available, then Eq. [8.19] can be modified to allow a graphical separation of K_S and K_D. Multiplication of the terms in parentheses yields

$$\frac{F_0}{F} = 1 + (K_D + K_S)[Q] + K_DK_S[Q]^2 \qquad [8.20]$$

$$= 1 + K_{app}[Q] \qquad [8.21]$$

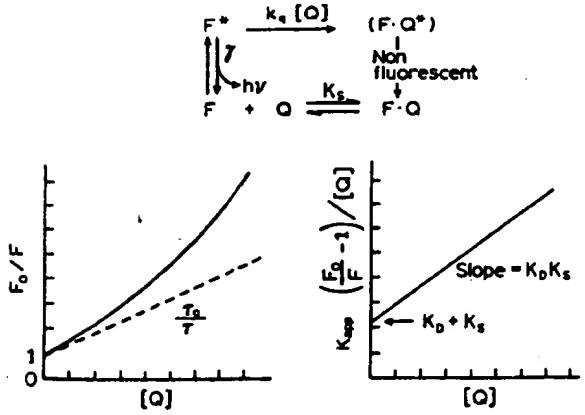

Figure 8.2. Dynamic and static quenching of the same population of fluorophores.

where

$$K_{app} = \left(\frac{F_0}{F} - 1\right)\frac{1}{[Q]} = (K_D + K_S) + K_DK_S[Q] \qquad [8.22]$$

The apparent quenching constant is calculated at each quencher concentration. A plot of K_{app} versus [Q] yields a straight line with an intercept of $K_D + K_S$ and a slope of K_DK_S (Figure 8.2). The individual values can be obtained from the two solutions of the quadratic equation obtained (see Eq. [8.23]). The dynamic component can generally be selected to be the solution comparable in magnitude to the expected diffusion-controlled value. Alternatively, the temperature or viscosity dependence of the values, or other available information, may be used as a basis for assigning the values.

8.5. EXAMPLES OF STATIC AND DYNAMIC QUENCHING

Before proceeding with additional theories and examples of quenching, it seems valuable to present some examples which illustrate both static and dynamic quenching. Data for oxygen quenching of tryptophan are shown in Figure 8.3.[14] The Stern–Volmer plot is linear, which indicates that only one type of quenching occurs. The proportional decrease in the fluorescence lifetime and yields proves that the observed quenching is due to a diffusive process. From the slope of the Stern–Volmer plot, one can calculate that $K_D = 32.5\,M^{-1}$, or that 50% of the fluorescence is quenched at an oxygen concentration of $0.031M$. The value of K_D and the fluorescence lifetime are adequate to calculate the bimolecular quenching constant, $k_q = 1.2 \times 10^{10}\,M^{-1}\,s^{-1}$. This is the value expected for the diffusion controlled bimolecular rate constant between oxygen and tryptophan (Eq. [8.11]), which indicates efficient quenching by molecular oxygen.

Static quenching is often observed if the fluorophore and quencher can have a stacking interaction. Such interactions often occur between purine and pyrimidine nucleotides and a number of fluorophores.[17–19] One example is quenching of the coumarin derivative C-120 by the nucleosides uridine (U) and deoxycytidine (dC). The intensity Stern–Volmer plot for quenching by U shows clear upward curvature (Figure 8.4). The lifetime Stern–Volmer plot is linear and shows less quenching than the intensity data. It is clear that the intensity of C-120 is being decreased by both complex formation with U as well as collisional quenching by U. Contrasting data were obtained for quenching of C-120 by dC. In this case, the Stern–Volmer plots are linear for both intensities and lifetimes, and F_0/F

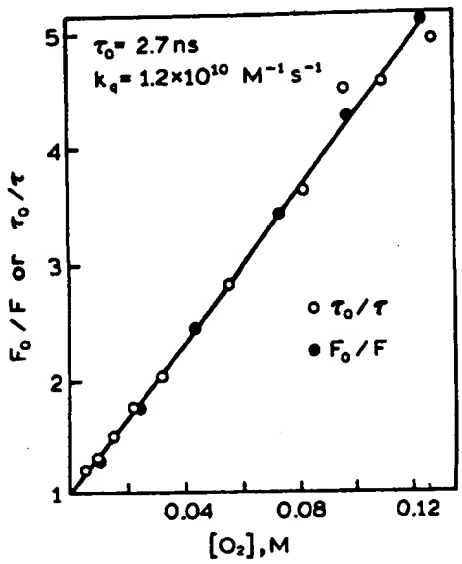

Figure 8.3. Oxygen quenching of tryptophan as observed from fluorescence lifetimes (o) and yields (●). Revised from Ref. 14.

$= \tau_0/\tau$. Hence, quenching of C-120 by dC is purely dynamic.

For quenching of C-120 by U, the static and dynamic quenching constants can be determined from a plot of K_{app} versus [U] (Figure 8.5). The slope (S) and intercept (I) were found to be 158 M^{-2} and 25.6 M^{-1}, respectively. Recalling that $I = K_D + K_S$ and $S = K_D K_S$, rearrangement yields

$$K_S^2 - K_S I + S = 0 \qquad [8.23]$$

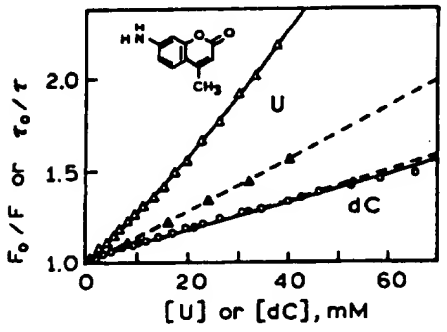

Figure 8.4. Quenching of coumarin C-120 by the nucleosides uridine (Δ, F_0/F; ▲, τ_0/τ) and deoxycytidine (O, F_0/F; ●, τ_0/τ). The sample was excited at the isosbestic point at 360 nm. Revised and reprinted, with permission, from Ref. 19, Copyright © 1996, American Chemical Society.

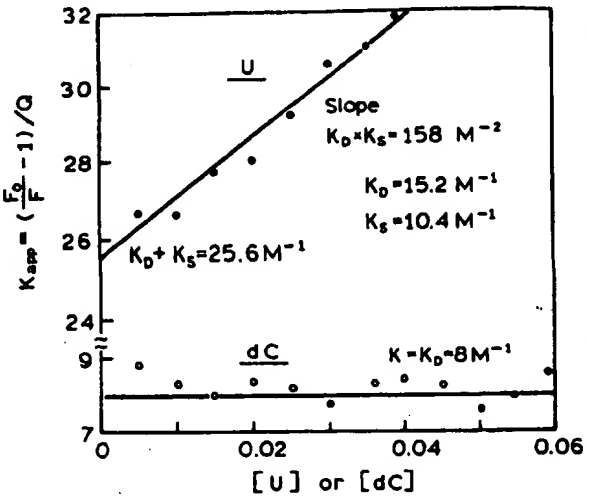

Figure 8.5. Separation of the dynamic and static quenching constants for quenching of C-120 by U or dC. Data from Ref. 19.

The solutions for this quadratic equation are K_S = 15.2 or 10.4 M^{-1}. From the lifetime data, we know that K_D is near 13.5 M^{-1}. The lower value of 10.4 M^{-1} was assigned as the static quenching constant. At a uridine concentration of 96mM, 50% of the ground state C-120 is complexed and thus nonfluorescent.

It is interesting to mention why the interactions of nucleosides and nucleotides with C-120 were studied. The goal was to develop a method for DNA sequencing using a single electrophoretic lane for all four nucleotides.[19] This would be possible if coumarin derivatives could be identified which display different lifetimes when adjacent to each nucleotide. The DNA sequence could then be determined from the lifetimes observed for each band on the sequencing gel. The use of lifetime measurements in fluorescence sensing is described in Section 19.2.B, and DNA sequencing is described in Section 21.1.

8.6. DEVIATIONS FROM THE STERN–VOLMER EQUATION; QUENCHING SPHERE OF ACTION

Positive deviations from the Stern–Volmer equation are frequently observed when the extent of quenching is large. Two examples of upward-curving Stern–Volmer plots are shown in Figures 8.6 and 8.7 for acrylamide quenching of NATA and of the fluorescent steroid dihydroequilenin (DHE), respectively. The upward-curving Stern–Volmer plots could be analyzed in terms of the static and dynamic quenching constants (Eq. [8.19]). This analysis yields K_S values near 2.8 and 5.2 M^{-1} for acrylamide quenching of

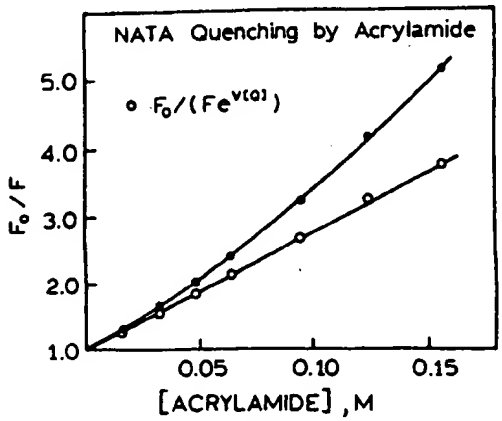

Figure 8.6. Acrylamide quenching of NATA in water. ●, F_0/F; ○, $F_0/(Fe^{V[Q]})$, where $V = 2.0\ M^{-1}$. Revised from Ref. 15.

NATA and DHE, respectively. These values imply that quencher concentrations near $0.3M$ are required to quench one-half of the fluorophores by a static process. Such a weak association suggests that the fluorophores and quenchers do not actually form a ground-state complex. Instead, it seems that the apparent static component is due to the quencher being adjacent to the fluorophore at the moment of excitation. These closely spaced fluorophore–quencher pairs are immediately quenched and thus appear to be dark complexes.

This type of apparent static quenching is usually interpreted in terms of a "sphere of action" within which the probability of quenching is unity. The modified form of the Stern–Volmer equation which describes this situation is

$$\frac{F_0}{F} = (1 + K_D[Q])\exp([Q]VN/1000) \qquad [8.24]$$

where V is the volume of the sphere.[21] The data in Figures 8.6 and 8.7 are consistent with a sphere radius near 10 Å, which is only slightly larger than the sum of the radii of

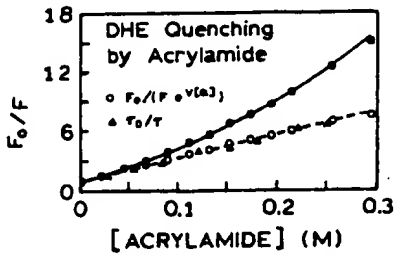

Figure 8.7. Acrylamide quenching of dihydroequilenin (DHE) in buffer containing 10% sucrose at 11 °C. ●, F_0/F; ▲, τ_0/τ; ○, $F_0/(Fe^{V[Q]})$, where $V = 2.4\ M^{-1}$. Revised and reprinted, with permission, from Ref. 20, Copyright © 1990, American Chemical Society.

the fluorophore and quencher. When the fluorophore and quencher are this close, there exists a high probability that quenching will occur before these molecules diffuse apart. As the quencher concentration increases, the probability increases that a quencher is within the first solvent shell of the fluorophore at the moment of excitation.

8.6.A. Derivation of the Quenching Sphere of Action

Assume the existence of a sphere of volume V within which the probability of immediate quenching is unity. Intuitively, if a fluorophore is excited when a quencher is immediately adjacent, then this fluorophore is quenched and is therefore unobservable. The only observable fluorophores are those for which there are no adjacent quenchers. The modified form of the Stern–Volmer equation (Eq. [8.24]) is derived by calculating the fraction of fluorophores which do not contain a quencher within their surrounding sphere of action.[21]

The Poisson probability distribution states that the probability of finding a volume V with n quenchers is

$$P(n) = \frac{\lambda^n}{n!}e^{-\lambda} \qquad [8.25]$$

where λ is the mean number of quenchers per volume V. The average concentration of quenchers (in molecules/cm^3) is given by $[Q]N/1000$, and hence the average number of molecules in the sphere is $\lambda = V[Q]N/1000$. Only those fluorophores without nearby quenchers are fluorescent. The probability that no quenchers are nearby is

$$P(0) = e^{-\lambda} \qquad [8.26]$$

Thus, the existence of the sphere of action reduces the proportion of observable fluorophores by the factor $\exp(-V[Q]N/1000)$, which in turn yields Eq. [8.24]. Division of the values of F_0/F by $\exp(V[Q]N/1000)$ corrects the steady-state intensities for this effect and reveals the dynamic portion of the observed quenching (Figures 8.6 and 8.7). For simplicity, the static term is often expressed in terms of reciprocal concentration.

8.7. EFFECTS OF STERIC SHIELDING AND CHARGE ON QUENCHING

The extent of quenching can be affected by the environment surrounding the fluorophore. One example is the quenching of the steroid DHE by acrylamide. When free in solution, DHE is readily quenched by acrylamide. How-

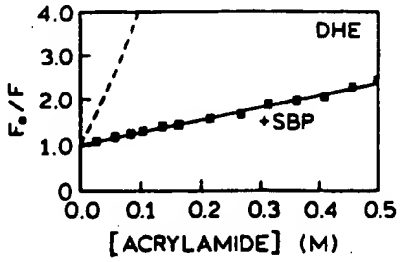

Figure 8.8. Acrylamide quenching of DHE when free in solution (---) and when bound to steroid binding protein (SBP; ■). Revised and reprinted, with permission, from Ref. 20, Copyright © 1990, American Chemical Society.

ever, when bound to a steroid binding protein (SBP), much less quenching occurs (Figure 8.8). In fact, the modest amount of quenching observed was attributed to dissociation of DHE from the protein.[20] Protection from quenching is frequently observed for probes bound to macromolecules[22,23] and even cyclodextrins.[24] In fact, binding of probes to cyclodextrins has been used as a means of obtaining room-temperature phosphorescence.[25] The macromolecules or cyclodextrins provide protection from the solvent but usually not complete protection from diffusing quenchers. Such solutions are usually purged to remove dissolved oxygen in order to observe phosphorescence.

The electronic charge on the quenchers can also have a dramatic effect on the extent of quenching (Figure 8.9). This is illustrated by quenching of 1-ethylpyrene (EP) in micelles, where the detergent molecules have different charges.[26] The quencher was *p*-*N*,*N*-dimethylaniline sulfonate (DMAS), which is negatively charged. The micelles were positively charged [dodecyltrimethylammonium chloride (DTAC)], neutral (Brij 35), or negatively charged [sodium dodecyl sulfate (SDS)]. There is extensive quenching of EP in the positively charged DTAC micelles, and essentially no quenching in the negatively charged SDS micelles. In general, one can expect charge effects to be present with charged quenchers such as iodide and to be absent for neutral quenchers like oxygen and acrylamide.

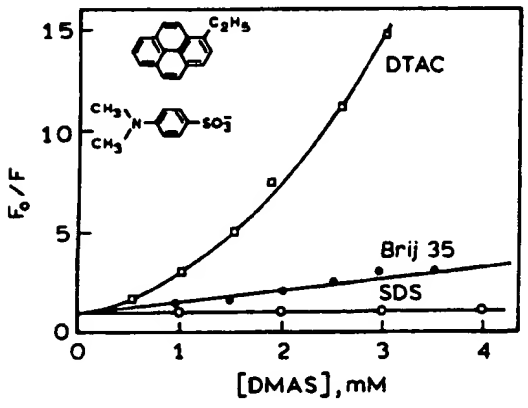

Figure 8.9. Quenching of 1-ethylpyrene (EP) by *p*-*N*,*N*-dimethylaniline sulfonate (DMAS), in positively charged micelles of dodecyltrimethylammonium chloride (DTAC), neutral micelles of Brij 35, or negatively charged micelles of sodium dodecyl sulfate (SDS). Revised from Ref. 26.

8.7.A. Accessibility of DNA-Bound Probes to Quenchers

The most dramatic effects of charge and shielding on quenching have been observed for fluorophores bound to DNA. One can expect the extent of quenching to be decreased by intercalation of probes into the DNA double helix. For instance, EB bound to DNA was found to be protected from oxygen quenching by a factor of 30 as compared to EB in solution.[14] Given the high negative charge density of DNA, one can expect the quenching to be sensitive to the charge of the quencher, the ionic strength of the solution, and the rate of quencher diffusion near the DNA helix.[27,28]

Collisional quenching by oxygen was used to study quenching of several DNA-bound probes.[29,30] Oxygen was chosen as the quencher because it is neutral and should thus be unaffected by the charge on the DNA. The probes were selected to have different sizes and different modes of binding to DNA (Figure 8.10). Proflavine intercalates into double-helical DNA and was expected to be protected from quenching. In fact, the bimolecular quenching constant was less than 10% of the diffusion-controlled rate

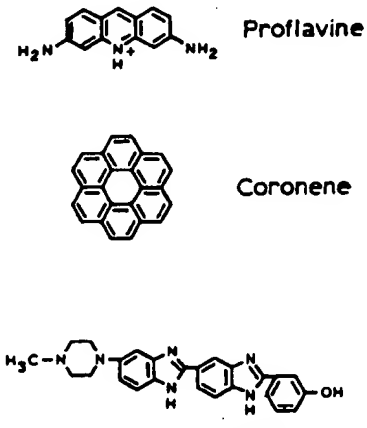

Figure 8.10. Structure of three probes bound to DNA (Table 8.2). From Ref. 30.

Table 8.2. Decay Times and Oxygen Quenching Constants of Probes Bound to DNA[a]

Fluorophore	Type of complex	τ_0 (ns)	k_q (M^{-1} s^{-1})
Proflavine	Intercalation	6.3	$<0.1 \times 10^{10}$
Coronene	Partial intercalation	225	0.17×10^{10}
Hoechst 33258	Minor groove	3.5	1.1×10^{10}

[a]Ref. 30.

(Table 8.2). The k_q value for proflavine may be smaller than shown, as there was little quenching under these experimental conditions. Hoechst 33258 is known to bind to the minor groove of DNA. Surprisingly, the k_q value for Hoechst 33258 bound to DNA was near the diffusion-controlled limit, suggesting complete accessibility by oxygen. The behavior of coronene was intermediate. Coronene is rather large and not able to fully fit into a DNA helix. The intermediate value of k_q, reflecting partial exposure to water, was explained as due to partial intercalation of coronene. These results illustrate how the extent of probe exposure can be correlated with the bimolecular quenching constant. Knowledge of the unquenched fluorescence lifetimes was essential for calculating the values of k_q from the Stern–Volmer quenching constants.

The extent of quenching can also be affected by the charge on the quenchers. This is illustrated by iodide quenching of Hoechst 33258 when free in solution and when bound to DNA (Figure 8.11). Hoechst 33258 is readily quenched by iodide when free in solution but is not quenched when bound to DNA. In the previous paragraph we saw that Hoechst 33258 bound to DNA was completely accessible to the neutral quencher oxygen. Apparently, the negative charges on DNA prevent iodide from coming into contact with Hoechst 33258 when bound to the minor groove of DNA.

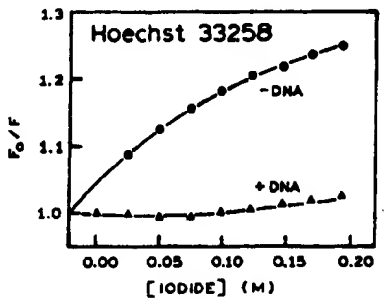

Figure 8.11. Iodide quenching of Hoechst 33258 in the absence (●) and presence (▲) of calf thymus DNA. The ionic strength was kept constant using KCl. Revised from Ref. 31.

8.7.B. Quenching of Ethenoadenine Derivatives

The nucleotide bases of DNA are mostly nonfluorescent. Fluorescent analogs of adenine nucleotides have been created by addition of an etheno bridge, the so-called ε-ATP derivatives (Chapter 3). Depending on the pH and extent of phosphorylation, the charge on the ethenoadenine nucleotides ranges from –3 for ε-ATP to 0 for ethenoadenosine. Hence, one expects the extent of quenching to depend on the charge of the quencher.

Stern–Volmer plots for the various ethenoadenine nucleotides are shown in Figure 8.12. For the neutral quencher acrylamide, there is no effect of charge. For the positively charged quencher Tl^+, the largest Stern–Volmer constant was observed for ε-ATP, with progressively smaller values as the number of negatively charged phosphates decreased. The opposite trend was observed for iodide quenching. Such effects of charge on quenching can be used to determine the local charge around fluorophores on proteins based on quenching by positive, neutral, and negatively charged quenchers.[32–34]

8.8. FRACTIONAL ACCESSIBILITY TO QUENCHERS

Proteins usually contain several tryptophan residues that are in distinct environments. Each residue can be differently accessible to quencher. Hence, one can expect complex Stern–Volmer plots and even spectral shifts due to selective quenching of exposed versus buried tryptophan residues. One example is quenching of lysozyme. This protein from egg white has six tryptophan residues, several of which are known to be near the active site. Lysozyme fluorescence was measured as a function of the concentration of trifluoroacetamide (TFA), which was found to be a collisional quencher of the fluorescence.[35] The Stern–Volmer plot curves downward toward the x-axis (Figure 8.13, left). As will be described below, this is a characteristic feature of two fluorophore populations, one of which is not accessible to the quencher. In the case of lysozyme, the emission spectrum shifts progressively to shorter wavelengths with increasing TFA concentration (Figure 8.13, right). This indicates that those tryptophan residues emitting at longer wavelengths are quenched more readily than the shorter-wavelength tryptophans.

The emission spectrum of the quenched residues can be calculated by taking the difference between the unquenched and quenched emission spectra. This difference spectrum (Figure 8.13, right) shows that the quenched residues display an emission maximum at 348 nm. The

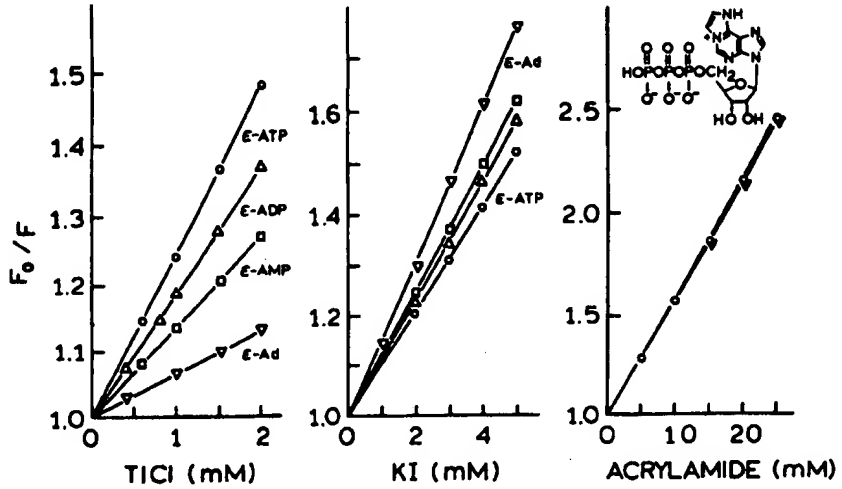

Figure 8.12. Quenching of (ε-ATP (○), ε-ADP (△), ε-AMP (□), and ε-Ad (▽) by Tl^+ (*left*), I^- (*middle*), and acrylamide (*right*) in 10m*M* phosphate buffer, 0.1*M* KCl, 20 °C, pH 7.0. Revised from Ref. 34.

protected residues display an emission maximum at 333 nm.

8.8.A. Modified Stern–Volmer Plots

The differing accessibilities of tryptophan residues in proteins have resulted in the frequent use of quenching to resolve the accessible and inaccessible residues.[36] Suppose that there are two populations of fluorophores, one being accessible (a) to quenchers and the other being inaccessible or buried (b). In this case the Stern–Volmer plot will display downward curvature (Figure 8.13). The total fluorescence in the absence of quencher (F_0) is given by

$$F_0 = F_{0a} + F_{0b} \qquad [8.27]$$

where the 0 subscript once again refers to the fluorescence intensity in the absence of quencher. In the presence of quencher, the intensity of the accessible fraction (f_a) is decreased according to the Stern–Volmer equation, whereas the buried fraction is not quenched. Therefore, the observed intensity is given by

$$F = \frac{F_{0a}}{1 + K_a[Q]} + F_{0b} \qquad [8.28]$$

where K_a is the Stern–Volmer quenching constant of the accessible fraction and [Q] is the concentration of quencher. Subtraction of Eq. [8.28] from Eq. [8.27] yields

$$\Delta F = F_0 - F = F_{0a}\left(\frac{K_a[Q]}{1 + K_a[Q]}\right) \qquad [8.29]$$

Inversion of Eq. [8.29] followed by division into Eq. [8.27] yields

$$\frac{F_0}{\Delta F} = \frac{1}{f_a K_a[Q]} + \frac{1}{f_a} \qquad [8.30]$$

where f_a is the fraction of the initial fluorescence which is accessible to quencher,

$$f_a = \frac{F_{0a}}{F_{0b} + F_{0a}} \qquad [8.31]$$

This modified form of the Stern–Volmer equation allows f_a and K_a to be determined graphically (Figure 8.14). A plot

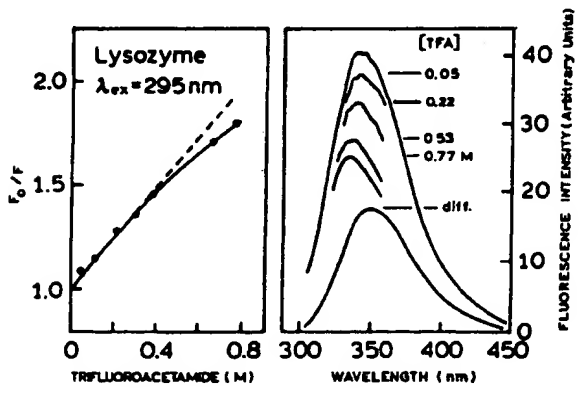

Figure 8.13. Quenching of lysozyme by trifluoroacetamide (TFA). *Left*: Stern–Volmer plot. *Right*: Emission spectra with increasing concentrations of TFA. Also shown is the difference spectrum (diff), 0.0*M* – 0.77*M* TFA. Revised and reprinted from Ref. 35, Copyright © 1984, with permission from Elsevier Science.

of $F_0/\Delta F$ versus 1/[Q] yields f_a^{-1} as the intercept and $(f_aK_a)^{-1}$ as the slope. A y-intercept of f_a^{-1} may be understood intuitively. The intercept represents the extrapolation to infinite quencher concentration (1/[Q] = O). The value of $F_0/(F_0 - F)$ at this quencher concentration represents the reciprocal of the fluorescence which was quenched. At high quencher concentration, only the inaccessible residues will be fluorescent.

In separation of the accessible and inaccessible fractions of the total fluorescence, it should be realized that there may be more than two classes of tryptophan residues. Also, even the presumed "inaccessible" fraction may be partially accessible to quencher. This possibility is illustrated by the dashed curves in Figure 8.14, which show the expected result if the Stern–Volmer constant for the buried fraction (K_b) is one-tenth of that for the accessible fraction ($K_b = 0.1K_a$). For a limited range of quencher concentrations, the modified Stern–Volmer plot can still appear to be linear. The extrapolated value of f_a would represent an apparent value somewhat larger than seen with $K_b = 0$. Hence, the modified Stern–Volmer plots provide a useful but arbitrary resolution of two assumed classes of tryptophan residues.

8.8.B. Experimental Considerations in Quenching

Although quenching experiments are straightforward, there are several potential problems. One should always examine the emission spectra under conditions of maximum quenching. As the intensity is decreased, the contribution from background fluorescence may begin to be significant. Quenchers are often used at high concentrations, and the quenchers themselves may contain fluorescent impurities. Also, the intensity of the Raman and Rayleigh scatter peaks is independent of quencher concentration. Hence, the relative contribution of scattered light always increases with quenching.

It is also important to consider the absorption spectra of the quenchers. Iodide and acrylamide absorb light below 290 nm. The inner filter effect due to their absorption can decrease the apparent fluorescence intensity and thereby distort the quenching data. Regardless of the quencher being used, it is important to determine if the inner filter effects are significant. If inner filter effects are present, the observed fluorescence intensities must be corrected. The lifetime measurements are mostly independent of inner filter effects because these measurements are relatively independent of total intensity.

When iodide or other ionic quenchers are used, it is important to maintain a constant ionic strength. This is usually accomplished by addition of KCl. When iodide is used, it is also necessary to add a reducing agent such as $Na_2S_2O_3$. Otherwise, I_2 is formed, which is reactive and can partition into the nonpolar regions of proteins and membranes.

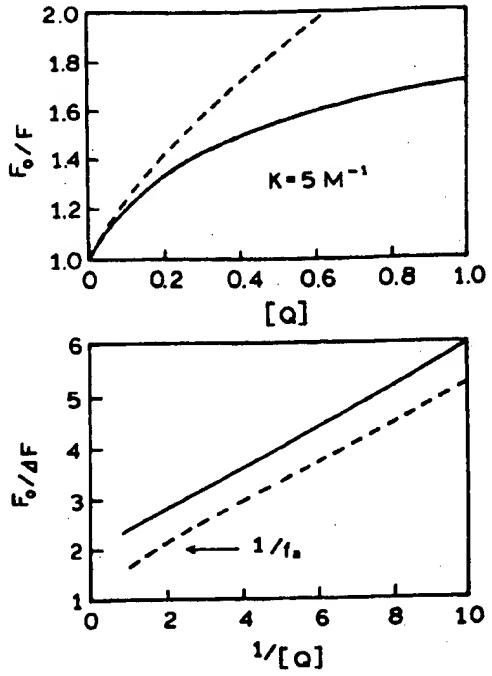

Figure 8.14. Stern–Volmer (*top*) and modified Stern–Volmer plots (*bottom*) for two populations of fluorophores, one of which is inaccessible to quencher. The dashed curves show the effect of the "inaccessible" population being quenched with a K value one-tenth of that for the accessible population.

8.9. APPLICATIONS OF QUENCHING TO PROTEINS

8.9.A. Fractional Accessibility of Tryptophan Residues in Endonuclease III

Since the pioneering study of lysozyme quenching,[36] there have been numerous publications on determining the fraction of protein fluorescence accessible to quenchers.[37–41] In Section 16.5 we show that proteins in the native state often display a fraction of the emission which is not accessible to water-soluble quenchers and that denaturation of the proteins usually results in accessibility of all the tryptophan residues to quenchers. The possibility of buried and exposed residues in a single protein is illustrated by endonuclease III (endo III). Endo III is a DNA repair enzyme which displays both *N*-glycosylase and apurinine/apyrimidinic lyase activities. The structure of

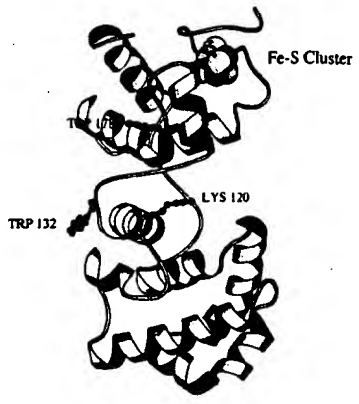

Figure 8.15. Structure of endo III, showing the exposed residue trp-132 and the buried residue trp-178 near the iron–sulfur cluster. Courtesy of Dr. Charles P. Scholes.

endo III shows two domains, with the DNA binding site in the cleft region. Endo III contains two tryptophan residues.[40] Trp-132 is exposed to the solvent, and trp-178 is buried in one of the domains (Figure 8.15). Hence, one expects these residues to be differently accessible to water-soluble quenchers.

The modified Stern–Volmer plot for quenching of endo III by iodide shows clear evidence for a shielded fraction (Figure 8.16). Extrapolation to high iodide concentrations yields an intercept near 2, indicating that only half of the emission can be quenched by iodide. This suggests that both trp residues in endo III are equally fluorescent and that only one residue (trp-132) can be quenched by iodide. Similar results have been obtained for a large number of proteins, and the extent of quenching is known to depend on the size and polarity of the quenchers.[6,7] Quenching of solvent-exposed residues in proteins is now a standard tool in the characterization of proteins.

8.9.B. Effect of Conformational Changes on Tryptophan Accessibility

The conformational state of a protein can have an influence on the exposure of its tryptophan residues to solvent. This is illustrated by the cyclic AMP receptor protein (CRP) from *Escherichia coli*.[41] This protein regulates the expression of over 20 genes in *E. coli*. CRP consists of two identical polypeptide chains, each containing 209 amino acids. It contains two nonidentical trp residues at positions 13 and 85.

Stern–Volmer plots for the quenching of CRP by acrylamide in the absence and in the presence of bound cyclic AMP (cAMP) are shown in Figure 8.17. In the absence of cAMP, the Stern–Volmer plot shows obvious downward curvature, indicating that one of the trp residues is inaccessible or only slightly accessible to acrylamide. Binding of cAMP results in a dramatic change in the Stern–Volmer plot, which becomes linear. Apparently, binding of cAMP to the CRP causes a dramatic conformational change which results in exposure of the previously shielded trp residue. Changes in accessibility due to conformational changes have been reported for other proteins.[42] Binding of substrates to proteins can also result in shielding of tryptophan, as has been observed for lysozyme[36] and for wheat germ agglutinin.[35]

8.9.C. Quenching of the Multiple Decay Times of Proteins

The intensity decays of proteins are typically multiexponential. Hence, it is natural to follow the individual decay times as the protein is exposed to increasing concentrations of quencher. One example is provided by the investigation of the CRP protein just described.[41] FD data for its intrinsic tryptophan emission yield decay times near 1.5 and 6.8 ns.

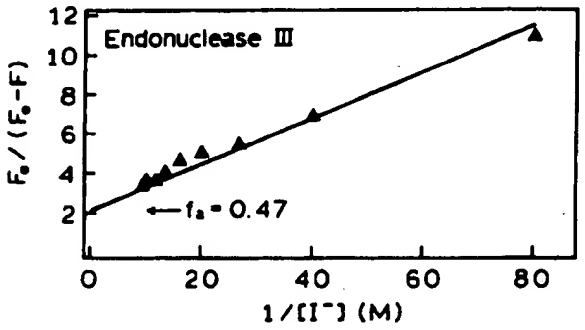

Figure 8.16. Modified Stern–Volmer plot for iodide quenching of endo III, showing evidence for two types of tryptophan residues. The inaccessible fraction is $f_a = 0.47$. Revised from Ref. 40.

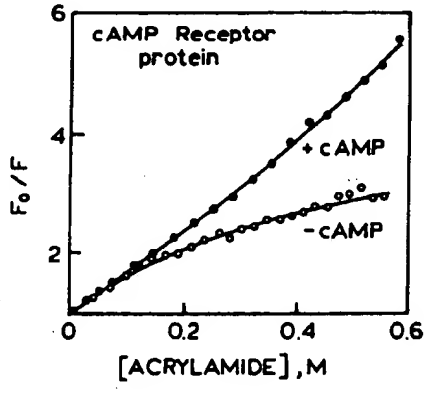

Figure 8.17 Stern–Volmer plot for acrylamide quenching of cAMP receptor protein in the absence (○) and in the presence (●) of cAMP. Revised from Ref. 41.

Similar decay times were observed in the absence and the presence of bound cAMP. For the protein without bound cAMP, the shorter decay time did not change with increasing iodide concentration (Figure 8.18, top), whereas the long lifetime decreased. This indicates that the 6.8-ns component is due to the exposed trp residue. The 1.5-ns component is not quenched by iodide and is assigned to the buried trp residue. In the presence of bound cAMP, both decay times are seen to decrease in the presence of iodide, indicating that both are quenched (Figure 8.18, bottom). These results agree with the linear Stern–Volmer plot found for CRP with bound cAMP (Figure 8.17).

While the results presented in Figure 8.18 show a clear separation of decay times, caution is needed when interpreting decay times in the presence of quencher. For many proteins, the decay times will be closer than 1.5 and 6.8 ns, and the decay time for each trp residue can depend on emission wavelength. Hence, it may not be possible to assign a unique decay time to each tryptophan residue. Additionally, collisional quenching results in nonexponential decays, even if the fluorophore shows a single decay time in the absence of quencher. This change in the intensity decay is due to transient effects in quenching, which are due to the rapid quenching of closely spaced flourophore–quencher pairs, followed by a slower quenching rate due to quencher diffusion. The presence of transient effects results in additional nanosecond decay times. The apparent lifetimes for each residue will be weighted averages that depend on the method of measurement. The assignment of decay times to trp residues in the presence of quenching can be ambiguous. Transient effects in quenching are described in the following chapter.

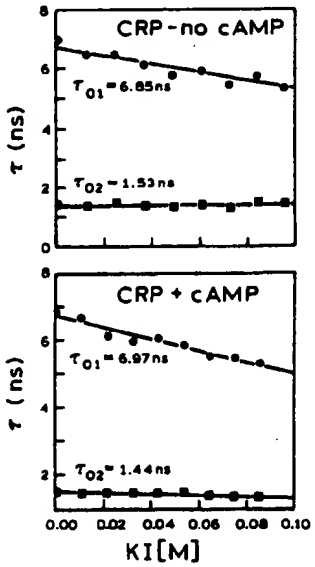

Figure 8.18. Iodide-dependent decay times of CRP in the absence (*top*) and in the presence (*bottom*) of bound cAMP. Revised from Ref. 41.

8.9.D. Effects of Quenchers on Proteins

When one performs quenching experiments, it is important to consider whether the quencher has an adverse effect on the protein. Some quenchers, such as 2,2,2-trichloroethanol, are known to bind to proteins and induce conformational changes.[43] For a time it was thought that acrylamide bound to proteins, but it is now accepted that such binding does not occur except in several specific cases.[44–46] However, even the nonperturbing quencher acrylamide can affect certain proteins, as was found for glyceraldehyde-3-phosphate dehydrogenase (GAPDH).[47] This protein contains three tryptophan residues in each subunit of the tetrameric enzyme. Quenching of the apoenzyme, which lacks NAD^+, by acrylamide yields a Stern–Volmer plot that is highly unusual. The extent of quenching increases rapidly above 0.4*M* acrylamide (Figure 8.19). This effect is not seen for the holoenzyme, which contains bound NAD^+. Acrylamide also caused a slow loss of activity and reduction in the number of thiol groups. Acrylamide appears to bind to GAPDH, reacting with the protein and destroying its activity.

8.9.E. Protein Folding of Colicin E1 • Advanced Topic •

Colicin E1 is a 522-residue polypeptide which is lethal to strains of *E. coli* that do not contain the resistance plasmid. Colicin E1 exerts its toxic effects by forming a channel in the cytoplasmic membrane which depolarizes and deenergizes the cell. The active channel-forming domain consists

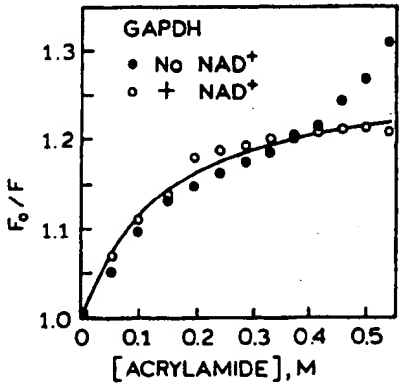

Figure 8.19. Acrylamide quenching of GAPDH in the absence (•) and in the presence (o) of the cofactor NAD^+. Revised from Ref. 47.

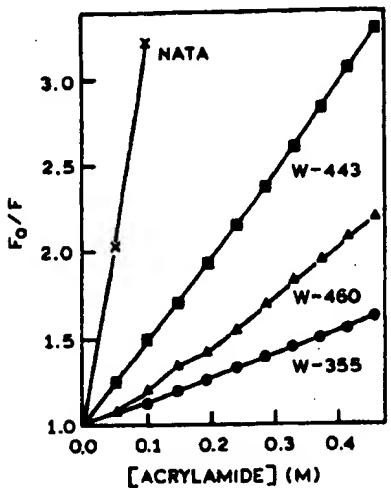

Figure 8.20. Stern–Volmer plots for acrylamide quenching of NATA (x) and three single-tryptophan mutants of the channel-forming peptide of colicin E1, W-355 (●), W-460 (▲), and W-443 (■). Revised from Ref. 48.

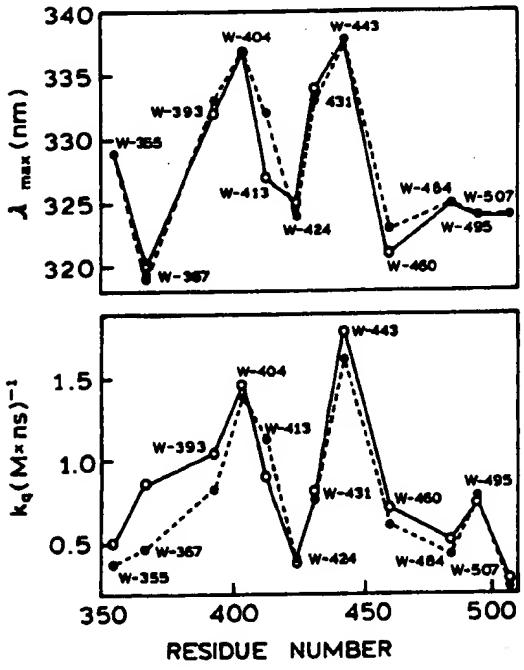

Figure 8.21. Emission maxima (*top*) and bimolecular quenching constants (*bottom*) of 12 single-tryptophan mutants of the channel-forming peptide of colicin E1. Revised and reprinted, with permission, from Ref. 48, Copyright © 1993, American Chemical Society.

of about 200 residues from the carboxy terminus, which form 10 α-helices spanning the membrane.

The conformation of the membrane-bound form of the colicin E1 channel peptide was studied by acrylamide quenching.[48] Twelve single-tryptophan mutants were formed by site-directed mutagenesis. The tryptophan residues were mostly conservative replacements, meaning that the trp residues were placed in positions previously containing phenylalanine or tyrosine. Stern–Volmer plots for acrylamide quenching of three of these mutant proteins and of NATA are shown in Figure 8.20. The accessibility to acrylamide quenching is strongly dependent on the location of the residue, and all residues are shielded relative to NATA. Depending on position, the trp residues also showed different emission maxima (Figure 8.21). The acrylamide bimolecular quenching constants were found to closely follow the emission maxima, with lower values of k_q for the shorter-wavelength tryptophans. Such data can be used to suggest a folding pattern for the channel-forming peptide and to reveal conformational changes that occur upon pH activation of colicin E1.

8.10. QUENCHING-RESOLVED EMISSION SPECTRA
• Advanced Topic •

8.10.A. Fluorophore Mixtures

As shown in Section 8.8, the emission spectra of proteins often shift in the presence of quenching. This effect occurs because the various trp residues are differently sensitive to quenching. Stated alternatively, for a mixture of fluorophores, quenching is expected to be dependent on the observation wavelength. This concept has been extended to calculation of the underlying emission spectra from the wavelength-dependent quenching data.[49–54] This is accomplished by measuring a Stern–Volmer plot for each emission wavelength (λ). For more than one fluorophore, the wavelength-dependent data can be described by

$$\frac{F(\lambda)}{F_0(\lambda)} = \sum_i \frac{f_i(\lambda)}{1 + K_i(\lambda)[Q]} \qquad [8.32]$$

where $f_i(\lambda)$ is the fractional contribution of the ith fluorophore to the steady-state intensity at wavelength λ, and $K_i(\lambda)$ is the Stern–Volmer quencher constant of the ith species at λ. For a single fluorophore, the quenching constant is usually independent of emission wavelength, i.e., $K_i(\lambda) = K_i$.

In order to resolve the individual emission spectra, the data are analyzed by nonlinear least-squares analysis.

Typically, one performs a global analysis in which the K_i values are global, and the $f_i(\lambda)$ values are variable at each wavelength. The result of the analysis is a set of K_i values, one for each component, and the fractional intensities $f_i(\lambda)$ at each wavelength, with $\sum f_i(\lambda) = 1.0$. The values of $f_i(\lambda)$ are used to calculate the emission spectrum of each component,

$$F_i(\lambda) = f_i(\lambda)F(\lambda) \qquad [8.33]$$

where $F(\lambda)$ is the steady-state emission spectrum of the sample.

The use of quenching-resolved spectra is illustrated by a sample containing both DPH and 5-((((2-iodoacetyl)amino)ethyl)amino)naphthalene-1-sulfonic acid (IAEDANS). These fluorophores were studied in SDS micelles, where their emission spectra are distinct (Figure 8.22). DPH is not soluble in water, so all the DPH is expected to be dissolved in the SDS micelles. IAEDANS is water-soluble and negatively charged, so it is not expected to bind to the negatively charged SDS micelles. Hence, IAEDANS is expected to be quenched by the water-soluble quencher acrylamide, and DPH is not expected to be accessible to acrylamide quenching.

Stern–Volmer plots for acrylamide quenching of the DPH–IAEDANS mixture as well as the individual fluorophores are shown in Figure 8.23. As predicted from the solubilities of the probes and acrylamide in water, DPH is weakly quenched by acrylamide. In contrast, IAEDANS is strongly quenched. The extent of quenching for the mixture is intermediate between that observed for each probe alone. As expected for a mixture of fluorophores, the

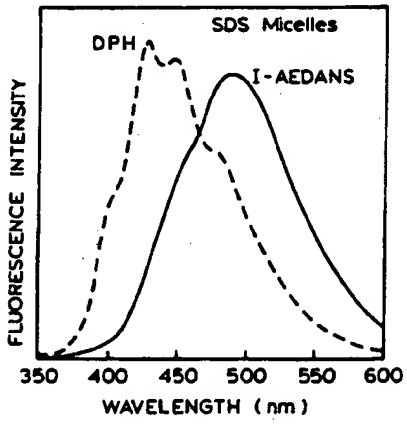

igure 8.22. Steady-state emission spectra of DPH (---) and IAEDANS —) in 1.2m*M* SDS micelles at 23 °C. The concentration of DPH was μ*M*, and that of IAEDANS was 170μ*M*. The excitation wavelength was 37 nm. Revised from Ref. 49.

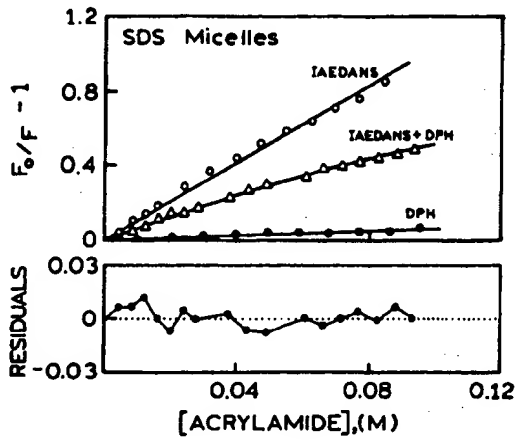

Figure 8.23. Stern–Volmer plots for acrylamide quenching of IAEDANS (○), DPH (●), and IAEDANS and DPH (△) in SDS micelles. For the mixture, the solid line represents the fit with calculated parameters $K_1 = 9.9\,M^{-1}$, $K_2 = 0\,M^{-1}$, $f_1 = 0.69$, and $f_2 = 0.31$ at 473 nm. The lower panel shows the residuals for this fit. Revised from Ref. 49.

Stern–Volmer plot curves downward due to the increasing fractional contribution of the more weakly quenched species at higher quencher concentrations.

The curvature in the Stern–Volmer plots was used to recover the values of $K_i(\lambda)$ and $f_i(\lambda)$ at each wavelength. In this case the $K_i(\lambda)$ values were not used as global parameters, so that $K_1(\lambda)$ and $K_2(\lambda)$ were obtained for each wavelength. At all wavelengths, there were two values near $0.5M^{-1}$ and $9.5M^{-1}$, representing the quenching constants of DPH and IAEDANS, respectively. At the shortest wavelength, below 420 nm, there is only one $K_i(\lambda)$ value because only DPH emits. The recovered values of $f_i(\lambda)$ were used to calculate the individual spectra from the spectrum of the mixture (Figure 8.24). In Chapters 4 and 5 we saw how the component spectra for heterogeneous samples could be resolved using the TD or the FD data. The use of wavelength-dependent quenching provides similar results, without the use of complex instrumentation. Of course, the method depends on the probes being differently sensitive to collisional quenching, which normally occurs if the decay times are different.

8.10.B. Quenching-Resolved Emission Spectra of the *E. coli* Tet Repressor

The Tet repressor from *E. coli* is a DNA-binding protein which controls the expression of genes that confer resistance to tetracycline. This protein contains two tryptophan residues at positions 43 and 75. W43 is thought to be an exposed residue, and W75 is thought to be buried in the protein matrix.[54] Earlier studies of single-tryptophan mu-

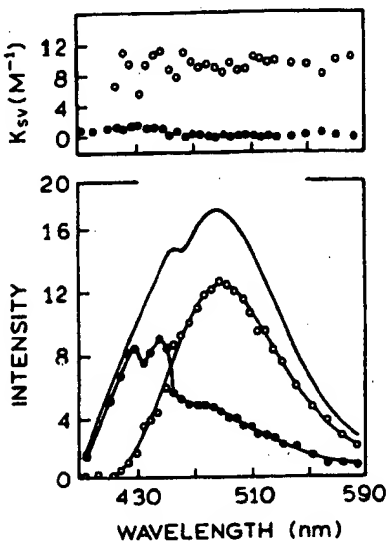

Figure 8.24. *Bottom*: Emission spectrum of the DPH–IAEDANS mixture and quenching-resolved emission spectra of DPH (●) and IAEDANS (○). *Top*: Wavelength dependence of the quenching constants, with average values of $K_1 = 9.6\ M^{-1}$ and $K_2 = 0.47\ M^{-1}$. Revised from Ref. 49.

tants of the Tet repressor confirmed the accessibility of W43 to iodide and the shielding of W75 from iodide quenching.[55] Hence, this protein provided an ideal model protein with which to attempt quenching resolution of the individual emission spectra of two tryptophan residues in a protein.

Stern–Volmer plots for iodide quenching of the Tet repressor were measured for various emission wavelengths[54] (Figure 8.25). A larger amount of quenching was observed for longer wavelengths. When the quenching data were analyzed in terms of two components, one of these components was found to be almost inaccessible to iodide. For instance, at 324 nm the recovered values are $f_1 = 0.34$, $K_1 = 16.2\ M^{-1}$, $f_2 = 0.66$, and $K_2 = 0$. The wavelength-dependent data were used to calculate the individual spectra (Figure 8.26). The blue-shifted spectrum with a maximum at 324 nm corresponds to the inaccessible fraction, and the red-shifted spectrum with a maximum at 349 nm is the fraction accessible to iodide quenching. These emission spectra are assigned to W-75 and W-43, respectively.

The results in the top panel of Figure 8.26 illustrate one difficulty often encountered in the determination of quenching-resolved spectra. The quenching constant for a single species can be dependent on emission wavelength. In this case the quenching constant of the accessible tryptophan changed about twofold across its emission spectrum. When this occurs, the values of $K_i(\lambda)$ cannot be treated as global parameters.

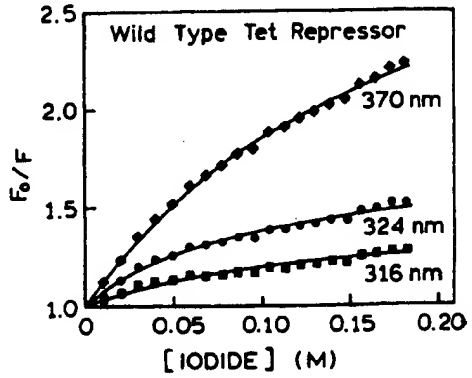

Figure 8.25. Stern–Volmer iodide plots for iodide quenching of the wild-type Tet repressor. The emission wavelengths are indicated on the figure. The solution contained 1 m*M* sodium thiosulfate to prevent formation of I_3^-. From Ref. 54.

The assignments of the quenching-resolved spectra are consistent with the results obtained using single-tryptophan mutants of the Tet repressor[55] (Figure 8.27). Little, if any, quenching was observed for the protein containing only W-75, and W-43 was readily quenched by iodide. Iodide quenching of the wild-type protein is intermediate between that of the two single-tryptophan mutants. While

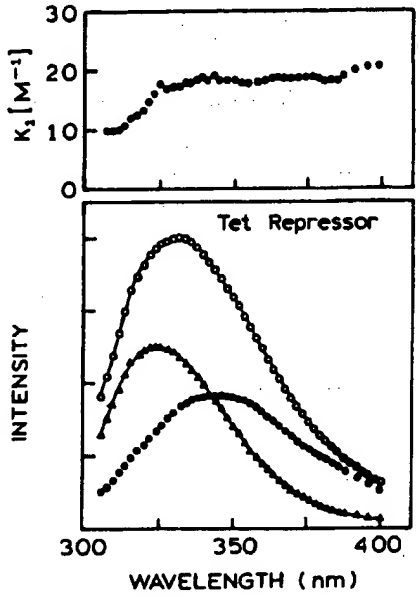

Figure 8.26. *Bottom*: Fluorescence quenching-resolved spectra of wild-type Tet repressor, obtained using potassium iodide as the quencher. *Top*: Wavelength-dependent values of K_1. From Ref. 54.

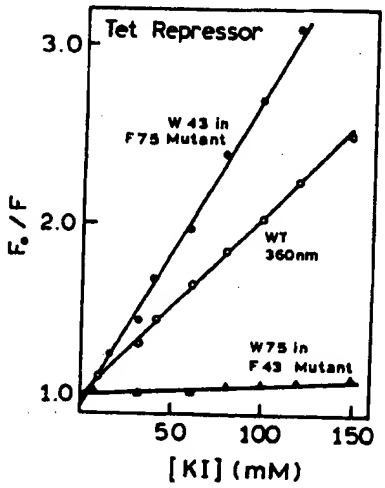

Figure 8.27. Stern–Volmer plots for the iodide quenching of *E. coli* Tet repressor (wild type, WT) and its mutants (F43 and F75). Revised from Ref. 55.

the same information is available from the mutant proteins, the use of quenching provided the resolved spectra with the use of only the wild-type protein.

It is valuable to notice a difference in the method of data analysis for the modified Stern–Volmer plots (Section 8.8.A) and for the quenching-resolved emission spectra. In analyzing a modified Stern–Volmer plot, one assumes that a fraction of the fluorescence is totally inaccessible to quenchers. This may not be completely true because one component can be more weakly quenched, but still quenched to some extent. If possible, it is preferable to analyze the Stern–Volmer plots by nonlinear least-squares analysis when the f_i and K_i values are variable. With this approach, one allows each component to contribute to the data according to its fractional accessibility, instead of forcing one component to be an inaccessible fraction. Of course, such an analysis is more complex, and the data may not be adequate to recover the values of f_i and K_i at each wavelength.

8.11. QUENCHING AND ASSOCIATION REACTIONS

8.11.A. Quenching Due to Specific Binding Interactions

In the preceding sections we considered quenchers that were in solution with the macromolecule but did not display any specific interactions. Such interactions can occur and can appear to be of static quenching.[56–59] One example is provided by serum albumin. Serum albumin consists of a single polypeptide chain, with a molecular weight near 65,000. Albumin is present in high concentrations in blood serum, 35–45 mg/ml, and is important for maintaining osmotic balance and for transport of hydrophobic species. Albumins have hydrophobic sites which are known to bind fatty acids and many fluorescent probes. Human serum albumin (HSA) has a single tryptophan residue, and bovine serum albumin (BSA) has two tryptophan residues.

BSA and HSA can bind halogenated anesthetics. This binding is seen by the effect of chloroform ($CHCl_3$) on the fluorescence intensity of BSA (Figure 8.28). Addition of $CHCl_3$ is seen to result in a progressive decrease in the fluorescence intensity of BSA. In the paper in which these results were reported,[58] there was no mention of photochemical effects, which we found surprising; in our experience, excitation of tryptophan in the presence of $CHCl_3$ results in the formation of blue fluorescent species.

The dependence of the BSA emission on the $CHCl_3$ concentration is shown in Figure 8.29 along with the effects of $CHCl_3$ on the emission of tryptophan and another protein, apomyoglobin. The effect of $CHCl_3$ on BSA is greater than that seen for trp or apomyoglobin, suggesting a specific interaction with BSA. The fact that there is hydrophobic binding of $CHCl_3$ to BSA is shown by the effect of trifluoroethanol (TFE), which disrupts hydrophobic binding. In 50% TFE, $CHCl_3$ no longer quenches BSA to the extent seen in water.

How can one determine whether the quenching seen for BSA in water is due to $CHCl_3$ binding or to collisional quenching? One method is to calculate the apparent bimolecular quenching constant (k_q^{app}). Assume that the decay time of BSA is near 5 ns. The data in Figure 8.29 indicate a K_{SV} value of 400 M^{-1}. The fluorescence is 50% quenched at 2.5mM $CHCl_3$. These values correspond to a bimolecular quenching constant of $k_q^{app} = 8 \times 10^{10}\ M^{-1}\ s^{-1}$, which is about 10-fold larger than the maximum value possible for diffusion-limited quenching

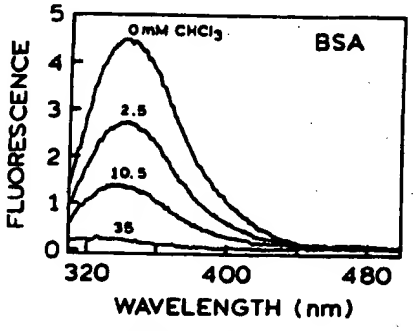

Figure 8.28. Emission spectra of BSA in the presence of various concentrations of chloroform. Revised from Ref. 58.

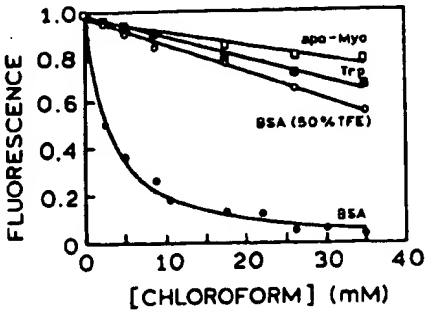

Figure 8.29. Fluorescence intensities of BSA (●), tryptophan (■), and apomyoglobin (□) in the presence of various amounts of dissolved $CHCl_3$. ○, BSA in 50% trifluoroethanol (TFE), which disrupts hydrophobic binding to BSA. Revised from Ref. 58.

in water. Hence, there must be some interaction that increases the local concentrations of $CHCl_3$ around the trp residues in BSA. Since there is no reason to expect ground-state complex formation between trp and $CHCl_3$, the quenching may be dynamic. However, the $CHCl_3$ is probably bound in close proximity to the trp residues, giving the appearance of a dark complex.

Another example of quenching due to a specific binding interaction is shown in Figure 8.30 for binding of caffeine to HSA, an experiment most of us start each morning. The Stern–Volmer plots show a value of $K_{SV} = 7150\ M^{-1}$. This value is obviously too large to be due to collisional quenching, especially for a lifetime near 5 ns. The value of k_q^{app} is $1.4 \times 10^{12}\ s^{-1}$, over 100-fold larger than the maximum diffusion-limited rate. Hence, the caffeine must be bound to the HSA. Caffeine is an electron-deficient molecule and may form ground-state complexes with indole. This possibility could be tested by examination of the absorption spectra of HSA in the absence and presence of caffeine. If ground-state association with indole occurs, then the trp absorption spectrum is expected to change. Another indicator of complex formation is the temperature dependence

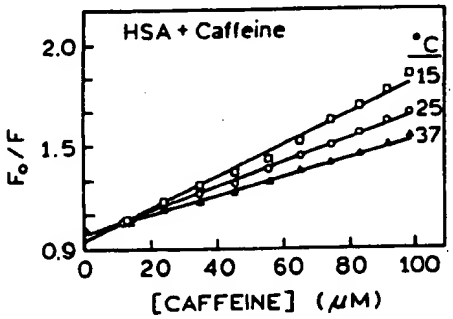

Figure 8.30. Quenching of HSA by caffeine at three temperatures. Revised from Ref. 59.

of the Stern–Volmer plots. For diffusive quenching, one expects more quenching at higher temperatures. In the case of HSA and caffeine, there is less quenching at higher temperatures (Figure 8.30), which suggests that the complex is less stable at higher temperatures.

8.11.B. Binding of Substrates to Ribozymes

The catalytic properties of highly structured RNAs have been the subject of numerous studies since 1982, when it was first reported that certain RNAs, termed ribozymes, could display enzymatic activity. One example is the hairpin ribozyme, which cleaves single-stranded RNA (Figure 8.31). The early observations of quenching by nucleotides[17,18] (Section 8.5) provided the opportunity to study substrate binding to ribozymes. The substrate contained a fluorescein residue covalently linked at the 3′-end. The hairpin ribozyme contains a guanosine residue at the 5′-end. Upon binding of substrate nucleotide to the ribozyme, the fluorescein emission is quenched (Figure 8.32). Quenching also occurs when the fluorescein-labeled substrate binds to the substrate-binding strand (SBS) which contains a 5′-guanosine residue (G-SBS). The guanosine residue is needed for quenching, and the emission of fluorescein is unchanged in the presence of the substrate-binding strand without a 5′-terminal guanosine residue (not shown in Figure 8.32). This example shows how

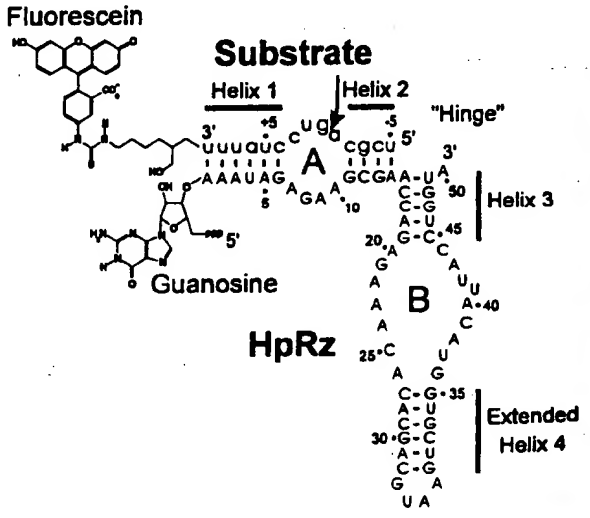

Figure 8.31. Structure of the hairpin ribozyme (HpRz) and the fluorescein-labeled substrate. The substrate-binding strand is the region adjacent to the substrate. Reprinted, with permission, from Ref. 60, Copyright © 1997, Cambridge University Press.

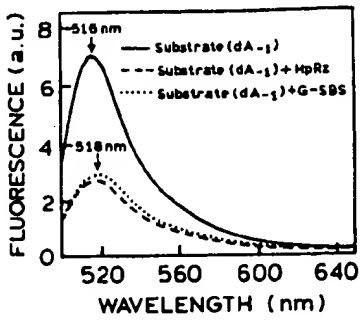

Figure 8.32. Emission spectra of the fluorescein-labeled substrate analog (dA_{-1}) in solution and when bound to the hairpin ribozyme (HpRz) or the guanosine-containing substrate-binding strand (G-SBS). From Ref. 60.

fundamental studies of nucleotide quenching have found useful applications in modern biochemistry.

8.11.C. Association Reactions and Quenching

Fluorescence is often used to measure association reactions. This requires that the fluorescence of one of the reactants changes upon binding. While this often occurs, it is not always the case. One example is the binding of ε-ADP to the DnaB helicase hexamer. The fluorescence of ε-ADP displayed only a small increase upon binding to the protein. Collisional quenching was used to induce a larger change in fluorescence on binding.[61] Acrylamide is an efficient quencher of ε-ADP, which should be quenched more strongly in solution than when bound to the helicase. Hence, if the binding is studied in a solution which contains acrylamide, there should be an increase in ε-ADP fluorescence on binding to the helicase.

Solutions of ε-ADP were titrated with the helicase (Figure 8.33). In the absence of acrylamide, there was little change in the ε-ADP fluorescence. The titrations were performed again, in solutions with increasing amounts of acrylamide. Under these conditions, ε-ADP showed an increase in fluorescence upon binding. This increase occurred because the ε-ADP became shielded from acrylamide upon binding to helicase. The authors also showed that acrylamide had no effect on the affinity of ε-ADP for helicase.[61] In this system the use of a quencher allowed measurement of a binding reaction that would otherwise be difficult to measure.

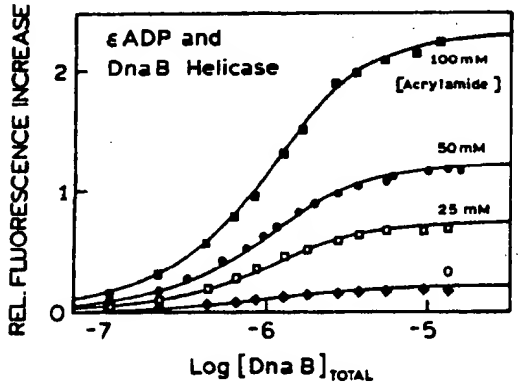

Figure 8.33. Fluorescence titration of ε-ADP, at a constant concentration of nucleotide, with the DnaB helicase in buffer containing different concentrations of acrylamide. Revised and reprinted from Ref. 61, Copyright © 1997, with permission from Elsevier Science.

8.12. INTRAMOLECULAR QUENCHING

Quenching can also occur between covalently linked fluorophore–quencher pairs.[62,63] One common example is the formation of exciplexes by covalently linked aromatic hydrocarbons and amines.[64,65] Another example is the covalent adduct formation by indole and acrylamide. For example, the lifetime of *N*-acetyltryptamine is near 5.1 ns. When the acetyl group is replaced by an acryloyl group, the lifetime is reduced to 31 ps (Figure 8.34). Similarly, covalent attachment of spin labels to a naphthalene derivative reduced its lifetime from 33.7 to 1.1 ns.

The concept of intramolecular quenching can be used to obtain structural information[66] as was demonstrated for a

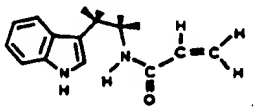

τ = 31 ps

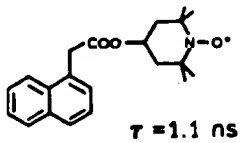

τ = 1.1 ns

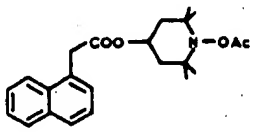

τ = 33.7 ns

Figure 8.34. Fluorophore–quencher conjugates which display intramolecular quenching.[62,63]

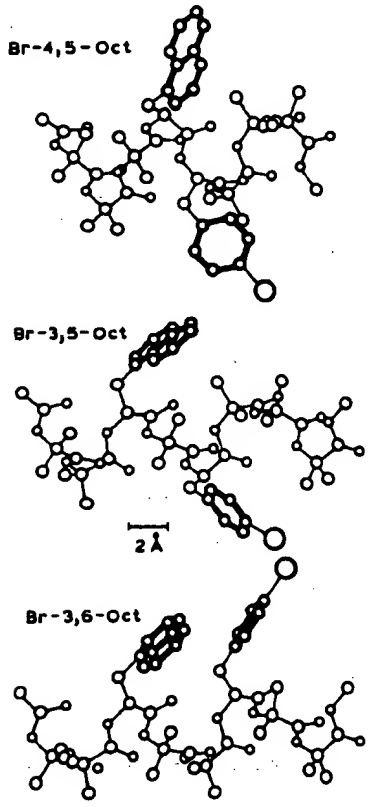

Figure 8.35. Structure of peptides containing naphthylalanine and *p*-bromophenylalanine, separated by 0 (*top*), 1 (*middle*), or 2 (*bottom*) amino acid residues. Revised and reprinted, with permission, from Ref. 66, Copyright © 1993, American Chemical Society.

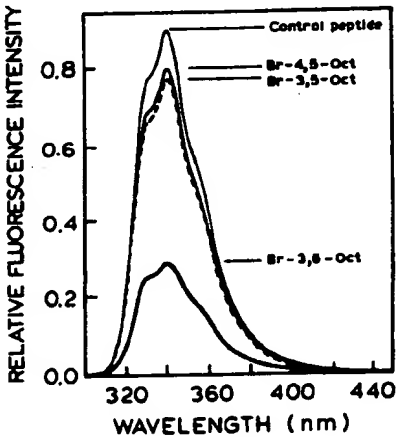

Figure 8.36. Emission spectra of the peptides shown in Figure 8.45. Also shown is the emission spectrum of a control peptide with a phenylalanine group in place of *p*-bromophenylalanine. Revised and reprinted, with permission, from Ref. 66, Copyright © 1993, American Chemical Society.

series of peptides containing a naphthylalanine fluorophore and a *p*-bromophenylalanine quencher (Figure 8.35). The probe and quencher were separated by 0, 1, or 2 amino acid residues. Emission spectra of these peptides show minimal quenching except for separation by 2 amino acid residues (Figure 8.36). In this case the fluorophore and quencher are adjacent, resulting in over 50% quenching of the naphthylalanine. These results suggest that, in solution, this peptide adopts a conformation with the bromo group near the indole ring.

8.13. QUENCHING OF PHOSPHORESCENCE

Phosphorescence is not usually observed in fluid solutions near room temperature. One reason for the absence of phosphorescence is the long phosphorescence lifetimes and the presence of dissolved oxygen and other quenchers. For instance, recent data for tryptophan revealed a phosphorescence lifetime of 1.2 ms at 20 °C.[67] Suppose that the oxygen bimolecular quenching constant is $1 \times 10^{10} M^{-1} s^{-1}$ and that the aqueous sample is in equilibrium with dissolved oxygen from the air (0.255mM O_2). Using Eq. [8.1], the intensity is expected to be quenched 3000-fold. For this reason, methods have been developed to remove dissolved oxygen from samples used to study phosphorescence.[68,69] In practice, other dissolved quenchers and nonradiative decay rates result in vanishingly small phosphorescence quantum yields in room-temperature solutions. Some exceptions are known, such as when fluorophores are located in highly protected environments within proteins.[70–73] Phosphorescence has also been observed at room temperature for probes bound to cyclodextrins, even in the pres-

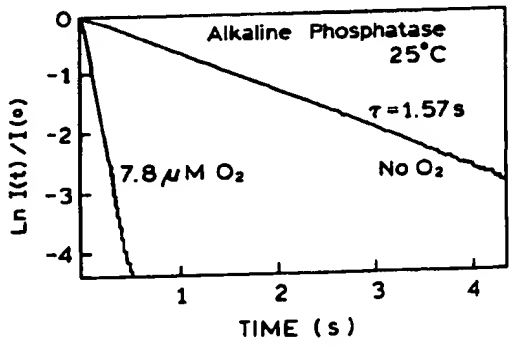

Figure 8.37. Phosphorescence decay of alkaline phosphatase at 25 °C in the absence of oxygen and in the presence of 7.8μM oxygen. Revised and reprinted, with permission, from Ref. 77, Copyright © 1987, Biophysical Society.

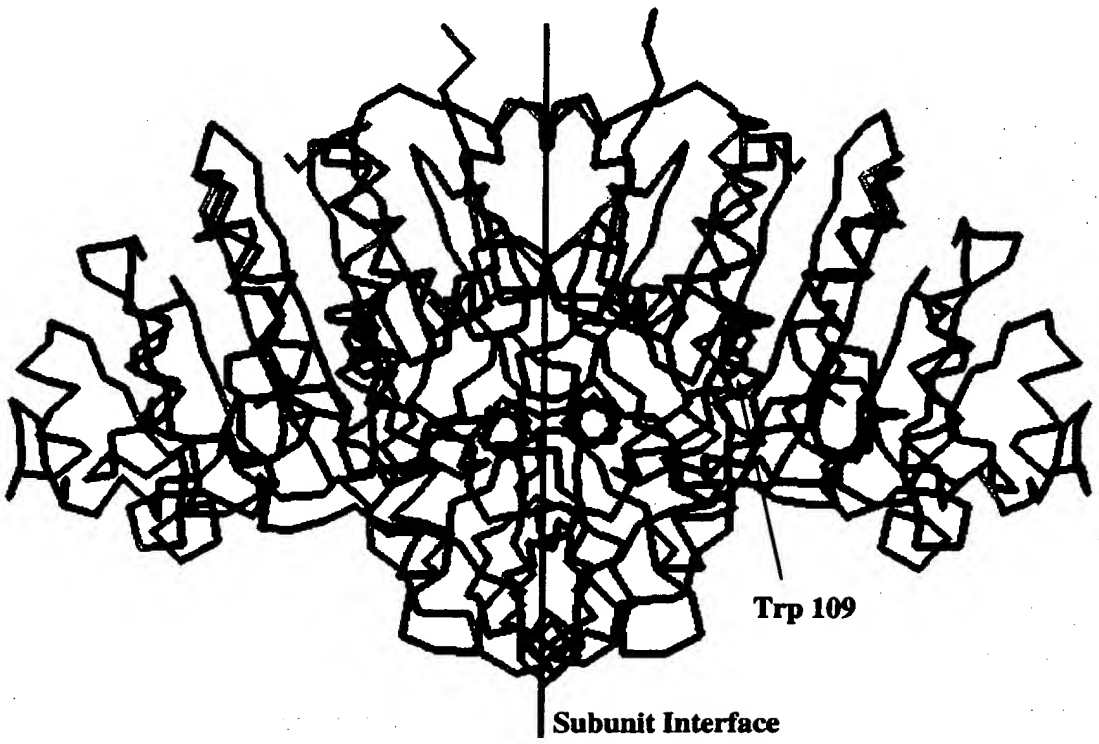

Figure 8.38. Structure of the alkaline phosphatase dimer, showing the phosphorescent residue trp-109. Courtesy of Dr. Ari Gafni, University of Michigan.

ence of oxygen.[74] However, in general, phosphorescence is not commonly observed near room temperature.

Protein phosphorescence can be quenched by a number of small molecules such as amino acids, H_2O, and CS_2,[75,76] in addition to oxygen. An example of the dramatic quenching of protein phosphorescence by even low concentrations of oxygen is shown for alkaline phosphatase phosphorescence[77] in Figure 8.37. It is now known that the phosphorescence from alkaline phosphatase results from one of its three nonidentical tryptophan residues, trp-109. This residue is located in a highly shielded environment near the dimer interface (Figure 8.38). In the presence of 7.8μM oxygen, the phosphorescence lifetime is reduced from 1.57 s to 0.1 s. Note that an oxygen concentration of 7.8μM would have an insignificant effect on nanosecond fluorescence. It is also important to notice that trp-109 in alkaline phosphatase is one of the most shielded residues identified to date in a protein. The lifetimes in the absence and presence of 7.8μM oxygen can be used to calculate a value of $1.2 \times 10^6\ M^{-1}\ s^{-1}$ for the bimolecular quenching constant k_q. If the residue were more typical, with a k_q value of $0.1 \times 10^9\ M^{-1}\ s^{-1}$, one can calculate that the decay time in 7.8μM oxygen would have been reduced to 1.28 ms, and thus quenched by over 1000-fold for a micromolar quencher concentration.

REFERENCES

1. Kautsky, H., 1939, Quenching of luminescence by oxygen, *Trans. Faraday Soc.* **35**:216–219.
2. Knibbe, H., Rehm, D., and Weller, A., 1968, Intermediates and kinetics of fluorescence quenching by electron transfer, *Ber. Bunsenges. Phys. Chem.* **72**:257–263.
3. Kasha, M., 1952, Collisional perturbation of spin–orbital coupling and the mechanism of fluorescence quenching. A visual demonstration of the perturbation, *J. Chem. Phys.* **20**:71–74.
4. Steiner, R. F., and Kirby, E. P., 1969, The interaction of the ground and excited states of indole derivatives with electron scavengers, *J. Phys. Chem.* **73**:4130–4135.
5. Eftink, M. R., and Ghiron, C., 1981, Fluorescence quenching studies with proteins, *Anal. Biochem.* **114**:199–227.
6. Eftink, M. R., 1991, Fluorescence quenching reactions: Probing biological macromolecular structures, in *Biophysical and Biochemical Aspects of Fluorescence Spectroscopy*, T. G. Dewey (ed.), Plenum Press, New York, pp. 1–41.
7. Eftink, M. R., 1991, Fluorescence quenching: Theory and applications, in *Topics in Fluorescence Spectroscopy, Volume 2, Principles*, J. R. Lakowicz (ed.), Plenum Press, New York, pp. 53–126.

8. Davis, G. A., 1973, Quenching of aromatic hydrocarbons by alkylpyridinium halides, *J. Chem. Soc., Chem. Commun.* **1973**:728–729.
9. Shinitzky, M., and Rivnay, B., 1977, Degree of exposure of membrane proteins determined by fluorescence quenching, *Biochemistry* **16**:982–986.
10. Spencer, R. D., and Weber, G., 1972, Thermodynamics and kinetics of the intramolecular complex in flavin-adenine dinucleotide, in *Structure and Function of Oxidation Reduction Enzymes*, A. Akeson and A. Ehrenberg (eds.), Pergamon Press, New York, pp. 393–399.
11. Scott, T. G., Spencer, R. D., Leonard, N. J., and Weber, G., 1970, Emission properties of NADH. Studies of fluorescence lifetimes and quantum efficiencies of NADH, AcPyADH, and simplified synthetic models, *J. Am. Chem. Soc.* **92**:687–695.
12. Ware, W. R., 1962, Oxygen quenching of fluorescence in solution: An experimental study of the diffusion process, *J. Phys. Chem.* **66**:455–458.
13. Othmer, D. F., and Thakar, M. S., 1953, Correlating diffusion coefficients in liquids, *Ind. Eng. Chem.* **45**:589–593.
14. Lakowicz, J. R., and Weber, G., 1973, Quenching of fluorescence by oxygen. A probe for structural fluctuations in macromolecules, *Biochemistry* **12**:4161–4170.
15. Eftink, M. R., and Ghiron, C. A., 1976, Fluorescence quenching of indole and model micelle systems, *J. Phys. Chem.* **80**:486–493.
16. Johnson, D. A., and Yguerabide, J., 1985, Solute accessibility to *N'*-fluorescein isothiocyanate-lysine-23, cobra α-toxin bound to the acetylcholine receptor, *Biophys. J.* **48**:949–955.
17. Kubota, Y., Nakamura, H., Morishita, M., and Fujisaki, Y., 1978, Interaction of 9-aminoacridine with 7-methylguanosine and $1,N^6$-ethenoadenosine monophosphate, *Photochem. Photobiol.* **27**:479–481.
18. Kubota, Y., Motoda, Y., Shigemune, Y., and Fujisaki, Y., 1979, Fluorescence quenching of 10-methylacridinium chloride by nucleotides, *Photochem. Photobiol.* **29**:1099–1106.
19. Seidel, C. A. M., Schulz, A., and Sauer, M. H. M., 1996, Nucleobase-specific quenching of fluorescent dyes. 1. Nucleobase one-electron redox potentials and their correlation with static and dynamic quenching efficiencies, *J. Phys. Chem.* **100**:5541–5553.
20. Casali, E., Petra, P. H., and Ross, J. B. A., 1990, Fluorescence investigation of the sex steroid binding protein of rabbit serum: Steroid binding and subunit dissociation, *Biochemistry* **29**:9334–9343.
21. Frank, I. M., and Vavilov, S. I., 1931, Über die wirkungssphäre der auslöschuns-vargänge in den fluresz ierenden flussigHeiten. *Z. Phys.* **69**:100–110.
22. Maniara, G., Vanderkooi, J. M., Bloomgarden, D. C., and Koloczek, H., 1988, Phosphorescence from 2-(*p*-toluidinyl)naphthalene-6-sulfonate and 1-anilinonaphthalene-8-sulfonate, commonly used fluorescence probes of biological structures, *Photochem. Photobiol.* **47**:207–208.
23. Kim, H., Crouch, S. R., and Zabik, M. J., 1989, Room-temperature phosphorescence of compounds in mixed organized media: Synthetic enzyme model-surfactant system, *Anal. Chem.* **61**:2475–2478.
24. Encinas, M. V., Lissi, E. A., and Rufs, A. M., 1993, Inclusion and fluorescence quenching of 2,3-dimethylnaphthalene in β-cyclodextrin cavities, *Photochem. Photobiol.* **57**:603–608.
25. Turro, N. J., Bolt, J. D., Kuroda, Y., and Tabushi, I., 1982, A study of the kinetics of inclusion of halonaphthalenes with β-cyclodextrin via time correlated phosphorescence, *Photochem. Photobiol.* **35**:69–72.
26. Waka, Y., Hamamoto, K., and Mataga, N., 1980, Heteroexcimer systems in aqueous micellar solutions, *Photochem. Photobiol.* **32**:27–35.
27. Atherton, S. J., and Beaumont, P. C., 1986, Quenching of the fluorescence of DNA-intercalated ethidium bromide by some transition metal ions, *J. Phys. Chem.* **90**:2252–2259.
28. Pasternack, R. F., Caccam, M., Keogh, B., Stephenson, T. A., Williams, A. P., and Gibbs, E. J., 1991, Long-range fluorescence quenching of ethidium ion by cationic porphyrins in the presence of DNA, *J. Am. Chem. Soc.* **113**:6835–6840.
29. Poulos, A. T., Kuzmin, V., and Geacintov, N. E., 1982, Probing the microenvironment of benzo[*a*]pyrene diol epoxide–DNA adducts by triplet excited state quenching methods, *J. Biochem. Biophys. Methods* **6**:269–281.
30. Zinger, D., and Geacintov, N. F., 1988, Acrylamide and molecular oxygen fluorescence quenching as a probe of solvent-accessibility of aromatic fluorophores complexed with DNA in relation to their conformations: Coronene-DNA and other complexes, *Photochem. Photobiol.* **47**:181–188.
31. Suh, D., and Chaires, J. B., 1995, Criteria for the mode of binding of DNA binding agents, *Bioorgan. Med. Chem.* **3**:723–728.
32. Ando, T., and Asai, H., 1980, Charge effects on the dynamic quenching of fluorescence of $1,N^6$-ethenoadenosine oligophosphates by iodide, thallium (I) and acrylamide, *J. Biochem.* **88**:255–264.
33. Ando, T., Fujisaki, H., and Asai, H., 1980, Electric potential at regions near the two specific thiols of heavy meromyosin determined by the fluorescence quenching technique, *J. Biochem.* **88**:265–276.
34. Miyata, H., and Asai, H., 1981, Amphoteric charge distribution at the enzymatic site of $1,N^6$-ethenoadenosine triphosphate-binding heavy meromyosin determined by dynamic fluorescence quenching, *J. Biochem.* **90**:133–139.
35. Midoux, P., Wahl, P., Auchet, J.-C., and Monsigny, M., 1984, Fluorescence quenching of tryptophan by trifluoroacetamide, *Biochim. Biophys. Acta* **801**:16–25.
36. Lehrer, S. S., 1971, Solute perturbation of protein fluorescence. The quenching of the tryptophan fluorescence of model compounds and of lysozyme by iodide ion, *Biochemistry* **10**:3254–3263.
37. Eftink, M. R., and Selvidge, L. A., 1982, Fluorescence quenching of liver alcohol dehydrogenase by acrylamide, *Biochemistry* **21**:117–125.
38. Eftink, M., and Hagaman, K. A., 1986, Fluorescence lifetime and anisotropy studies with liver alcohol dehydrogenase and its complexes, *Biochemistry* **25**:6631–6637.
39. Sontag, B., Reboud, A.-M., Divita, G., Di Pietro, A., Guillot, D., and Reboud, J.P., 1993, Intrinsic tryptophan fluorescence of rat liver elongation factor eEF-2 to monitor the interaction with guanylic and adenylic nucleotides and related conformational changes, *Biochemistry* **32**:1976–1980.
40. Xing, D., Dorr, R., Cunningham, R. P., and Scholes, C. P., 1995, Endonuclease III interactions with DNA substrates. 2. The DNA repair enzyme endonuclease III binds differently to intact DNA and to apyrimidinic/apurinic DNA substrates as shown by tryptophan fluorescence quenching, *Biochemistry* **34**:2537–2544.
41. Wasylewski, M., Malecki, J., and Wasylewski, Z., 1995, Fluorescence study of *Escherichia coli* cyclic AMP receptor protein, *J. Protein Chem.* **14**:299–308.
42. Wells, T. A., Nakazawa, M., Manabe, K., and Song, P.-S., 1994, A conformational change associated with the phototransformation of *Pisum* phytochrome A as probed by fluorescence quenching, *Biochemistry* **33**:708–712.

43. Eftink, M. R., Zajicek, J. L., and Ghiron, C. A., 1977, A hydrophobic quencher of protein fluorescence: 2,2,2-Trichloroethanol, *Biochim. Biophys. Acta* **491**:473–481.
44. Blatt, E., Husain, A., and Sawyer, W. H., 1986, The association of acrylamide with proteins. The interpretation of fluorescence quenching experiments, *Biochim. Biophys. Acta* **871**:6–13.
45. Eftink, M. R., and Ghiron, C. A., 1987, Does the fluorescence quencher acrylamide bind to proteins? *Biochim. Biophys. Acta* **916**:343–349.
46. Punyiczki, M., Norman, J. A., and Rosenberg, A., 1993, Interaction of acrylamide with proteins in the concentration range used for fluorescence quenching studies, *Biophys. Chem.* **47**:9–19.
47. Bastyns, K., and Engelborghs, Y., 1992, Acrylamide quenching of the fluorescence of glyceraldehyde-3-phosphate dehydrogenase: Reversible and irreversible effects, *Photochem. Photobiol.* **55**:9–16.
48. Merrill, A. R., Palmer, L. R., and Szabo, A. G., 1993, Acrylamide quenching of the intrinsic fluorescence of tryptophan residues genetically engineered into the soluble colicin E1 channel peptide. Structural characterization of the insertion-competent state, *Biochemistry* **32**:6974–6981.
49. Wasylewski, Z., Kaszycki, P., Guz, A., and Stryjewski, W., 1988, Fluorescence quenching resolved spectra of fluorophores in mixtures and micellar solutions, *Eur. J. Biochem.* **178**:471–476.
50. Wasylewski, Z., Kołoczek, H., and Wasniowska, A., 1988, Fluorescence quenching resolved spectroscopy of proteins, *Eur. J. Biochem.* **172**:719–724.
51. Laws, W. R., and Shore, J. D., 1978, The mechanism of quenching of liver alcohol dehydrogenase fluorescence due to ternary complex formation, *J. Biol. Chem.* **23**:8593–8597.
52. Stryjewski, W., and Wasylewski, Z., 1986, The resolution of heterogeneous fluorescence of multitryptophan-containing proteins studied by a fluorescence quenching method, *Eur. J. Biochem.* **158**:547–553.
53. Blicharska, Z., and Wasylewski, Z., 1995, Fluorescence quenching studies of trp repressor using single-tryptophan mutants, *J. Protein Chem.* **14**:739–746.
54. Wasylewski, Z., Kaszycki, P., and Drwiega, M., 1996, A fluorescence study of Tn10-encoded tet repressor, *J. Protein Chem.* **15**:45–52.
55. Hansen, D., Altschmied, L., and Hillen, W., 1987, Engineered tet repressor mutants with single tryptophan residues as fluorescent probes, *J. Biol. Chem.* **29**:14030–14035.
56. Lange, R., Anzenbacher, P., Müller, S., Maurin, L., and Balny, C., 1994, Interaction of tryptophan residues of cytochrome P45scc with a highly specific fluorescence quencher, a substrate analogue, compared to acrylamide and iodide, *Eur. J. Biochem.* **226**:963–970.
57. Johansson, J. S., Eckenhoff, R. G., and Dutton, L., 1995, Binding of halothane to serum albumin demonstrated using tryptophan fluorescence, *Anesthesiology* **83**:316–324.
58. Johansson, J. S., 1997, Binding of the volatile anesthetic chloroform to albumin demonstrated using tryptophan fluorescence quenching, *J. Biol. Chem.* **272**:17961–17965.
59. Gonzalez-Jimenez, J., Frutos, G., and Cayre, I., 1992, Fluorescence quenching of human serum albumin by xanthines, *Biochem. Pharmacol.* **44**:824–826.
60. Walter, N. G., and Burke, J. M., 1997, Real-time monitoring of hairpin ribozyme kinetics through base-specific quenching of fluorescein-labeled substrates, *RNA* **3**:392–404.
61. Jezewska, M. J., and Bujalowski, W., 1997, Quantitative analysis of ligand–macromolecule interactions using differential dynamic quenching of the ligand fluorescence to monitor the binding, *Biophys. Chem.* **64**:253–269.
62. Eftink, M. R., Jia, Y.-W., Graves, D. E., Wiczk, W., Gryczynski, I., and Lakowicz, J. R., 1989, Intramolecular fluorescence quenching in covalent acrylamide–indole adducts, *Photochem. Photobiol.* **49**:725–729.
63. Green, S. A., Simpson, D. J., Zhou, G., Ho, P. S., and Blough, N. V., 1990, Intramolecular quenching of excited singlet states by stable nitroxyl radicals, *J. Am. Chem. Soc.* **112**:7337–7346.
64. Chuang, T. J., Cox, R. J., and Eisenthal, K. B., 1974, Picosecond studies of the excited charge-transfer interactions in anthracene-$(CH_2)_3$-*N,N*-dimethylaniline systems, *J. Am. Chem. Soc.* **96**:6828–6831.
65. Migita, M., Okada, T., Mataga, N., Sakata, Y., Misumi, S., Nakashima, N., and Yoshihara, K., 1981, Picosecond laser spectroscopy of intramolecular heteroexcimer systems. Time-resolved fluorescence studies of *p*-$(CH_3)_2NC_6H_4$-$(CH_2)_n$-(9-anthryl), *p*-$(CH_3)_2NC_6H_4$-$(CH_2)_n$-(1-pyrenyl) systems and 9,9′-bianthryl, *Bull. Chem. Soc. Jpn.* **54**:3304–3311.
66. Basu, G., Anglos, D., and Kuki, A., 1993, Fluorescence quenching in a strongly helical peptide series: The role of noncovalent pathways in modulating electronic interactions, *Biochemistry* **32**:3067–3076.
67. Strambini, G. B., and Gonnelli, M., 1995, Tryptophan phosphorescence in fluid solution, *J. Am. Chem. Soc.* **117**:7646–7651.
68. Englander, S. W., Calhoun, D. B., and Englander, J. J., 1987, Biochemistry without oxygen, *Anal. Biochem.* **161**:300–306.
69. Zhang, H. R., Zhang, J., Wei, Y. S., Jin, E. J., and Liu, C. S., 1997, Study of new facile deoxygenation methods in cyclodextrin induced room temperature phosphorescence, *Anal. Chim. Acta* **357**:119–125.
70. Cioni, P., Puntoni, A., and Strambini, G. B., 1993, Tryptophan phosphorescence as a monitor of the solution structure of phosphoglycerate kinase from yeast, *Biophys. Chem.* **46**:47–55.
71. Gonnelli, M., and Strambini, G. B., 1993, Glycerol effects on protein flexibility: A tryptophan phosphorescence study, *Biophys. J.* **65**:131–137.
72. Strambini, G. B., and Gabellieri, E., 1996, Proteins in frozen solutions: Evidence of ice-induced partial unfolding, *Biophys. J.* **70**:971–976.
73. Vanderkooi, J. M., Calhoun, D. B., and Englander, S. W., 1987, On the prevalence of room-temperature protein phosphorescence, *Science* **236**:568–569.
74. Turro, N. J., Cox, G. S., and Li, X., 1983, Remarkable inhibition of oxygen quenching of phosphorescence by complexation with cyclodextrins, *Photochem. Photobiol.* **37**:149–153.
75. Gonnelli, M., and Strambini, G. B., 1995, Phosphorescence lifetime of tryptophan in proteins, *Biochemistry* **34**:13847–13857.
76. Wright, W. W., Owen, C. S., and Vanderkooi, J. M., 1992, Penetration of analogues of H_2O and CO_2 in proteins studied by room temperature phosphorescence of tryptophan, *Biochemistry* **31**:6538–6544.
77. Strambini, G. B., 1987, Quenching of alkaline phosphatase phosphorescence by O_2 and NO, *Biophys. J.* **52**:23–28.
78. Boaz, H., and Rollefson, G. K., 1950, The quenching of fluorescence. Deviations from the Stern–Volmer law, *J. Am. Chem. Soc.* **72**:3425–3443.
79. Eftink, M. R., and Ghiron, C. A., 1976, Exposure of tryptophanyl residues in proteins. Quantitative determination by fluorescence quenching studies, *Biochemistry* **15**:672–680.
80. Kuzmin, M. G., and Guseva, L. N., 1969, Donor–acceptor complexes of singlet excited states of aromatic hydrocarbons with aliphatic amines, *Chem. Phys. Lett.* **3**:71–72.
81. Rehm, D., and Weller, A., 1970, Kinetics of fluorescence quenching by electron and H-atom transfer, *Israel J. Chem.* **8**:259–271.

82. Obyknovennaya, I. E., Vasileva, I. M., and Cherkasov, A. S., 1986, Quenching of the fluorescence of anthracene by dimethylaniline in aqueous-micellar solvent and formation of luminescent exciplexes, *Opt. Spectrosc.* **60**:169–171.
83. Lewis, F. D., and Bassani, D. M., 1992, Formation and decay of styrene–amine exciplexes, *J. Photochem. Photobiol. A: Chem.* **66**:43–52.
84. Schneider, S., Stammler, W., Bierl, R., and Jager, W., 1994, Ultrafast photoinduced charge separation and recombination in weakly bound complexes between oxazine dyes and *N,N*-dimethylaniline, *Chem. Phys. Lett.* **219**:433–439.
85. Yoshihara, K., Yartsev, A., Nagasawa, Y., Kandori, H., Douhal, A., and Kemnitz, K., 1993, Femtosecond intermolecular electron transfer between dyes and electron-donating solvents, *Pure Appl. Chem.* **65**:1671–1675.
86. Bisht, P. B., and Tripathi, H. B., 1993, Fluorescence quenching of carbazole by triethylamine: Exciplex formation in polar and nonpolar solvents, *J. Lumin.* **55**:153–158.
87. Sikaris, K. A., and Sawyer, W. H., 1982, The interaction of local anaesthetics with synthetic phospholipid bilayers, *Biochem. Pharmacol.* **31**:2625–2631.
88. Fernandez, M. S., and Calderon, E., 1990, The local anaesthetic tetracaine as a quencher of perylene fluorescence in micelles, *J. Photochem. Photobiol. B: Biol.* **7**:75–86.
89. Winkler, M. H., 1969, A fluorescence quenching technique for the investigation of the configurations of binding sites for small molecules, *Biochemistry* **8**:2586–2590.
90. Berlman, I. B., 1973, Empirical study of heavy-atom collisional quenching of the fluorescence state of aromatic compounds in solution, *J. Phys. Chem.* **77**:562–567.
91. James, D. R., and Ware, W. R., 1985, Multiexponential fluorescence decay of indole-3-alkanoic acids, *J. Phys. Chem.* **89**:5450–5458.
92. Illsley, N. P., and Verkman, A. S., 1987, Membrane chloride transport measured using a chloride-sensitive fluorescent probe, *Biochemistry* **26**:1215–1219.
93. Chao, A. C., Dix, J. A., Sellers, M. C., and Verkman, A. S., 1989, Fluorescence measurement of chloride transport in monolayer cultured cells, *Biophys. J.* **56**:1071–1081.
94. Verkman, A. S., 1990, Development and biological applications of chloride-sensitive fluorescent indicators, *Am. J. Phys.* **253**:C375–C388.
95. Martin, A., and Narayanaswamy, R., 1997, Studies on quenching of fluorescence of reagents in aqueous solution leading to an optical chloride-ion sensor, *Sensors Actuators B* **38–39**:330–333.
96. Daems, D., Boens, N., and Schryver, F. C., 1989, Fluorescence quenching with lindane in small unilamellar L,α-dimyristoylphosphatidylcholine vesicles, *Eur. Biophys. J.* **17**:25–36.
97. Namiki, A., Nakashima, N., and Yoshihara, K., 1979, Fluorescence quenching due to the electron transfer. Indole-chloromethanes in rigid ethanol glass, *J. Chem. Phys.* **71**:925–930.
98. Johnson, G. E., 1980, Fluorescence quenching of carbazoles, *J. Phys. Chem.* **84**:2940–2946.
99. Jones, O. T., and Lee, A. G., 1985, Interactions of hexachlorocyclohexanes with lipid bilayers, *Biochim. Biophys. Acta* **812**:731–739.
100. Hariharan, C., Vijaysree, V., and Mishra, A. K., 1997, Quenching of 2,5-diphenyloxazole (PPO) fluorescence by metal ions, *J. Lumin.* **75**:205–211.
101. Morris, S. J., Bradley, D., and Blumenthal, R., 1985, The use of cobalt ions as a collisional quencher to probe surface charge and stability of fluorescently labeled bilayer vesicles, *Biochim. Biophys. Acta* **818**:365–372.
102. Homan, R., and Eisenberg, M., 1985, A fluorescence quenching technique for the measurement of paramagnetic ion concentrations at the membrane/water interface. Intrinsic and X537A-mediated cobalt fluxes across lipid bilayer membranes, *Biochim. Biophys. Acta* **812**:485–492.
103. Salthammer, T., Dreeskamp, H., Birch, D. J. S., and Imhof, R. E., 1990, Fluorescence quenching of perylene by Co^{2+} ions via energy transfer in viscous and non-viscous media, *J. Photochem. Photobiol., A: Chem.* **55**:53–62.
104. Holmes, A. S., Birch, D. J. S., Suhling, K., Imhof, R. E., Salthammer, T., and Dreeskamp, H., 1991, Evidence for donor–donor energy transfer in lipid bilayers: Perylene fluorescence quenching by Co^{2+} ions, *Chem. Phys. Lett.* **186**:189–194.
105. Birch, D. J. S., Suhling, K., Holmes, A. S., Salthammer, T., and Imhof, R. E., 1992, Fluorescence energy transfer to metal ions in lipid bilayers, *Proc. SPIE* **1640**:707–718.
106. Perochon, E., and Tocanne, J.-F., 1991, Synthesis and phase properties of phosphatidylcholine labeled with 8-(2-anthroyl)octanoic acid, a solvatochromic fluorescent probe, *Chem. Phys. Lipids* **58**:7–17.
107. Fucaloro, A. F., Forster, L. S., and Campbell, M. K., 1984, Fluorescence quenching of indole by dimethylformamide, *Photochem. Photobiol.* **39**:503–506.
108. Swadesh, J. K., Mui, P. W., and Scheraga, H. A., 1987, Thermodynamics of the quenching of tyrosyl fluorescence by dithiothreitol, *Biochemistry* **26**:5761–5769.
109. Valentino, M. R., and Boyd, M. K., 1995, Ether quenching of singlet excited 9-arylxanthyl cations, *J. Photochem. Photobiol.* **89**:7–12.
110. Medinger, T., and Wilkinson, F., 1965, Mechanism of fluorescence quenching in solution I. Quenching of bromobenzene, *Trans. Faraday Soc.* **61**:620–630.
111. Ahmad, A., and Durocher, G., 1981, How hydrogen bonding of carbazole to ethanol affects its fluorescence quenching rate by electron acceptor quencher molecules, *Photochem. Photobiol.* **34**:573–578.
112. Bowen, E. J., and Metcalf, W. S., 1951, The quenching of anthracene fluorescence, *Proc. R. Soc. London* **206A**:437–447.
113. Schmidt, R., Janssen, W., and Brauer, H.-D., 1989, Pressure effect on quenching of perylene fluorescence by halonaphthalenes, *J. Phys. Chem.* **93**:466–468.
114. Encinas, M. V., Rubio, M. A., and Lissi, E., 1983, Quenching and photobleaching of excited polycyclic aromatic hydrocarbons by carbon tetrachloride and chloroform in micellar systems, *Photochem. Photobiol.* **37**:125–130.
115. Behera, P. K., Mukherjee, T., and Mishra, A. K., 1995, Quenching of substituted naphthalenes fluorescence by chloromethanes, *J. Lumin.* **65**:137–142.
116. Behera, P. K., and Mishra, A. K., 1993, Static and dynamic model for 1-naphthol fluorescence quenching by carbon tetrachloride in dioxane–acetonitrile mixtures, *J. Photochem. Photobiol., A: Chem.* **71**:115–118.
117. Behera, P. K., Mukherjee, T., and Mishra, A. K., 1995, Simultaneous presence of static and dynamic component in the fluorescence quenching for substituted naphthalene–CCl_4 system, *J. Lumin.* **65**:131–136.
118. Zhang, J., Roek, D. P., Chateauneuf, J. E., and Brennecke, J. F., 1997, A steady-state and time-resolved fluorescence study of quenching reactions of anthracene and 1,2-benzanthracene by carbon tetrabromide and bromoethane in supercritical carbon dioxide, *J. Amer. Chem. Soc.* **119**:9980–9991.
119. Tucker, S. A., Cretella, L. E., Waris, R., Street, K. W., Acree, W. E., and Fetzer, J. C., 1990, Polycyclic aromatic hydrocarbon solute probes. Part VI: Effect of dissolved oxygen and halogenated sol-

vents on the emission spectra of select probe molecules, *Appl. Spectrosc.* 44:269–273.
120. Wiczk, W. M., and Latowski, T., 1992, The effect of temperature on the fluorescence quenching of perylene by tetrachloromethane in mixtures with cyclohexane and benzene, *Z. Naturforsch. A* 47:533–535.
121. Wiczk, W. M., and Latowski, T., 1986, Photophysical and photochemical studies of polycyclic aromatic hydrocarbons in solutions containing tetrachloromethane. I. Fluorescence quenching of anthracene by tetrachloromethane and its complexes with benzene, *p*-xylene and mesitylene, *Z. Naturforsch. A* 41:761–766.
122. Goswami, D., Sarpal, R. S., and Dogra, S. K., 1991, Fluorescence quenching of few aromatic amines by chlorinated methanes, *Bull. Chem. Soc. Jpn.* 64:3137–3141.
123. Takahashi, T., Kikuchi, K., and Kokubun, H., 1980, Quenching of excited 2,5-diphenyloxazole by CCl_4, *J. Photochem.* 14:67–76.
124. Alford, P. C., Cureton, C. G., Lampert, R. A., and Phillips, D., 1983, Fluorescence quenching of tertiary amines by halocarbons, *Chem. Phys.* 76:103–109.
125. Khwaja, H. A., Semeluk, G. P., and Unger, I., 1984, Quenching of the singlet and triplet state of benzene in condensed phase, *Can. J. Chem.* 62:1487–1491.
126. Washington, K., Sarasua, M. M., Koehler, L. S., Koehler, K. A., Schultz, J. A., Pedersen, L. G., and Hiskey, R. G., 1984, Utilization of heavy-atom effect quenching of pyrene fluorescence to determine the intramembrane distribution of halothane, *Photochem. Photobiol.* 40:693–701.
127. Lopez, M. M., and Kosk-Kosicka, D., 1998, Spectroscopic analysis of halothane binding to the plasma membrane Ca^{2+}-ATPase, *Biophys. J.* 74:974–980.
128. Cavatorta, P., Favilla, R., and Mazzini, A., 1979, Fluorescence quenching of tryptophan and related compounds by hydrogen peroxide, *Biochim. Biophys. Acta* 578:541–546.
129. Vos, R., and Engelborghs, Y., 1994, A fluorescence study of tryptophan–histidine interactions in the peptide alantin and in solution, *Photochem. Photobiol.* 60:24–32.
130. Mae, M., Wach, A., and Najbar, J., 1991, Solvent effects on the fluorescence quenching of anthracene by iodide ions, *Chem. Phys. Lett.* 176:167–172.
131. Blatt, E., Ghiggino, K. P., and Sawyer, W. H., 1982, Fluorescence depolarization studies of *n*-(9-anthroyloxy) fatty acids in cetyltrimethylammonium bromide micelles, *J. Phys. Chem.* 86:4461–4464.
132. Fraiji, L. K., Hayes, D. M., and Werner, T. C., 1992, Static and dynamic fluorescence quenching experiments for the physical chemistry laboratory, *J. Chem. Educ.* 69:424–428.
133. Zhu, C., Bright, F. V., and Hieftje, G. M., 1990, Simultaneous determination of Br^- and I^- with a multiple fiber-optic fluorescence sensor, *Appl. Spectrosc.* 44:59–64.
134. Lakowicz, J. R., and Anderson, C. J., 1980, Permeability of lipid bilayers to methylmercuric chloride: Quantification by fluorescence quenching of a carbazole-labeled phospholipid, *Chem.-Biol. Interact.* 30:309–323.
135. Boudou, A., Desmazes, J. P., and Georgescauld, D., 1982, Fluorescence quenching study of mercury compounds and liposome interactions: Effect of charged lipid and pH, *Ecotoxicol. Environ. Saf.* 6:379–387.
136. Holmes, A. S., Suhling, K., and Birch, D. J. S., 1993, Fluorescence quenching by metal ions in lipid bilayers, *Biophys. Chem.* 48:193–204.
137. Birch, D. J. S., Suhling, K., Holmes, A. S., Salthammer, T., and Imhof, R. E., 1993, Metal ion quenching of perylene fluorescence in lipid bilayers, *Pure Appl. Chem.* 65:1687–1692.
138. Sawicki, E., Stanley, T. W., and Elbert, W. C., 1964, Quenchofluorometric analysis for fluoranthenic hydrocarbons in the presence of other types of aromatic hydrocarbon, *Talanta* 11:1433–1441.
139. Dreeskamp, H., Koch, E., and Zander, M., 1975, On the fluorescence quenching of polycyclic aromatic hydrocarbons by nitromethane, *Z. Naturforsch. A* 30:1311–1314.
140. Pandey, S., Fletcher, K. A., Powell, J. R., McHale, M. E. R., Kauppila, A-S. M., Acree, W. E., Fetzer, J. C., Dai, W., and Harvey, R. G., 1997, Spectrochemical investigations of fluorescence quenching agents. Part 5. Effect of surfactants on the ability of nitromethane to selectively quench fluorescence emission of alternant PAHs, *Spectrochim. Acta, Part A* 53:165–172.
141. Pandey, S., Acree, W. E., Cho, B. P., and Fetzer, J. C., 1997, Spectroscopic properties of polycyclic aromatic compounds. Part 6. The nitromethane selective quenching rule visited in aqueous micellar zwitterionic surfactant solvent media, *Talanta* 44:413–421.
142. Acree, W. E., Pandey, S., and Tucker, S. A., 1997, Solvent-modulated fluorescence behavior and photophysical properties of polycyclic aromatic hydrocarbons dissolved in fluid solution, *Curr. Top. Solution Chem.* 2:1–27.
143. Tucker, S. A., Acree, W. E., Tanga, M. J., Tokita, S., Hiruta, K., and Langhals, H., 1992, Spectroscopic properties of polycyclic aromatic compounds: Examination of nitromethane as a selective fluorescence quenching agent for alternant polycyclic aromatic nitrogen hetero-atom derivatives, *Appl. Spectrosc.* 46:229–235.
144. Tucker, S. A., Acree, W. E., and Upton, C., 1993, Polycyclic aromatic nitrogen heterocycles. Part V: Fluorescence emission behavior of select tetraaza- and diazaarenes in nonelectrolyte solvents, *Appl. Spectrosc.* 47:201–206.
145. Green, J. A., Singer, L. A., and Parks, J. H., 1973, Fluorescence quenching by the stable free radical di-*t*-butylnitroxide, *J. Chem. Phys.* 58:2690–2695.
146. Bieri, V. G., and Wallach, D. F. H., 1975, Fluorescence quenching in lecithin:cholesterol liposomes by paramagnetic lipid analogues: Introduction of new probe approach, *Biochim. Biophys. Acta* 389:413–427.
147. Encinas, M. V., Lissi, E. A., and Alvarez, J., 1994, Fluorescence quenching of pyrene derivatives by nitroxides microheterogeneous systems, *Photochem. Photobiol.* 59:30–34.
148. Matko, J., Ohki, K., and Edidin, M., 1992, Luminescence quenching by nitroxide spin labels in aqueous solution: Studies on the mechanism of quenching, *Biochemistry* 31:703–711.
149. Jones, P. F., and Siegel, S., 1971, Quenching of naphthalene luminescence by oxygen and nitric oxide, *J. Chem. Phys.* 54:3360–3366.
150. Harper, J., and Sailor, M. J., 1996, Detection of nitric oxide and nitrogen dioxide with photoluminescent porous silicon, *Anal. Chem.* 68:3713–3717.
151. Denicola, A., Souza, J. M., Radi, R., and Lissi, E., 1996, Nitric oxide diffusion in membranes determined by fluorescence quenching, *Arch. Biochem. Biophys.* 328:208–212.
152. Ware, W. R., Holmes, J. D., and Arnold, D. R., 1974, Exciplex photophysics. II. Fluorescence quenching of substituted anthracenes by substituted 1,1-diphenylethylenes, *J. Am. Chem. Soc.* 96:7861–7864.
153. Labianca, D. A., Taylor, G. N., and Hammond, G. S., 1972, Structure–reactivity factors in the quenching of fluorescence from naphthalenes by conjugated dienes, *J. Am. Chem. Soc.* 94:3679–3683.
154. Encinas, M. V., Guzman, E., and Lissi, E. A., 1983, Intramicellar aromatic hydrocarbon fluorescence quenching by olefins, *J. Phys. Chem.* 87:4770–4772.

155. Abuin, E. B., and Lissi, E. A., 1993, Quenching rate constants in aqueous solution: Influence of the hydrophobic effect, *J. Photochem. Photobiol.* **71**:263–267.
156. Chang, S. L. P., and Schuster, D. I., 1987, Fluorescence quenching of 9,10-dicyanoanthracene by dienes and alkenes, *J. Phys. Chem.* **91**:3644–3649.
157. Eriksen, J., and Foote, C. S., 1978, Electron-transfer fluorescence quenching and exciplexes of cyano-substituted anthracenes, *J. Phys. Chem.* **82**:2659–2662.
158. Fischkoff, S., and Vanderkooi, J. M., 1975, Oxygen diffusion in biological and artificial membranes determined by the fluorochrome pyrene, *J. Gen. Phys.* **65**:663–676.
159. Jameson, D. M., Gratton, E., Weber, G., and Alpert, B., 1984, Oxygen distribution and migration within $MB^{DES\,FE}$ and $HB^{DES\,FE}$, *Biophys. J.* **45**:795–803.
160. Subczynski, W. K., Hyde, J. S., and Kusumi, A., 1989, Oxygen permeability of phosphatidylcholine-cholesterol membranes, *Proc. Natl. Acad. Sci. U.S.A.* **86**:4474–4478.
161. Dumas, D., Muller, S., Gouin, F., Baros, F., Viriot, M.-L., and Stoltz, J.-F., 1997, Membrane fluidity and oxygen diffusion in cholesterol-enriched erythrocyte membrane, *Arch. Biochem. Biophys.* **341**:34–39.
162. Camyshan, S. V., Gritsan, N. P., Korolev, V. V., and Bazhin, N. M., 1990, Quenching of the luminescence of organic compounds by oxygen in glassy matrices, *Chem. Phys.* **142**:59–68.
163. Kikuchi, K., Sato, C., Watabe, M., Ikeda, H., Takahashi, Y., and Miyashi, T., 1993, New aspects on fluorescence quenching by molecular oxygen, *J. Am. Chem. Soc.* **115**:5180–5184.
164. Vaughan, W. M., and Weber, G., 1970, Oxygen quenching of pyrenebutyric acid fluorescence in water. A dynamic probe of the microenvironment, *Biochemistry* **9**:464–473.
165. Abuin, E. B., and Lissi, E. A., 1991, Diffusion and concentration of oxygen in microheterogeneous systems. Evaluation from luminescence quenching data, *Prog. React. Kinet.* **16**:1–33.
166. Parasassi, T., and Gratton, E., 1992, Packing of phospholipid vesicles studied by oxygen quenching of laurdan fluorescence, *J. Fluoresc.* **2**:167–174.
167. Encinas, M. V., and Lissi, E. A., 1983, Intramicellar quenching of 2,3-dimethylnaphthalene fluorescence by peroxides and hydroperoxides, *Photochem. Photobiol.* **37**:251–255.
168. Holmes, L. G., and Robbins, F. M., 1974, Quenching of tryptophyl fluorescence in proteins by *N*'-methylnicotinamide chloride, *Photochem. Photobiol.* **19**:361–366.
169. Martin, M. M., and Ware, W. R., 1978, Fluorescence quenching of carbazole by pyridine and substituted pyridines. Radiationless processes in the carbazole–amine hydrogen bonded complex, *J. Phys. Chem.* **82**:2770–2776.
170. Seely, G. R., 1978, The energetics of electron-transfer reactions of chlorophyll and other compounds, *Photochem. Photobiol.* **27**:639–654.
171. Schroeder, J., and Wilkinson, F., 1979, Quenching of triplet states of aromatic hydrocarbons by quinones due to favourable charge-transfer interactions, *J. Chem. Soc., Faraday Trans. 2* **75**:896–904.
172. Dreeskamp, H., Laufer, A., and Zander, M., 1983, Löschung der perylen-fluoreszenz durch Ag^+-ionen, *Z. Naturforsch. A* **38**:698–700.
173. Badley, R. A., 1975, The location of protein in serum lipoproteins: A fluorescence quenching study, *Biochim. Biophy. Acta* **379**:517–528.
174. Eftink, M. R., and Ghiron, C. A., 1984, Indole fluorescence quenching studies on proteins and model systems: Use of the inefficient quencher succinimide, *Biochemistry* **23**:3891–3899.
175. Moore, H.-P. H., and Raftery, M. A., 1980, Direct spectroscopic studies of cation translocation by *Torpedo* acetylcholine receptor on a time scale of physiological relevance, *Proc. Natl. Acad. Sci. U.S.A.* **77**:4509–4513.
176. Mac, M., Najbar, J., Phillips, D., and Smith, T. A., 1992, Solvent dielectric relaxation properties and the external heavy atom effect in the time-resolved fluorescence quenching of anthracene by potassium iodide and potassium thiocyanate in methanol and ethanol, *J. Chem. Soc., Faraday Trans.* **88**:3001–3005.
177. Carrigan, S., Doucette, S., Jones, C., Marzzacco, C. J., and Halpern, A. M., 1996, The fluorescence quenching of 5,6-benzoquinoline and its conjugate acid by Cl^-, Br^-, SCN^- and I^- ions, *J. Photochem. Photobiol., A: Chem.* **99**:29–35.
178. Horrochs, A. R., Kearvell, A., Tickle, K., and Wilkinson, F., 1966, Mechanism of fluorescence quenching in solution II. Quenching by xenon and intersystem crossing efficiencies, *Trans. Faraday Soc.* **62**:3393–3399.

PROBLEMS

8.1. *Separation of Static and Dynamic Quenching of Acridone by Iodide*: The following data were obtained for quenching of acridone in water at 26 °C.[78] KNO_2 is used to maintain a constant ionic strength and does not quench the fluorescence of arcidone.

[KI] (*M*)	[KNO_2] (*M*)	F_0/F
0.0	1.10	[1.0]
0.04	1.06	4.64
0.10	1.00	10.59
0.20	0.90	23.0
0.30	0.80	37.2
0.50	0.60	68.6
0.80	0.30	137

A. Construct a Stern–Volmer plot.
B. Determine the dynamic (K_D) and static (K_S) quenching constants. Use the quadratic equation to obtain K_D and K_S from the slope and intercept of a plot of K_{app} versus [Q].
C. Calculate the observed bimolecular quenching constant. The unquenched lifetime $\tau_0 = 17.6$ ns.
D. Calculate the diffusion-limited bimolecular quenching constant and the quenching efficiency. The diffusion constant of KI in water is 2.065×10^{-5} cm^2/s for 1*M* KI (*Handbook of Chemistry and Physics*, 55th ed.).
E. Comment on the magnitude of the sphere of action and the static quenching constant, with regard to the nature of the complex.

8.2. *Separation of Static and Dynamic Quenching*: The following table lists the fluorescence lifetimes and relative quantum yields of 10-methylacridinium chloride (MAC) in the presence of adenosine monophosphate (AMP).[18]

[AMP] (m*M*)	τ (ns)	Intensity
0	32.9	1.0
1.75	26.0	0.714
3.50	21.9	0.556
5.25	18.9	0.426
7.00	17.0	0.333

A. Is the quenching dynamic, static, or both?
B. What is (are) the quenching constant(s)?
C. What is the association constant for the MAC–AMP complex?
D. Comment on the magnitude of the static quenching constant.
E. Assume that the AMP–MAC complex is completely nonfluorescent and that complex formation shifts the absorption spectrum of MAC. Will the corrected excitation spectrum of MAC, in the presence of nonsaturating amounts of AMP, be comparable to the absorption spectrum of MAC or that of the MAC–AMP complex?

8.3. *Effects of Dissolved Oxygen on Fluorescence Intensities and Lifetimes*: Oxygen is known to dissolve in aqueous and organic solutions and is a collisional quencher of fluorescence. Assume that your measurements are accurate to 3%. What are the lifetimes above which dissolved oxygen from the atmosphere will result in changes in the fluorescence intensities or lifetimes that are outside your accuracy limits? Indicate these lifetimes for both aqueous and ethanolic solutions. The oxygen solubility in water is 0.001275*M* for a partial pressure of 1 atm. Oxygen is fivefold more soluble in ethanol than in water. The following information is needed to answer this question: k_q (in water) = $1 \times 10^{10}\ M^{-1}\ s^{-1}$; k_q (in ethanol) = $2 \times 10^{10}\ M^{-1}\ s^{-1}$.

8.4. *Intramolecular Complex Formation by Flavin Adenine Dinucleotide (FAD)*: FAD fluorescence is quenched both by static complex formation between the flavin and adenine rings and by collisions between these two moieties. Flavin mononucleotide (FMN) is similar to FAD except that it lacks the adenine ring. Use the following data for FAD and FMN to calculate the fraction complexed (f) and the collisional deactivation rate (k) of the flavin by the adenine ring. Q is the relative quantum yield. Note that the deactivation rate is in units of s^{-1}.
τ (FMN) = 4.6 ns
τ (FAD) = 2.4 ns
Q(FMN) = 1.0 (assumed unity)
Q(FAD) = 0.09

8.5. *Quenching of Protein Fluorescence; Determination of the Fraction of the Total Fluorescence Accessible to Iodide:* Assume that a protein contains four identical subunits, each containing two tryptophan residues. The following data are obtained in the presence of iodide.

$[I^-]$ (*M*)	Fluorescence intensity
0.00	1.0
0.01	0.926
0.03	0.828
0.05	0.767
0.10	0.682
0.20	0.611
0.40	0.563

A. What fraction of the total tryptophan fluorescence is accessible to quenching?
What property of the Stern–Volmer plots indicates an inaccessible fraction?
B. Assume that all the tryptophans have equal quantum yields and lifetimes (5 ns). How many tryptophan residues are accessible to quenching?
C. What are the bimolecular quenching constants for the accessible and inaccessible residues?
D. Assume that you could selectively excite the accessible tryptophans by excitation at 300 nm. Draw the predicted Stern–Volmer and modified Stern–Volmer plots for the accessible and the inaccessible residues.

8.6. *Quenching of Endonuclease III:* Figure 8.39 shows the effect of a 19-mer of poly(dA-dT) on the intrinsic tryptophan emission of endo nuclease III (Endo III). Explain the data in terms of the structure of endo III (Figure 8.15). Is the quenching collisional or static? Assume that the unquenched decay time is 5 ns. The concentration of endo III is 0.8μ*M*.

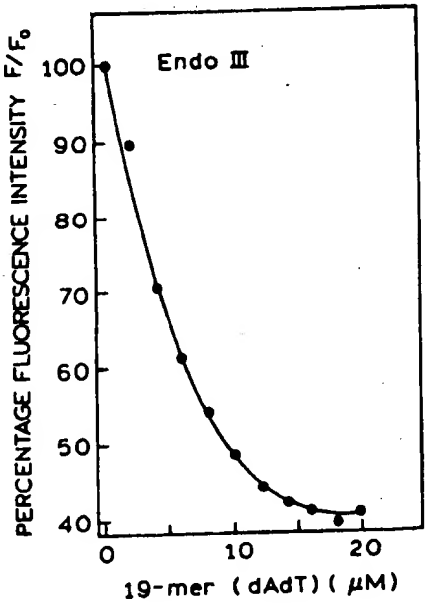

Figure 8.39. Fluorescence intensity of endo III with increasing concentrations of a 19-mer of poly(dA-dT). Revised from Ref. 40.

Principles of Fluorescence Spectroscopy
(Ed. Joseph R. Lakowicz,
Kluwer Academic/Plenum Publisher, 2nd Ed.1999)

13 Energy Transfer

Fluorescence resonance energy transfer (FRET) is transfer of the excited-state energy from the initially excited donor (D) to an acceptor (A). The donor molecules typically emit at shorter wavelengths which overlap with the absorption spectrum of the acceptor. Energy transfer occurs without the appearance of a photon and is the result of long-range dipole–dipole interactions between the donor and acceptor. The term resonance energy transfer (RET) is preferred because the process does not involve the appearance of a photon. The rate of energy transfer depends upon the extent of spectral overlap of the emission spectrum of the donor with the absorption spectrum of the acceptor, the quantum yield of the donor, the relative orientation of the donor and acceptor transition dipoles, and the distance between the donor and acceptor molecules. The distance dependence of RET has resulted in its widespread use to measure distances between donors and acceptors.

The most common application of RET is to measure the distances between two sites on a macromolecule. Typically, a protein is covalently labeled with a donor and an acceptor (Figure 13.1). The donor is often a tryptophan residue, but extrinsic donors are also used. If there is a single donor and acceptor, and if the D–A distance does not change during the excited-state lifetime, then the D–A distance can be determined from the efficiency of energy transfer. The transfer efficiency can be determined by steady-state measurements of the extent of donor quenching due to the acceptor.

Resonance energy transfer is also used to study macromolecular systems in which a single D–A distance is not present, such as assemblies of proteins and membranes or unfolded proteins where there is a distribution of D–A distances. The extent of energy transfer can also be influenced by the presence of donor-to-acceptor diffusion during the donor lifetime. Although information can be obtained from the steady-state data, such systems are usually studied using time-resolved measurements. These more advanced applications of RET are presented in Chapters 14 and 15.

An important characteristic of energy transfer is that it occurs over distances comparable to the dimensions of biological macromolecules. The distance at which RET is 50% efficient, called the Förster distance,[1] is typically in the range of 20–60 Å. The rate of energy transfer from a donor to an acceptor (k_T) is given by

$$k_T = \frac{1}{\tau_D}\left(\frac{R_0}{r}\right)^6 \qquad [13.1]$$

where τ_D is the decay time of the donor in the absence of acceptor, R_0 is the Förster distance, and r is the donor-to-acceptor (D–A) distance. Hence, the rate of transfer is equal to the decay rate of the donor in the absence of acceptor ($1/\tau_D$) when the D–A distance (r) is equal to the Förster distance (R_0). When the D–A distance is equal to the Förster distance ($r = R_0$), then the transfer efficiency is 50%. At this distance ($r = R_0$), the donor emission would be decreased to one-half of its intensity in the absence of acceptor. The rate of RET depends strongly on distance, being inversely proportional to r^6 (Eq. [13.1]).

Förster distances ranging from 20 to 90 Å are convenient for studies of biological macromolecules. These distances are comparable to the diameter of many proteins, the thickness of biological membranes, and the distance between sites on multisubunit proteins. Any phenomenon which affects the D–A distance will affect the transfer rate, allowing the phenomenon to be quantified. Energy-transfer measurements have been used to estimate the distances between sites on macromolecules and the effects of conformational changes on these distances. In this type of application, one uses the extent of energy transfer between a fixed donor and acceptor to calculate the D–A distance and thus obtain structural information about the macromolecule (Figure 13.1). Such distance measurements have resulted in the description of RET as a "spectroscopic ruler."[2,3] For instance, energy transfer can be used to

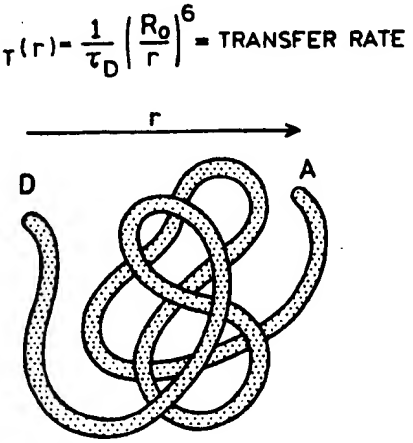

Figure 13.1. Fluorescence resonance energy transfer for a protein with a single donor (D) and a single acceptor (A).

measure the distance from a tryptophan residue to a ligand binding site when the ligand serves as the acceptor.

In the case of multidomain proteins, RET has been used to measure conformational changes which move the domains closer or further apart. Energy transfer can also be used to measure the distance between a site on a protein and a membrane surface, association between protein subunits, and lateral association of membrane-bound proteins. In the case of macromolecular association reactions, one relies less on determination of a precise D–A distance, and more on the simple fact that energy transfer occurs whenever the donors and acceptors are in close proximity comparable to the Förster distance.

The use of energy transfer as a proximity indicator illustrates an important characteristic of energy transfer. Energy transfer can be reliably assumed to occur whenever the donors and acceptors are within the characteristic Förster distance, and whenever suitable spectral overlap occurs. The value of R_0 can be reliably predicted from the spectral properties of the donors and acceptors. Energy transfer is a through-space interaction which is mostly independent of the intervening solvent and/or macromolecule. In principle, the orientation of the donors and acceptors can prevent energy transfer between a closely spaced D–A pair, but such a result is rare, and possibly nonexistent in biomolecules. Hence, one can assume that RET will occur if the spectral properties are suitable and the D–A distance is comparable to R_0. A wide variety of biochemical interactions result in changes in distance and are thus measurable using RET.

RET is a process which does not involve emission and reabsorption of photons. The theory of energy transfer is based on the concept of a fluorophore as an oscillating dipole, which can exchange energy with another dipole with a similar resonance frequency.[4] Hence, RET is similar to the behavior of coupled oscillators, like two swings on a common supporting beam. In contrast, radiative energy transfer is due to emission and reabsorption of photons and is thus due to inner filter effects. Radiative transfer depends upon less interesting optical properties of the sample, such as the size of the sample container, the path length, the optical densities of the sample at the excitation and emission wavelengths, and the geometric arrangement of the excitation and emission light paths. In contrast, nonradiative energy transfer contains a wealth of structural information concerning the donor–acceptor pair.

RET contains molecular information which is different from that revealed by solvent relaxation, excited-state reactions, fluorescence quenching, or fluorescence anisotropy. These other fluorescence phenomena depend on interactions of the fluorophore with other molecules in the surrounding solvent shell. These nearby interactions are less important for energy transfer, except for their effects on the spectral properties of the donor and acceptor. Nonradiative energy transfer is effective over much longer distances, and the intervening solvent or macromolecule has little effect on the efficiency of energy transfer, which depends primarily on the D–A distance. In this chapter we will describe the basic theory of nonradiative energy transfer. This theory is applicable to a D–A pair separated by a fixed distance, but we also describe examples of RET from membrane-bound proteins to randomly distributed lipid acceptors and the use of RET to study association reactions. More complex formalisms are needed to describe other commonly encountered situations, such as distance distributions (Chapter 14) and the presence of multiple acceptors (Chapter 15).

13.1. THEORY OF ENERGY TRANSFER FOR A DONOR–ACCEPTOR PAIR

The theory for RET is moderately complex, and similar equations have been derived from classical and quantum-mechanical considerations. We will describe only the final equations. Readers interested in the physical basis of RET are referred to the excellent review by Clegg.[4] RET is best understood by considering a single donor and acceptor separated by a distance r. The rate of transfer for a donor and acceptor separated by a distance r is given by

$$k_T(r) = \frac{Q_D\kappa^2}{\tau_D r^6}\left(\frac{9000\,(\ln 10)}{128\,\pi^5 N n^4}\right)\int_0^\infty F_D(\lambda)\varepsilon_A(\lambda)\lambda^4\,d\lambda \qquad [13.2]$$

where Q_D is the quantum yield of the donor in the absence of acceptor; n is the refractive index of the medium, which

is typically assumed to be 1.4 for biomolecules in aqueous solution; N is Avogadro's number; τ_D is the lifetime of the donor in the absence of acceptor; $F_D(\lambda)$ is the corrected fluorescence intensity of the donor in the wavelength range λ to $\lambda + \Delta\lambda$, with the total intensity (area under the curve) normalized to unity; $\varepsilon_a(\lambda)$ is the extinction coefficient of the acceptor at λ, which is typically in units of M^{-1} cm^{-1}; κ^2 is a factor describing the relative orientation in space of the transition dipoles of the donor and acceptor and is usually assumed to be equal to $\frac{2}{3}$, which is appropriate for dynamic random averaging of the donor and acceptor (see Section 13.1.A below). In Eq. [13.2] we wrote the transfer rate k_T as a function of r, $k_T(r)$, to emphasize its dependence on distance.

The overlap integral $J(\lambda)$ expresses the degree of spectral overlap between the donor emission and the acceptor absorption,

$$J(\lambda) = \int_0^\infty F_D(\lambda)\varepsilon_A(\lambda)\lambda^4\, d\lambda = \frac{\int_0^\infty F_D(\lambda)\varepsilon_A(\lambda)\lambda^4\, d\lambda}{\int_0^\infty F_D(\lambda)\, d\lambda} \qquad [13.3]$$

$F_D(\lambda)$ is dimensionless. If $\varepsilon_A(\lambda)$ is expressed in units of M^{-1} cm^{-1} and λ is in nanometers, then $J(\lambda)$ is in units of M^{-1} cm^{-1} nm^4. If λ is in centimeters, then $J(\lambda)$ is in units of M^{-1} cm^3. In calculating $J(\lambda)$, one should use the corrected emission spectrum with its area normalized to unity (Eq. [13.3], middle) or normalize the calculated value of $J(\lambda)$ by the area (Eq. [13.3], right). The overlap integral has been defined in several ways, each with different units. In our experience, we find that it is easy to get confused so we recommend the units of nanometers or centimeters for the wavelength and units of M^{-1} cm^{-1} for the extinction coefficient.

Because the transfer rate $k_T(r)$ depends on r, it is inconvenient to use this rate constant in the design of biochemical experiments. For this reason, Eq. [13.2] is written in terms of the Förster distance R_0, at which the transfer rate $k_T(r)$ is equal to the decay rate of the donor in the absence of acceptor (τ_D^{-1}). At this distance, one-half of the donor molecules decay by energy transfer and one-half decay by the usual radiative and nonradiative rates. From Eqs. [13.1] and [13.2] with $k_T(r) = \tau_D^{-1}$, one obtains

$$R_0^6 = \frac{9000(\ln 10)\kappa^2 Q_D}{128\,\pi^5 N n^4} \int_0^\infty F_D(\lambda)\varepsilon_A(\lambda)\lambda^4\, d\lambda \qquad [13.4]$$

This expression allows the Förster distance to be calculated from the spectral properties of the donor and the acceptor and the donor quantum yield. While Eq. [13.4] looks complex, many of the terms are simple physical constants. It is convenient to have simpler expressions for R_0 in terms of the experimentally known values, which is accomplished by combining the constant terms in Eq. [13.4]. If the wavelength is expressed in nanometers, then $J(\lambda)$ is in units of M^{-1} cm^{-1} (nm)^4 and the Förster distance, in angstroms, is given by

$$R_0 = 0.211[\kappa^2 n^{-4} Q_D J(\lambda)]^{1/6} \quad \text{(in Å)} \qquad [13.5]$$

and

$$R_0^6 = 8.79 \times 10^{-5}[\kappa^2 n^{-4} Q_D J(\lambda)] \quad \text{(in Å}^6\text{)} \qquad [13.6]$$

If the wavelength is expressed in centimeters and $J(\lambda)$ is in units of M^{-1} cm^3, then the Förster distance is given by

$$R_0^6 = 8.79 \times 10^{-25}[\kappa^2 n^{-4} Q_D J(\lambda)] \quad \text{(in cm}^6\text{)} \qquad [13.7]$$

or

$$R_0 = 9.78 \times 10^{3}[\kappa^2 n^{-4} Q_D J(\lambda)]^{1/6} \quad \text{(in Å)} \qquad [13.8]$$

and

$$R_0^6 = 8.79 \times 10^{23}[\kappa^2 n^{-4} Q_D J(\lambda)] \quad \text{(in Å}^6\text{)} \qquad [13.9]$$

It is important to recognize that the Förster distances are usually reported for an assumed value of κ^2, typically $\kappa^2 = \frac{2}{3}$. Once the value of R_0 is known, the rate of energy transfer can be easily calculated using

$$k_T(r) = \frac{1}{\tau_D}\left(\frac{R_0}{r}\right)^6 \qquad [13.10]$$

One can then readily determine whether the rate of transfer will be competitive with the decay rate (τ_D^{-1}) of the donor. If the transfer rate is much faster than the decay rate, then energy transfer will be efficient. If the transfer rate is slower than the decay rate, then little transfer will occur during the excited-state lifetime, and RET will be inefficient.

The efficiency of energy transfer (E) is the fraction of photons absorbed by the donor that are transferred to the acceptor. This fraction is given by

$$E = \frac{k_T}{\tau_D^{-1} + k_T} \qquad [13.11]$$

which is the ratio of the transfer rate to the total decay rate of the donor. Recalling that $k_T = \tau_D^{-1}(R_0/r)^6$, one can easily rearrange Eq. [13.11] to yield

$$E = \frac{R_0^6}{R_0^6 + r^6} \qquad [13.12]$$

This equation shows that the transfer efficiency is strongly dependent on distance when the D–A distance is near R_0 (Figure 13.2). The efficiency quickly increases to 1.0 as the D–A distance decreases below R_0. For instance, if $r = 0.1R_0$, one can readily calculate that the transfer efficiency is 0.999999, so that the donor emission would not be observable. Conversely, the transfer efficiency quickly decreases to zero if r is greater than R_0. Because E depends so strongly on distance, measurements of the distance (r) are only reliable when r is within a factor of 2 of R_0 (see Problem 13.7). If r is twice the Förster distance ($r = 2R_0$), then the transfer efficiency is 1.56%.

The transfer efficiency is typically measured using the relative fluorescence intensity of the donor, in the absence (F_D) and presence (F_{DA}) of acceptor. The transfer efficiency can also be calculated from the lifetimes under these respective conditions (τ_D and τ_{DA}):

$$E = 1 - \frac{\tau_{DA}}{\tau_D} \qquad [13.13]$$

$$E = 1 - \frac{F_{DA}}{F_D} \qquad [13.14]$$

It is important to remember the assumptions involved in the derivation of these equations. Equations [13.13] and [13.14] are only applicable to donor–acceptor pairs which are separated by a fixed distance. This situation is frequently encountered for labeled proteins. However, a single fixed donor–acceptor distance is not found for a mixture of donors and acceptors in solution, nor for donors and acceptors dispersed randomly in membranes. More complex expressions are required in these cases, and such expressions are generally derived by averaging the transfer rate over the assumed spatial distribution of donor–acceptor pairs.[5]

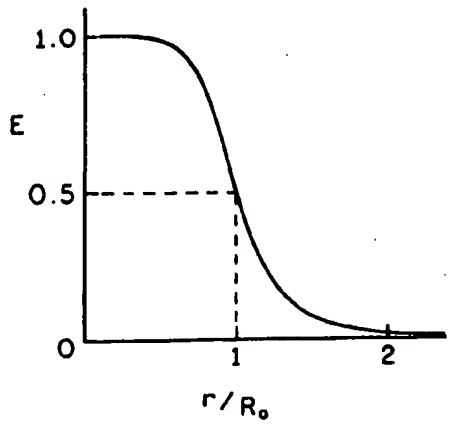

Figure 13.2. Dependence of the energy transfer efficiency (E) on distance. R_0 is the Förster distance.

The use of lifetimes in Eq. [13.13] has been a source of confusion. In Eq. [13.13] we have assumed that the decay of the donor is a single exponential in the absence (τ_D) and presence (τ_{DA}) of acceptor. Single-exponential decays are rare in biomolecules. If the intensity decays are multiexponential, then it is important to use average decay times in Eq. [13.13] which are proportional to the steady-state intensities. These averages are given by the sum of the $\alpha_i\tau_i$ products. Also, even if the donor decay is a single exponential, the decay rate in the presence of acceptor will only remain a single exponential if there is a single D–A distance. The presence of acceptors at more than one distance can result in more complex decays (Chapter 14).

Assuming that the single-distance model is appropriate, one sees that the rate of energy transfer is dependent upon R_0, which in turn depends upon κ^2, n, Q_D, and $J(\lambda)$. These factors must be known in order to calculate the distance. The refractive index is generally known from the solvent composition or is estimated for the macromolecule. The refractive index is often assumed to be close to that of water (n = 1.33) or small organic molecules (n = 1.39). The quantum yield of the donor, Q_D, is determined by comparison with standard fluorophores. Since Q_D is used as the sixth root in the calculation of R_0, small errors in Q_D do not have a large effect on R_0. The overlap integral must be evaluated for each D–A pair. The greater the overlap of the emission spectrum of the donor with the absorption spectrum of the acceptor, the higher is the value of R_0. Acceptors with larger extinction coefficients result in larger R_0 values. In the equations presented above, it was assumed that the lifetime of the donor was not altered by binding of the acceptor, other than by the rate of energy transfer. For labeled macromolecules, this may not always be the case. Allosteric interactions between the donor and acceptor sites could alter the donor lifetime by enhancement of other decay processes, or by protection from these processes. Under these circumstances, more complex analysis of the apparent transfer efficiency is required, typically by a comparison of the apparent efficiency by donor quenching and enhanced acceptor emission (Section 13.3.D).

The dependence of R_0 on spectral overlap is illustrated in Figure 13.3 for RET from structural isomers of dansyl-labeled phosphatidylethanolamine (DPE) to the eosin-labeled lipid (EPE). Each of the dansyl derivatives of DPE displays a different emission spectrum.[5] As the spectra of the DPE isomers shift to longer wavelengths, the overlap

with the absorption spectrum of EPE increases and the R_0 values increase (Table 13.1). One notices that R_0 is not very dependent upon $J(\lambda)$. For instance, for two of the D–A pairs, a 120-fold change in the overlap integral results in a 2.2-fold change in the Förster distance. This is because of the sixth-root dependence in Eq. [13.5]. It should also be noted that the visual impression of overlap is somewhat misleading because the value of $J(\lambda)$ depends on λ^4 (Eq. [13.3]). Comparison of the spectral overlap for 2,5-DPE and 1,5-DPE suggests a larger Förster distance for 1,5-DPE, whereas the calculated value is smaller. The larger Förster distance for 2,5-DPE is due to its larger quantum yield.

Because of the complexity in calculating overlap integrals and Förster distances, it is convenient to have several examples. Values of the overlap integral corresponding to the spectra in Figure 13.3 are summarized in Table 13.1.

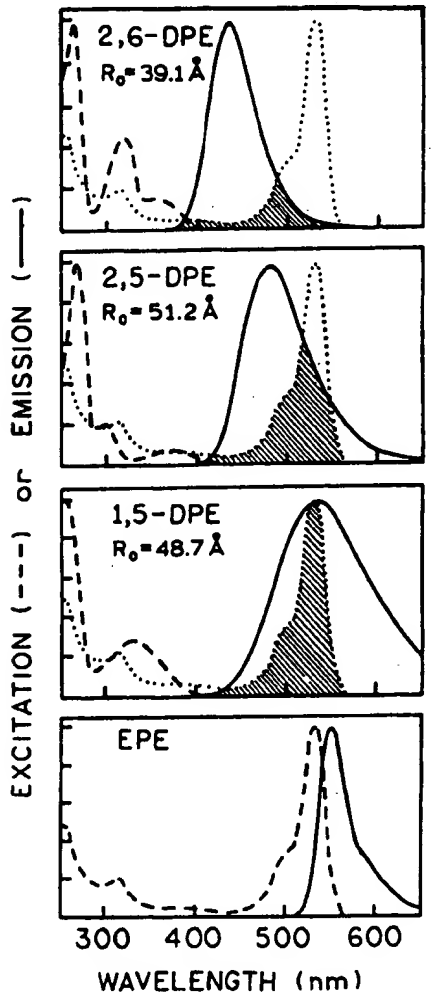

Figure 13.3. Excitation (---) and emission (—) spectra of dansyl-labeled lipids and an eosin-labeled lipid. The eosin- and dansyl-labeled compounds are N-derivatives of phosphatidylethanolamine (PE). In the designations of the dansyl-PE (DPE) derivatives, the numbers refer to the location of the dimethylamino and sulfonyl residues on the naphthalene ring of the dansyl group. The extinction coefficient of eosin-PE (EPE) is 85,000 M^{-1} cm^{-1} at 527 nm. In the top three panels, the long-wavelength absorption spectrum of eosin-PE is shown as a dotted curve. Revised from Ref. 5.

Brief Biographical Sketch of Theodor Förster

The theory for resonance energy transfer was developed by Professor Theodor Förster (Figure 13.4). He was born in Frankfurt, Germany, in 1910. He received a Ph.D. in 1933 for studies of the polarization of reflected electrons. He then became a research assistant in Leipzig, Germany, where he studied light absorption of organic compounds until 1942. In this phase of his work, he applied the newly developed principles of quantum mechanics to chemistry. His most productive period followed World War II. From 1942 to 1945, he held a professorship in Poznan, Poland, where he did not appear to publish any papers, but he did get married. In 1945 he joined the Max-Planck Institute for Physical Chemistry in Göttingen, where he wrote his classic book *Fluoreszenz Organischer Verbindungen*, which has been described as a concentrated "house bible" for the German community of spectroscopists. By 1946 Professor Förster had written his first paper on energy transfer and pointed out the importance of energy transfer in photosynthesis systems. Professor Förster was also among the first scientists to observe excited-state proton transfer, which is now described by the Förster cycle. In 1954 he discovered excimer formation. Professor Förster died of a heart attack in his car on the way to work in 1974. (For additional biographical information, see Ref. 6 and the Introduction about Theodor Förster in Ref. 7.)

13.1.A. Orientation Factor κ^2

A final factor in the analysis of the energy-transfer efficiencies is the orientation factor κ^2, which is given by

$$\kappa^2 = (\cos\theta_T - 3\cos\theta_D \cos\theta_A)^2 \qquad [13.15]$$

$$= (\sin\theta_D \sin\theta_A \cos\phi - 2\cos\theta_D \cos\theta_A)^2 \qquad [13.16]$$

In these equations, θ_T is the angle between the emission transition dipole of the donor and the absorption transition

Table 13.1. Calculated R_0 Values for RET from Structural Isomers of Dansyl-Labeled Phosphatidylethanolamine (DPE) to Eosin-Labeled Ethanolamine (EPE) and from 2,6-DPE to 2,5-DPE[a]

Donor	Acceptor	ϕ_D	$J(M^{-1}\,cm^3)$	$J(M^{-1}\,cm^3\,(nm)^4)^b$	R_0 (Å)
1,5-DPE	EPE	0.37	2.36×10^{-13}	2.36×10^{15}	48.7
2,5-DPE	EPE	0.76	1.54×10^{-13}	1.54×10^{15}	51.2
2,6-DPE	EPE	0.71	3.31×10^{-14}	3.31×10^{14}	39.1
2,6-DPE	2,5-DPE	0.71	1.3×10^{-15}	1.3×10^{13}	22.8

[a]From Ref. 5. R_0 was calculated using $n = 1.4$ and $\kappa^2 = \frac{2}{3}$.
[b]The factor of 10^{28} between $J(\lambda)$ in $M^{-1}\,cm^3$ and $M^{-1}\,cm^3\,nm^4$ arises from 1 nm = 10^{-7} cm, raised to the fourth power.

dipole of the acceptor, θ_D and θ_A are the angles between these dipoles and the vector joining the donor and the acceptor, and ϕ is the angle between the planes (Figure 13.5). Depending upon the relative orientation of donor and acceptor, κ^2 can range from 0 to 4. For collinear and parallel transition dipoles, $\kappa^2 = 4$, and for parallel dipoles, $\kappa^2 = 1$. Since the sixth root of κ^2 is taken in calculating the distance, variation of κ^2 from 1 to 4 results in only a 26% change in r. With $\kappa^2 = \frac{2}{3}$, as is usually assumed, the calculated distance can be in error by no more than 35%. However, if the dipoles are oriented perpendicular to one another, $\kappa^2 = 0$, which would result in serious errors in the calculated distance. This problem has been discussed in detail.[8–10] By measurements of the fluorescence anisotropy of the donor and the acceptor, one can set limits on κ^2 and thereby minimize uncertainties in the calculated distance.[9–11] An example of calculating the range of possible values of κ^2 is given in Section 13.2.B. In general, variation of κ^2 seems to have not resulted in major errors in the calculated distances.[12,13] Generally, κ^2 is assumed equal to $\frac{2}{3}$, which is the value for donors and acceptors that randomize by rotational diffusion prior to energy transfer. This value is generally assumed for calculation of R_0. Alternatively, one may assume that a range of static donor—acceptor orientations are present and that these orientations do not change during the lifetime of the excited state. In this case, $\kappa^2 = 0.476$.[3] For fluorophores bound to macromolecules, segmental motions of the donor and acceptor tend to randomize the orientations. Further, many

Figure 13.4. Professor Theodor Förster, May 15, 1910–May 20, 1974. Reprinted, with permission, from Ref. 6, Copyright © 1974, Springer-Verlag.

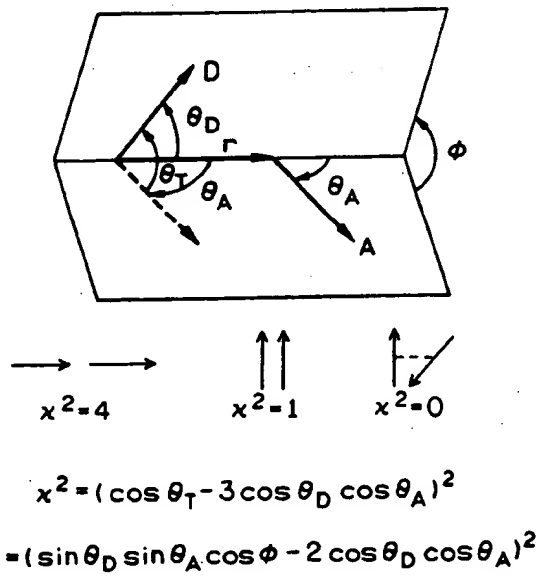

Figure 13.5. Dependence of the orientation factor κ^2 on the directions of the emission dipole of the donor and the absorption dipole of the acceptor.

donors and acceptors display fundamental anisotropies less than 0.4 owing to overlapping electronic transitions. In this case, the range of possible κ^2 values is more limited, and errors in distance are likely to be less than 10%.[14]

13.1.B. Dependence of the Transfer Rate on Distance (r), the Overlap Integral (J), and κ^2

The theory of Förster predicts that $k_T(r)$ depends on $1/r^6$ (Eq. [13.1]) and linearly on the overlap integral (Eq. [13.2]). Given the complexity and assumptions of RET theory,[4] it was important to demonstrate experimentally that these dependencies are valid. The predicted $1/r^6$ dependence on distance was confirmed experimentally.[15–17] One demonstration used oligomers of poly-L-proline, labeled on opposite ends with a naphthyl (donor) and a dansyl (acceptor) group.[15,16] Poly-L-proline forms a rigid helix of known atomic dimensions, providing fixed distances between the donor and acceptor moieties. By measuring the transfer efficiency with different numbers of proline residues, it was possible to demonstrate that the transfer efficiency in fact decreased as $1/r^6$. These data are described in detail in Problem 13.3.

The linear dependence of k_T on the overlap integral J has also been experimentally proven.[18] This was accomplished using a D–A pair linked by a rigid steroid spacer. The extent of spectral overlap was altered by changing the solvent, which shifted the indole donor emission spectrum and the carbonyl acceptor absorption spectrum. The rate of transfer was found to decrease linearly as the overlap integral decreased. These data are shown in Problem 13.4. To date, there has not been experimental confirmation of the dependence of the transfer rate on κ^2.

Another important characteristic of RET is that the transfer rate is proportional to the decay rate of the fluorophore (Eq. [13.1]). This means that for a D–A pair spaced by the R_0 value, the rate of transfer will be $k_T = \tau_D^{-1}$ whether the decay time is 10 ns or 10 ms. Hence, long-lived lanthanides are expected to display RET over distances comparable to those for the nanosecond-decay-time fluorophores, as demonstrated by transfer from Tb^{3+} to Co^{2+} in thermolysin.[19] This fortunate result occurs because the transfer rate is proportional to the emission rate of the donor. The proportionality to the emissive rate is due to the term Q_D/τ_D in Eq. [13.2]. It is interesting to speculate what would happen if the transfer rate were independent of the decay rate. In this case, a longer-lived donor would allow more time for energy transfer. Then energy transfer would occur over longer distances where the smaller rate of transfer would still be comparable to the donor decay rate.

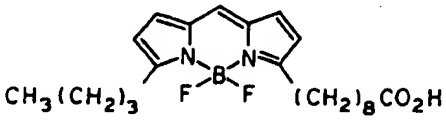

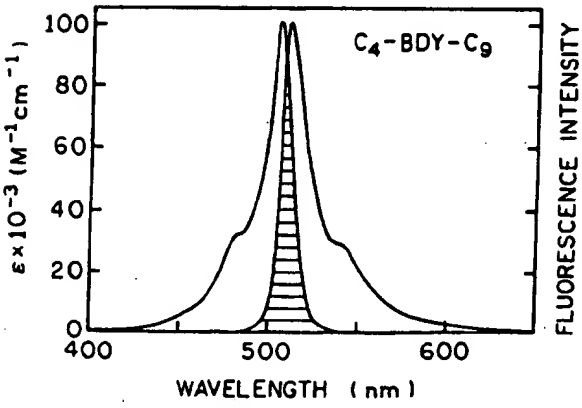

Figure 13.6. Absorption and corrected fluorescence emission (bandpass 2.5 nm) spectra of the BODIPY derivative C_4-BDY-C_9 in methanol, with shaded area representing spectral overlap. Revised and reprinted, with permission, from Ref. 20, Copyright © 1991, Academic Press, Inc.

13.1.C. Homotransfer and Heterotransfer

In the preceding sections we considered only energy transfer between chemically distinct donors and acceptors, which is called heterotransfer. RET can also occur between chemically identical molecules. Such transfer, termed homotransfer, typically occurs for fluorophores which display small Stokes' shifts. One example of homotransfer is provided by the relatively new class of fluorophores referred to as BODIPY* dyes.[20] The absorption and emission spectra of one BODIPY derivative are shown in Figure 13.6. Because of the small Stokes' shift and high extinction coefficient of these probes, the Förster distance for homotransfer is near 57 Å.[20]

At first glance, homotransfer may seem like an unlikely phenomenon, but its occurrence is rather common. For example, it is well known that antibodies labeled with fluorescein do not become more highly fluorescent with higher degrees of labeling.[21] Antibodies are typically brightest with about four fluoresceins per antibody, after which the intensity starts to decrease. This effect is attributed to the small Stokes' shift of fluorescence and homotransfer. In fact, homotransfer among fluorescent molecules was one of the earliest observations in fluores-

*BODIPY, 4,4-difluoro-4-bora-3a,4a-diaza-s-indacene. BODIPY is a trademark of Molecular Probes, Inc.

cence and was detected by a decrease in the anisotropy of fluorophores at higher concentrations.[22] The possibility of homotransfer can be readily evaluated by examination of the absorption and emission spectra. For instance, perylene would be expected to display homotransfer, but homotransfer is unlikely for quinine (Figure 1.3).

13.2. DISTANCE MEASUREMENTS USING RET

13.2.A. Distance Measurements in α-Helical Melittin

Because RET can be reliably assumed to depend on $1/r^6$, the transfer efficiency can be used to measure distances between sites in proteins. This use of energy transfer has been recently summarized in useful reviews.[12,23] These articles contain R_0 values for a number of commonly used D–A pairs and offer practical advice. The use of RET in structural biochemistry is illustrated in Figure 13.7 for the peptide melittin.[24] This peptide has 26 amino acids. A single tryptophan residue at position 19 serves as the donor. A single dansyl acceptor was placed on the N-terminal amino group. The spectral properties of this D–A pair are shown in Figure 13.8. These spectral properties result in a Förster distance of 23.6 Å (Problem 13.5).

Depending upon the solvent conditions, melittin can exist in the monomer, tetramer, α-helix, and/or random-coil state.[25–27] In the methanol–water mixture specified on Figure 13.7, melittin is in the rigid α-helical state and exists as a monomer. There is a single dansyl acceptor adjacent to each tryptophan donor, and the helical structure ensures a single D–A distance. Hence, we can use the theory

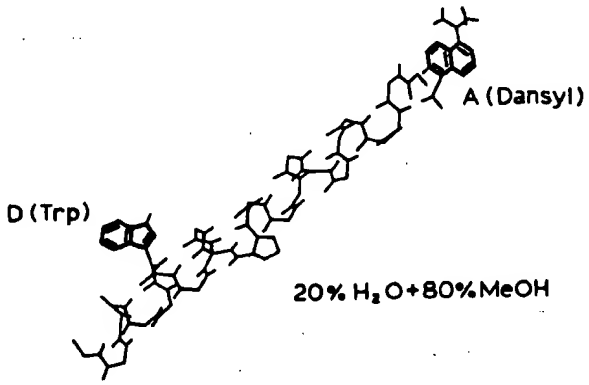

Figure 13.7. Structure of melittin in the α-helical state. The donor is tryptophan-19, and the acceptor is an N-terminal dansyl group. Revised from Ref. 24.

described above, and in particular Eqs. [13.12] and [13.14], to calculate the D–A distance.

In order to calculate the D–A distance, it is necessary to determine the efficiency of energy transfer. This can only be accomplished by comparing the intensity of the donor in the presence of acceptor (F_{DA}) with the donor intensity from a control molecule which lacks the acceptor (F_D). From Figure 13.9 one sees that the value of F_{DA}/F_D is near 0.55, so that the transfer efficiency is less than 50% ($E = 0.45$). Since E is less than 0.5, we know that the D–A distance must be larger than the R_0 value. Using Eq. [13.12], and the R_0 value of 23.6 Å, one can readily calculate that the tryptophan-to-dansyl distance is 24.4 Å.

It is important to notice the assumptions used in calculating the distance. We assumed that the orientation factor κ^2 was equal to the dynamic average of $\frac{2}{3}$. In the case of melittin, this is a good assumption because both the trp

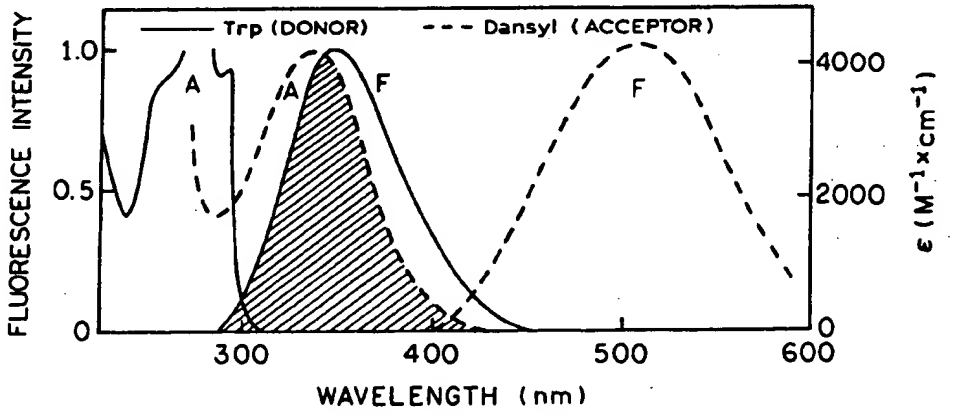

Figure 13.8. Overlap integral (shaded area) for energy transfer from a tryptophan donor to a dansyl acceptor on melittin. $R_0 = 23.6$ Å. Data from Ref. 24.

nor and dansyl acceptor are fully exposed to the liquid ase, which is highly fluid. The rotational correlation ıes for such groups are typically near 100 ps, so that the ɔoles can randomize during the excited-state lifetime. rhaps the most dangerous assumption is that the sample 100% labeled with acceptor. If melittin were incom-:tely labeled with acceptor, the measured value of F_{DA} ıuld be larger than the true value, and the calculated tance too large. Suppose that the fractional labeling with :eptor is given by f_A, so that the fractional donor popu-ion lacking acceptor is given by $1 - f_A$. In this case, Eq. 3.14] becomes[11]

$$E = 1 - \frac{F_{DA} - F_D(1 - f_A)}{F_D f_A} = \left(1 - \frac{F_{DA}}{F_D}\right)\frac{1}{f_A} \qquad [13.17]$$

r a high degree of RET donor quenching ($F_{DA}/F_D \ll 1$), mall percentage of unlabeled acceptor can result in a ge change in the calculated transfer efficiency (Problem .9).

Another assumption in calculating the trp to dansyl tance in melittin is that a single conformation exists, i.e., t there is a single D–A distance. This assumption is ɔbably safe for many proteins in the native state, particu-ly for single-domain proteins. For unfolded peptides or ıltidomain proteins, a variety of conformations can exist, ulting in a range of D–A distances. In this case, calcu-on of a single distance using Eq. [13.12] would result an apparent distance, which would be weighted toward shorter distances. Such systems are best analyzed in ms of a distance distribution (Chapter 14).

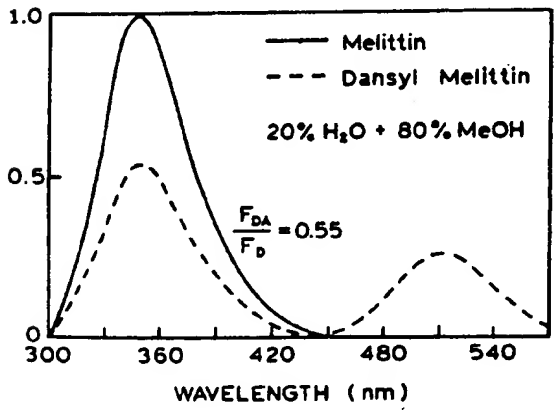

ıre 13.9. Emission spectra of the melittin donor (D) and acceptor-led melittin (D–A). Excitation at 282 nm. Revised from Ref. 24.

13.2.B. Effect of κ^2 on the Possible Range of Distances

In distance measurements using RET, there is often concern about the effects of the orientation factor κ^2. At present, there is no way to measure κ^2, short of determination of the X-ray crystal structure, in which case the distance would be known and thus there would be no reason to use energy transfer. However, it is possible to set limits on κ^2, which in turn sets limits on the range of possible D–A distances. These limits are determined from the anisotropies of the donor and acceptor, which reflect the extent of orientational averaging toward the dynamic average of $\kappa^2 = \frac{2}{3}$.

The problem of κ^2 has been discussed in detail by Dale and co-workers[8–10] and summarized by Cheung.[11] The basic idea is that the donor and acceptor move freely within a cone and that energy transfer is rapidly averaged over all available D–A orientations. Interpretation of the formalism described by Dale and co-workers[8–10] is not always straightforward, and we present the method preferred in our laboratory.[28] Although it is not possible to calculate the values of κ^2, it is possible to set upper and lower limits. These values are given by

$$\kappa^2_{min} = \frac{2}{3}\left[1 - \frac{(d_D^x + d_A^x)}{2}\right] \qquad [13.18]$$

$$\kappa^2_{max} = \frac{2}{3}(1 + d_D^x + d_A^x + 3d_D^x d_A^x) \qquad [13.19]$$

where

$$d_i^x = \left(\frac{r_i}{r_0}\right)^{1/2} \qquad [13.20]$$

The value of d_i^x represents the depolarization factor due to segmental motion of the donor (d_D^x) or acceptor (d_A^x), but not the depolarization due to overall rotational diffusion of the protein. Overall rotational diffusion is not important because it does not change the D–A orientation. The values of r_i and r_0 are often taken as the steady-state and fundamental anisotropies, respectively, of the donor or acceptor. If the donor and acceptor do not rotate relative to each other during the excited-state lifetime, then $d_D^x = d_A^x = 1.0$, and $\kappa^2_{min} = 0$ and $\kappa^2_{max} = 4$. If both D and A are independently and rapidly rotating over all space, $\kappa^2_{min} = \kappa^2_{max} = \frac{2}{3}$.

There are several ways to obtain the values of d_D^x and d_A^x. The easiest method is to determine the anisotropy decays of the donor and acceptor, the latter when directly excited. This calculation of a range of κ^2 values is illustrated by the anisotropy decays measured for the trypto-

phan donor and dansyl acceptor in α-helical melittin (Table 13.2). Both the donor and the acceptor display two correlation times, one near 2 ns due to overall protein rotation, and a shorter correlation time near 0.3 ns due to segmental motions of the donor and the acceptor. It is these faster motions which randomize κ^2. The values of d_D^x and d_A^x are given by the ratio of the long-correlation-time amplitude to the total anisotropy. Hence, for melittin,

$$d_D^x = \left(\frac{0.174}{0.294}\right)^{1/2} = 0.77 \qquad [13.21]$$

$$d_A^x = \left(\frac{0.135}{0.300}\right)^{1/2} = 0.67 \qquad [13.22]$$

Using these values and Eqs. [13.18] and [13.19], one can calculate the limits on κ^2, $\kappa^2_{min} = 0.19$ and $\kappa^2_{max} = 2.66$.

Once the limiting values of κ^2 are known, one may use these values to calculate the maximum and minimum values of the distance that are consistent with the data. In calculating these distances, one must remember that R_0 was calculated with an assumed value of $\kappa^2 = \frac{2}{3}$. Hence, the minimum and maximum distances are given by

$$r_{min} = \left(\frac{\kappa^2_{min}}{2/3}\right)^{1/6} r\left(\frac{2}{3}\right) \qquad [13.23]$$

$$r_{max} = \left(\frac{\kappa^2_{max}}{2/3}\right)^{1/6} r\left(\frac{2}{3}\right) \qquad [13.24]$$

where $r(\frac{2}{3})$ is the distance calculated assuming $\kappa^2 = \frac{2}{3}$. Using the limiting values of κ^2, one finds for the example given above that the distance can be from 0.81 to 1.26 of $r(\frac{2}{3})$, the distance calculated with the assumed value of $\kappa^2 = \frac{2}{3}$. While this range may seem large, it should be remembered that there is an additional depolarization factor due to the transfer process itself, which will further randomize κ^2 toward $\frac{2}{3}$. Equations [13.18]–[13.20] provide a worst-case estimate, which usually overestimates the effects of κ^2 on the calculated distance. For fluorophores with mixed polarization, $r_0 < 0.3$, the error in distance is thought to be below 10%.[14]

Table 13.2. Anisotropy Decays for α-Helical Melittin[a]

Fluorophore	r_{0i}	ϕ_i (ns)
Tryptophan-19[b]	0.120	0.23
	0.174	1.77
N-terminal dansyl	0.165	0.28
	0.135	2.18

[a]From Ref. 24.

[b]Determined for donor-only melittin. Similar amplitudes and correlation times were found for trp-19 in dansyl-melittin.

There are two other ways to obtain the depolarization factors. One method is to construct a Perrin plot in which the steady-state polarization is measured for various viscosities. Upon extrapolation to the high-viscosity limit, the $1/r_0^{app}$ intercept (Section 10.5) is typically larger than $1/r_0$ in frozen solution. This difference is usually attributed to segmental probe motions and can be used to estimate the depolarization factor, $d_i^x = (r_0^{app}/r_0)^{1/2}$. Another method is to estimate the expected steady-state anisotropy from the lifetime and correlation time of the protein and to use these data to estimate d_D^x and d_A^x (Problem 13.8). The basic idea is to estimate d_A^x and d_D^x by correcting for the decrease in anisotropy resulting from rotational diffusion of the protein. Any loss in anisotropy, beyond that calculated for overall rotation, is assumed to be due to segmental motions of the donor or acceptor.

13.2.C. Protein Folding Measured by RET

Energy transfer has also been widely useful for measurements of protein folding. One example is for the protein serine hydroxymethyltransferase. This protein typically has three tryptophan residues, at positions 16, 183, and 385.[29] The acceptor was a pyridoxyl 5′-phosphate (PyP) residue covalently linked to lysine-229. One expects protein folding or unfolding to affect the distance from each of the tryptophan residues to PyP, and thus one expects the extent of RET to be different for the native and folded proteins.

The presence of three tryptophan residues results in emission from three donors, which would be practically impossible to interpret. For this reason, single-tryptophan mutants were prepared which each lacked the other two trp residues. This procedure results in a single trp–PyP pair for each mutant protein. Emission spectra are shown for the trp-183 mutant in Figure 13.10. The protein was initially in 8*M* urea, resulting in a random-coil state; the initial emission spectrum is shown as the dashed curve in Figure 13.10. Upon dilution into buffer without urea, the protein began to refold, as seen by a decrease in the trp-donor emission and an increase in the PyP-acceptor emission. The intensity of the PyP emission increases upon refolding due to increased RET from trp-183. (Enhancement of acceptor emission is described in more detail in Section 13.3.D.) The availability of three single-tryptophan mutants allowed studies of refolding of specific sites on the protein. The PyP acceptor emission at 380 nm was

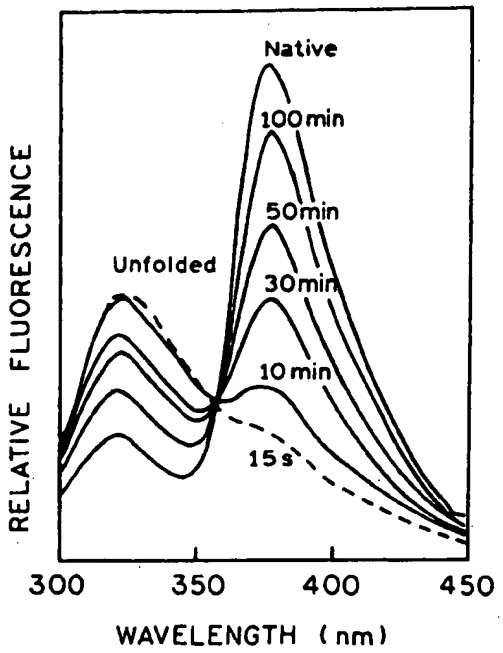

Figure 13.10. Emission spectra of trp-183 in PyP-5'-serine hydroxymethyltransferase during refolding. Excitation at 290 nm. Revised from Ref. 29.

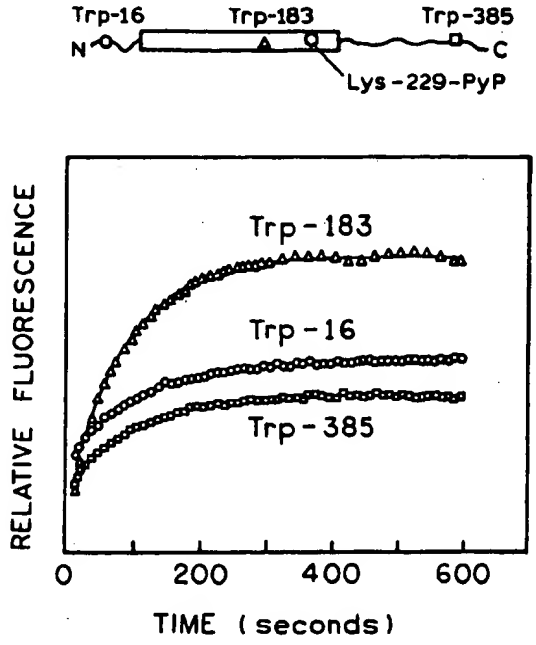

Figure 13.11. Time-dependent intensity of PyP at 380 nm in serine hydroxymethyltransferase during refolding of the single-tryptophan mutants. Excitation at 290 nm. Revised from Ref. 29.

neasured during refolding for each of the mutants (trp-183, trp-16, and trp-385 in Figure 13.11), providing information about the folding pathway. For this protein, the greatest acceptor enhancement is seen for the trp-183 nutant, suggesting that trp-183 is closest to PyP in the olded protein. Less transfer is seen from the other two ryptophan residues. The extent of energy transfer from ach tryptophan residue allowed determination of the trp-o-PyP distances. By such experiments, one can determine vhich region of the protein folds first and thus gain an nderstanding of the folding pathway. These experiments n protein folding represent an important class of experiments based on protein engineering and site-directed mutagenesis. These techniques of molecular biology make it ossible to simplify the spectral signal from multitrypto-han proteins to obtain structural information.

3.2.D. Orientation of a Protein-Bound eptide

n the presence of calcium, calmodulin is known to interact vith a number of proteins and peptides. One example is inding of a peptide from myosin light-chain kinase MLCK) to calmodulin.[30] Such peptides are known to bind n the cleft between the two domains of calmodulin (Figure 3.12). When bound to calmodulin, the MLCK peptide

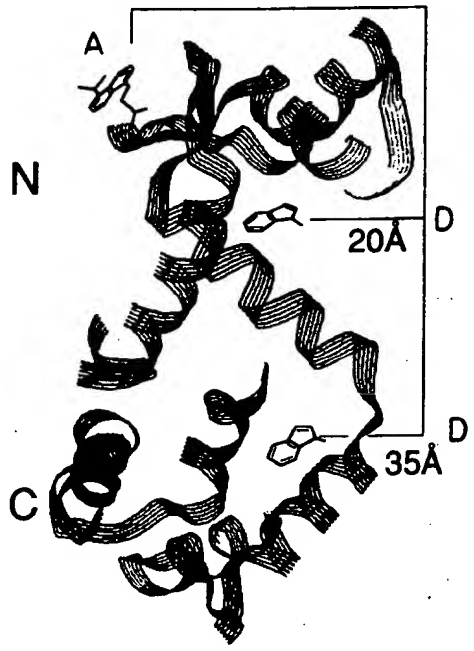

Figure 13.12. Structure of spinach calmodulin. The acceptor is AEDANS on cysteine-26 of calmodulin. The tryptophan donor is on the MLCK peptides shown in Figure 13.13. Revised and reprinted, with permission, from Ref. 30, Copyright © 1992, American Chemical Society.

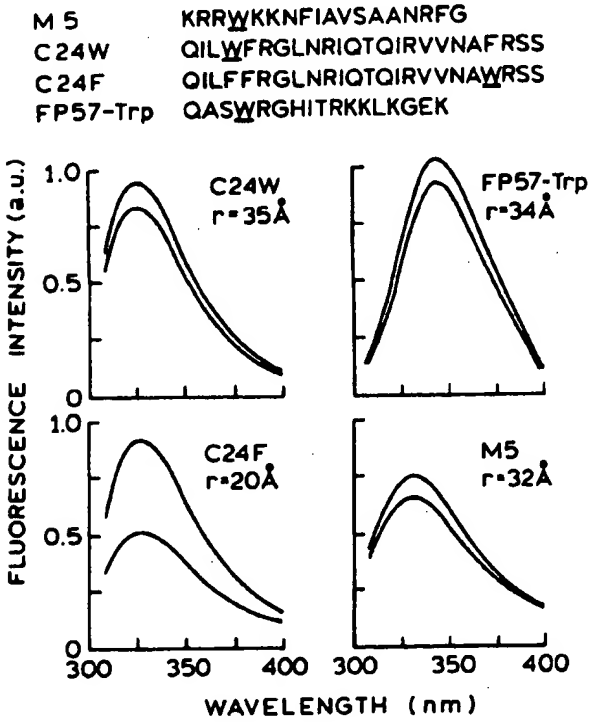

Figure 13.13. Emission spectra of MLCK peptides when free in solution and when bound to AEDANS-calmodulin. The upper and lower spectra in each panel correspond to the peptide emission spectra in the absence and in the presence of AEDANS-calmodulin, respectively. The peptide sequences are shown at the top of the figure, and the calculated distances are shown with the spectra. Excitation was at 295 nm. Revised and reprinted, with permission, from Ref. 30, Copyright © 1992, American Chemical Society.

was known to adopt an α-helical conformation. However, the direction of peptide binding to calmodulin was not known.

Information on the direction of binding was obtained by studying four similar peptides, each of which contained a single tryptophan residue, which served as the donor (Figure 13.13). Calmodulin typically contains only tyrosine residues, so an intrinsic acceptor was not available. This problem was solved by using calmodulin from spinach, which contains a single cysteine residue at position 26. This residue was labeled with 1,5-IAEDANS, which contains a thiol-reactive iodoacetyl group. The Förster distances for trp-to-AEDANS energy transfer ranged from 21 to 24 Å.

Emission spectra of the tryptophan-containing peptides are shown in Figure 13.13. The excitation wavelength was 295 nm to avoid excitation of the tyrosine residues in calmodulin. Upon binding of AEDANS-calmodulin, the tryptophan emission of each peptide was quenched. One of the peptides showed a transfer efficiency of 54%, and the remaining three peptides showed efficiencies ranging from 5 to 16%. These results demonstrated that the N-terminal region of the peptides bound closely to the N-terminal domain of calmodulin and illustrate how structural information can be obtained by comparative studies of analogous structures.

13.3. USE OF RET TO MEASURE MACROMOLECULAR ASSOCIATIONS

Energy transfer is widely useful in biochemistry even apart from its application for the measurement of distances. This is because energy transfer occurs independently of the linker joining the donor and acceptor and depends only on the D–A distance. Hence, any process bringing the donor and acceptor into close proximity will result in energy transfer. This includes biochemical association reactions, as will be illustrated below for protein subunits and DNA oligomers.

13.3.A. Dissociation of the Catalytic and Regulatory Subunits of a Protein Kinase

Cyclic 3′,5′-adenosine monophosphate (cAMP) is an important second messenger in cellular transduction pathways, and it is thus important to develop optical means to detect cAMP. Nucleotides are weakly fluorescent or nonfluorescent, so that it is not practical to use the intrinsic emission of cAMP. One method to detect cAMP is based on the effect of cAMP on the cAMP-dependent protein kinase.[31] The basic idea is to label the protein subunits with donors and acceptors. The presence of cAMP alters the extent of RET, which can be monitored by the donor or acceptor emission.

The cAMP-dependent protein kinase (PK) is composed of four units, two catalytic (C) and two regulatory (R) subunits. These subunits were thought to dissociate in the presence of the substrate cAMP and in the presence of protein kinase inhibitor (PKI). The association of the catalytic (C) and regulatory (R) subunits was examined by covalently labeling the subunits with a fluorescein (Fl-C) and a rhodamine (Rh-R) derivative, respectively.[32] The actual probes used were carboxyfluorescein succinimidyl ester and Texas Red sulfonyl chloride, which is a rhodamine derivative. Absorption and emission spectra are shown in Figure 13.14. The Förster distance for this D–A pair was 51.3 Å and was thus suited for distance measurements between protein subunits. For calculation of R_0, the quantum yield of the donor was taken as 0.5, κ^2 was

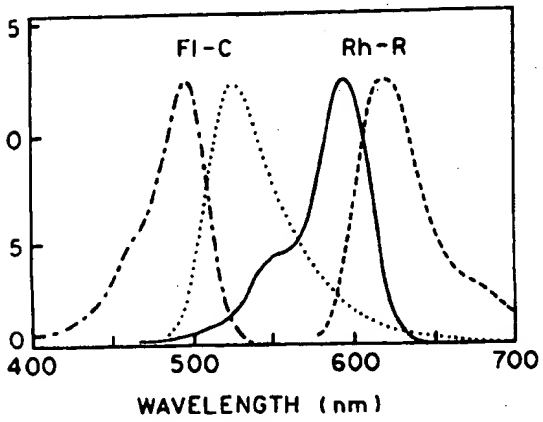

e 13.14. Spectral overlap of the fluorescein-labeled catalytic it (Fl-C) and the Texas Red-labeled regulator subunit (Rh-R) of a -dependent protein kinase. –·–, Absorption spectrum of Fl-C; ···, on spectrum of Fl-C; ———, absorption spectrum of Rh-R; – –, on spectrum of Rh-R. Revised and reprinted, with permission, from 2, Copyright © 1993, American Chemical Society.

ned equal to $\frac{2}{3}$, and the maximum extinction coeffi- of the acceptor was set equal to 85,000 M^{-1} cm^{-1}. on addition of cAMP, the extent of energy transfer ased (Figure 13.15), consistent with a 10-Å increase e D–A distance. This decrease in RET could be preted in terms of a displacement of the donor and otor to more distant regions of the protein (Figure 5). While the extent of RET allows a distance calcula- this is not necessary. The fact that energy transfer still rs in the protein kinase with bound cAMP demon-

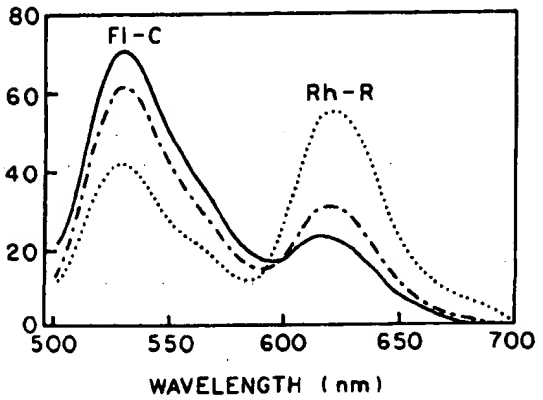

e 13.15. Effect of cAMP and protein kinase inhibitor (PKI) on ission spectrum of a donor- and acceptor-labeled cAMP-dependent n kinase. The emission spectrum of the holoenzyme without cAMP (···) and the emission spectra recorded following addition of cAMP and PKI (———) are shown. Revised and reprinted, with permis- rom Ref. 32, Copyright © 1993, American Chemical Society.

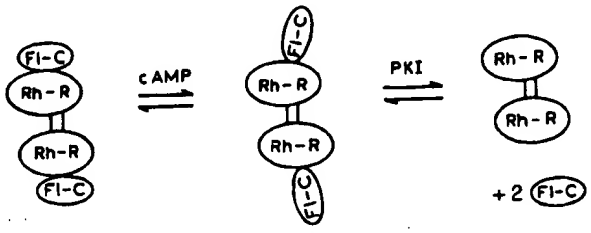

Figure 13.16. Effect of cAMP and protein kinase inhibitor (PKI) on the structure and association of cAMP-dependent protein kinase. The holoenzyme consists of two catalytic and two regulatory subunits. Revised from Refs. 31 and 32.

strates that the subunits are still associated in the presence of cAMP. If the subunits were dissociated by cAMP, energy transfer would be eliminated. This is because for unlinked donors and acceptors, the acceptor concentrations need to be in the millimolar range for Förster transfer to occur (Chapter 15).

The protein kinase was examined further by addition of PKI, which resulted in elimination of energy transfer (Figure 13.15). While one could argue about changes in D–A distance versus protein dissociation as the cause of this effect, the important point from these data is that RET can be used as a proximity sensor. For dilute biochemical solutions, energy transfer between nonassociated species can usually be ignored unless the acceptor concentrations are very high (millimolar). Binding will bring donor and acceptor within the Förster distance, resulting in energy transfer. This example shows how RET can be used to measure the extent of association even without knowledge of the Förster distance. Of course, such data could be used to measure the dissociation constant of cAMP from the protein (Problem 13.6). Calculation of the distance is not needed to calculate the dissociation constant. Use of the donor intensity provides a simple method to monitor the rates and extents of any association reaction.

It is important to remember the possibility of inner filter effects, which can distort the measured intensities of the donors or acceptors.[33] For instance, in the previous example suppose that the fluorescence emission was measured at 550 nm, where the acceptor extinction coefficient is near 33,000 M^{-1} cm^{-1}. To maintain the acceptor absorbance below 0.05, the concentration of the acceptor-labeled protein must be below 1.5μM. If higher acceptor concentrations are used, the intensity values must be corrected for the absorption at the excitation and/or emission wavelength.

13.3.B. RET Calcium Indicators

The dependence of RET on proximity has been used to develop indicators for calcium. One example used a pep-

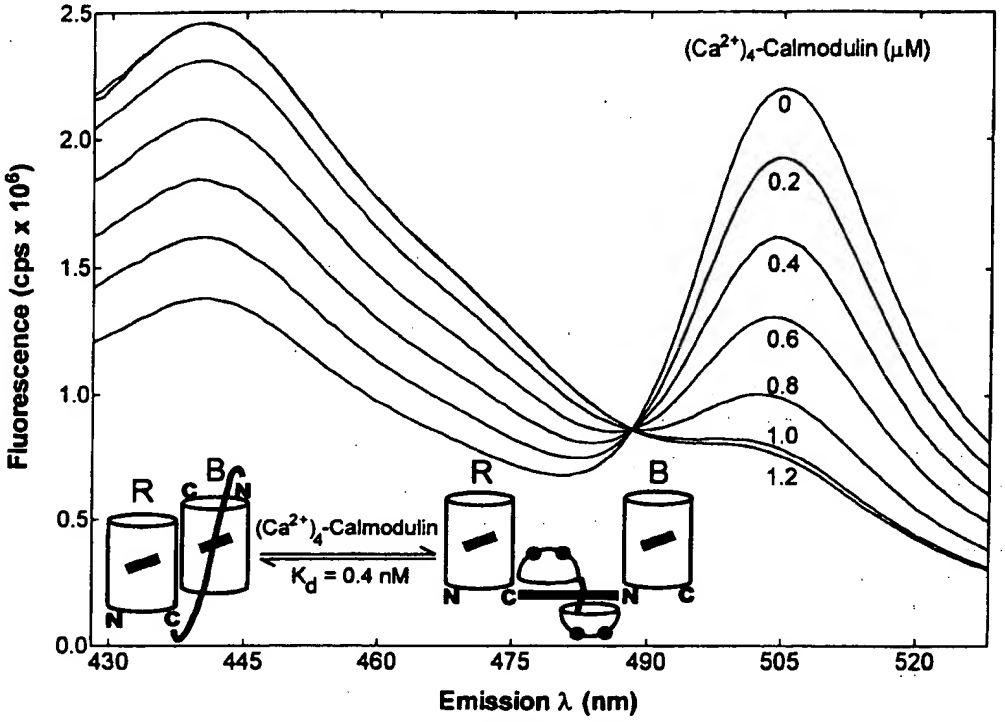

Figure 13.17. An RET calcium indicator composed of calmodulin and two GFP mutants (R and B) linked by the MLCK which binds to calmodulin. From Ref. 34.

tide from MLCK to link two mutants of green fluorescent protein (GFP).[34] By modification of the amino acid sequence of GFP, it is possible to create mutant proteins that emit at shorter or longer wavelengths. Two GFP mutants which would undergo energy transfer, a red (R) and a blue (B) GFP, were selected. These GFPs were placed on opposite ends of the MLCK peptide. In the presence of calcium, calmodulin exposes a hydrophobic surface, which can bind to a number of proteins, including the MLCK peptide. When calmodulin bound the MLCK peptide, the R and B GFPs became more widely separated, and the extent of energy transfer decreased (Figure 13.17). Similar results were obtained for calmodulin covalently linked to the MLCK peptide and the GFPs.[35] An important aspect of this work is that the genes for GFP-labeled proteins can be prepared by molecular biology and expressed in bacteria. This approach bypasses the usual difficulties associated with covalent labeling of specific sites on proteins.

13.3.C. Association Kinetics of DNA Oligomers

The general usefulness of RET in investigations of association reactions is illustrated by studies of donor- and acceptor-labeled DNA oligomers that have a complementary base sequence.[36–38] In such studies, one strand is typically labeled with fluorescein (Fl), and the complementary DNA strand is labeled with rhodamine (Rh) (Figure 13.18). Upon association, the fluorescein donor is quenched.[38] The fluorescence of the donor can be used to measure the rates of association or dissociation of the DNA oligomers (Figure 13.19). In other studies, the extent of RET has been used to detect changes in the melting temperature of DNA oligomers. The melting temperature was found to be sensitive to even a single base pair mismatch.[37]

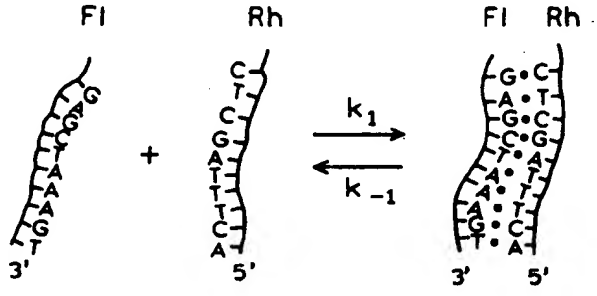

Figure 13.18. DNA association kinetics observed using oligonucleotides labeled with fluorescein (Fl) and rhodamine (Rh). Revised from Ref. 38.

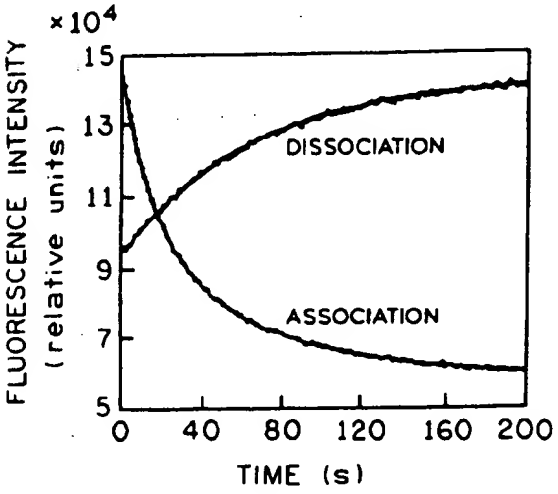

Figure 13.19. Association and dissociation kinetics of complementary donor- and acceptor-labeled oligonucleotides, observed using the donor (fluorescein) emission intensity. Revised and reprinted, with permission, from Ref. 38, Copyright © 1993, American Chemical Society.

RET has also been used to measure the catalytic activity of restriction enzymes, which cleave DNA at specific sites in the sequence. One example of this application is on investigation of the PaeR7 endonuclease.[39] For this restriction enzyme, the recognition site consists of a CTCGAG sequence. Fluorescein-donor- and rhodamine-acceptor-labeled oligonucleotides served as the substrate (Figure 13.20). Binding of the DNA strands resulted in donor quenching and acceptor enhancement. Digestion with the endonuclease resulted in an increase in donor fluorescence equivalent to that in the donor-only control. When the donors and acceptors are on separate DNA fragments, the solution is too dilute for energy transfer.

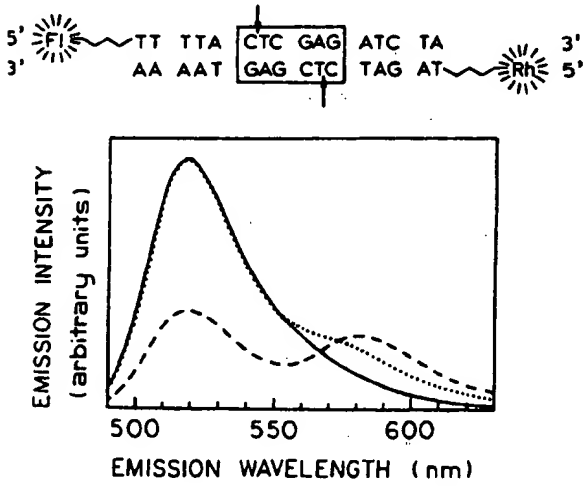

Figure 13.20. Principle of the RET endonuclease assay. The emission spectrum of a 16-mer donor strand (—) is quenched upon addition of its complementary rhodamine-labeled strand (– – –). The fluorescence spectrum taken after addition of PaeR7 endonuclease (· · ·) shows full recovery of the fluorescein emission intensity of the donor strand, indicating complete cleavage of the DNA duplex substrate. The peak at 580 nm in the emission spectra of duplex samples is due to the rhodamine acceptor fluorescence. Revised from Ref. 39.

The concept used in the endonuclease assay was the elimination of RET by enzymatic breakage of a covalently linked D–A pair. This concept has been applied in a variety of other circumstances,[40] including assay of an HIV-1 endonuclease,[41] which is involved in integrating the HIV into the host DNA. RET has also been used to measure the activity of an HIV protease,[42] proteolytic cleavage of linked derivatives of GFP,[43] and the activity of ribozymes in cleaving RNA[44] and as the basis of a general assay for DNA cleavage.[45]

13.3.D. Energy Transfer Efficiency from Enhanced Acceptor Fluorescence

In a RET experiment the acceptor must absorb light at donor emission wavelengths, but the acceptor does not need to be fluorescent. However, fluorescent acceptors are often used. In these cases, light absorbed by the donor and transferred to the acceptor appears as enhanced acceptor emission. This enhanced acceptor emission can be seen in Figure 13.15 at 620 nm for the Rh-labeled subunits of protein kinase when bound to the Fl-labeled subunits and in Figure 13.20 at 580 nm when the donor and acceptor DNA oligomers are associated. By extrapolating the emission spectrum of the donor, one can see that its emission extends to the acceptor wavelengths. Hence, the intensity measured at the acceptor wavelength typically contains some contribution from the donor.

Use of the acceptor intensities is complicated by the need to account for directly excited acceptor emission, which is almost always present.[11,46] In the case of protein kinase, the acceptor emission without RET (shown as the solid curve in Figure 13.15) is about 40% of the intensity with RET. This occurs because the acceptor absorbs at the excitation wavelength used to excite the donor, resulting in acceptor emission without RET.

Calculation of the transfer efficiency from the enhanced acceptor emission requires careful consideration of all the interrelated intensities. Assuming that the donor does not emit at the acceptor wavelength, the efficiency of transfer is given by

$$E = \frac{\varepsilon_A(\lambda_D^{ex})}{\varepsilon_D(\lambda_D^{ex})}\left[\frac{F_{AD}(\lambda_A^{em})}{F_A(\lambda_A^{em})} - 1\right]\left(\frac{1}{f_D}\right) \qquad [13.25]$$

In this expression, $\varepsilon_A(\lambda_D^{ex})$ and $\varepsilon_D(\lambda_D^{ex})$ are the extinction coefficients (single D–A pairs) or absorbance (multiple acceptors) of the acceptor and the donor at the donor excitation wavelength (λ_D^{ex}), and f_D is the fractional labeling with the donor. The acceptor intensities are measured at an acceptor emission wavelength (λ_A^{em}) in the absence [$F_A(\lambda_A^{em})$] and in the presence [$F_{AD}(\lambda_A^{em})$] of donor. This expression with $f_D = 1.0$ can be readily obtained by noting that $F_A(\lambda_A^{em})$ is proportional to $\varepsilon_A(\lambda_D^{ex})$ and $F_{AD}(\lambda_A^{em})$ is proportional to $\varepsilon_A(\lambda_D^{ex}) + E\varepsilon_D(\lambda_D^{ex})$. The accuracy of the measured E value is typically less than when using the donor emission (Eq. [13.14]).

It is also important to remember that it may be necessary to correct further for the donor emission at λ_A, which is not accounted for in Eq. [13.25]. The possibility of donor emission at λ_A is easily seen from the donor emission spectra in Figures 13.15 and 13.20. The presence of donor emission at the acceptor wavelength, if not corrected for in measuring the acceptor intensities, will result in an apparent transfer efficiency larger than the actual value (see Problem 13.11). Equation [13.25] can also be applied when multiple acceptors are present, that is, in the case of unlinked donor and acceptor pairs (Chapter 15). In this case, $\varepsilon_D(\lambda_D^{ex})$ and $\varepsilon_A(\lambda_D^{ex})$ are replaced by the optical densities of the donor [$OD_D(\lambda_D^{ex})$] and of the acceptor [$OD_A(\lambda_D^{ex})$] at the donor excitation wavelength. The factor $1/f_D$ in Eq. [13.25] is the fractional labeling with the donor. When measuring the acceptor emission, it is important to have complete donor labeling, $f_D = 1.0$.

Occasionally, it is difficult to obtain the transfer efficiency from the sensitized acceptor emission. One difficulty is a precise comparison of the donor-alone and donor–acceptor pair at precisely the same concentration. The need for two samples at the same concentration can be avoided if the donor- and acceptor-labeled sample can be enzymatically digested so as to eliminate energy transfer.[47] Additionally, methods allowing comparison of the donor-alone and donor–acceptor spectra without requiring the concentrations to be the same have been developed. This is accomplished by relying on the shape of the donor emission to subtract its contribution from the emission spectrum of the D–A pair. These methods are best understood by reading the original descriptions.[48,49]

Finally, one should be aware of the possibility that the presence of the acceptor affects the donor fluorescence by a mechanism other than RET. Such effects could occur due to allosteric interactions between the donor and acceptor sites. For example, the acceptor may block diffusion of a quencher to the donor, or it may cause a shift in protein conformation that exposes the donor to solvent. If binding of the acceptor results in quenching of the donor by some other mechanism, then the transfer efficiency determined from the donor will be larger than the true value. In such cases, the transfer efficiency determined from enhanced acceptor emission is thought to be the correct value. The possibility of non-RET donor quenching can be addressed by comparison of the transfer efficiencies observed from donor quenching and acceptor sensitization[50] (see Problem 13.11).

13.4. ENERGY TRANSFER IN MEMBRANES

In the examples of RET described so far, there was a single acceptor attached to each donor molecule. The situation becomes more complex for unlinked donors and acceptors. In this case the bulk concentration of acceptors is important because the acceptor concentration determines the D–A proximity. Also, one needs to consider the presence of more than a single acceptor around each donor. In spite of the complexity, RET has considerable potential for studies of lateral organization in membranes. For example, consider a membrane which contains regions that are in the liquid phase and regions that are in the solid phase. If the donor and acceptor both partition into the same region, one expects the extent of energy transfer to be increased, relative to that expected for a random distribution of donors and acceptors between the phases. Conversely, if donor and acceptor partition into different phases, the extent of energy transfer will decrease relative to a random distribution, an effect which has been observed.[51] Alternatively, consider a membrane-bound protein. If acceptor-labeled lipids cluster around the protein, then the extent of energy transfer will be greater than expected for acceptor randomly dispersed in the membrane. Energy transfer to membrane-localized acceptors can be used to measure the distance of closest approach to a donor site on the protein or the distance from the donor to the membrane surface.

RET in membranes is typically investigated by measuring the transfer efficiency as the membrane acceptor concentration is increased. Quantitative analysis of such data requires knowledge of the extent of energy transfer expected for fluorophores randomly distributed on the surface of a membrane. This is a complex problem which requires one to consider the geometric form of the bilayer (planar or spherical) and transfer between donors and acceptors which are on the same side of the bilayer as well as those on opposite sides. A variety of approaches have been used,[5,52–60] and, in general, numerical simulations and/or computer analyses are necessary. These theories are complex and not easily summarized. The complexity of the problem is illustrated by the fact that an analytical expression for the donor intensity for energy transfer in two

ıensions only appeared in 1964[61] and was extended to ›w an excluded volume around the donor in 1979.[53] T to multiple acceptors in one, two, and three dimens ns is described in more detail in Chapter 15. Several of se results are presented here to illustrate the general m of the expected data.

\ general description of energy transfer on a two-dimenal surface has been given by Fung and Stryer.[5] Assumno homotransfer between the donors, and no diffusion ing the donor excited-state lifetime, the intensity decay he donor is given by

$$I_D(t) = I_D^0 \exp(-t/\tau_D) \exp[-\sigma S(t)] \qquad [13.26]$$

ere

$$S(t) = \int_{r_c}^{\infty} \{1 - \exp[-(t/\tau_D)(R_0/r)^6]\} 2\pi r\, dr \qquad [13.27]$$

hese equations $\exp[-\sigma S(t)]$ describes that portion of the ıor decay due to RET, σ is the surface density of the eptor, and r_c is the distance of closest approach between donor and acceptors. The energy-transfer efficiency be calculated by an equation analogous to Eqs. [13.13] [13.14], except that the intensities or lifetimes are :ulated from integrals of the donor intensity decay:

$$E = 1 - \frac{1}{\tau_D} \int \frac{I_D(t)}{I_D^0}\, dt \qquad [13.28]$$

quations [13.26]–[13.28] are moderately complex to /e and require use of numerical integration. However, approach is quite general and can be applied to a wide ety of circumstances by using different expressions for that correspond to different geometric conditions. ure 13.21 shows the calculated transfer efficiencies for se in which the donor and acceptors are constrained to lipid–water interface region of a bilayer. Several fea- s of these predicted data are worthy of mention. The :iency of transfer increases with R_0 and is independent he concentration of donor. The absence of energy sfer between donors is generally a safe assumption :ss the donor displays a small Stokes' shift or the donor :entration is high, conditions which favor homotrans- Only small amounts of acceptor, 0.4 mol %, can result asily measured quenching. For example, with $R_0 = 40$ ıe transfer efficiency is near 50% for just 0.8 mol % :ptor, or one acceptor per 125 phospholipid molecules. ne may readily visualize how energy quenching data ıd be used to determine whether the distributions of or and acceptor are random. Using the calculated value $_0$, one compares the measured extent of donor quenching with the observed efficiency. If the measured quenching efficiency exceeds the calculated value, then a preferential association of donors and acceptors within the membrane is indicated.[62] Less quenching would be observed if the donor and acceptor are localized in different regions of the membrane or if the distance of closest approach is restricted due to steric factors. We note that these calculated values shown in Figure 13.21 are strictly true only for transfer between immobilized donor and acceptor on one side of a planar bilayer. However, this simple model is claimed to be a good approximation for a spherical bilayer.[5] For smaller values of R_0, transfer across the bilayer is not significant.

It is also instructive to examine the time-resolved decays of the donor in the presence of acceptor (Figure 13.22). In the presence of acceptor, the donor decays become significantly nonexponential, especially at higher acceptor concentrations. The origin of this nonexponential decay is the time-dependent distribution of acceptors around the excited donors. At short times following excitation, there exist more donors with nearby acceptors. The donors with nearby acceptors decay more rapidly because of the dis-

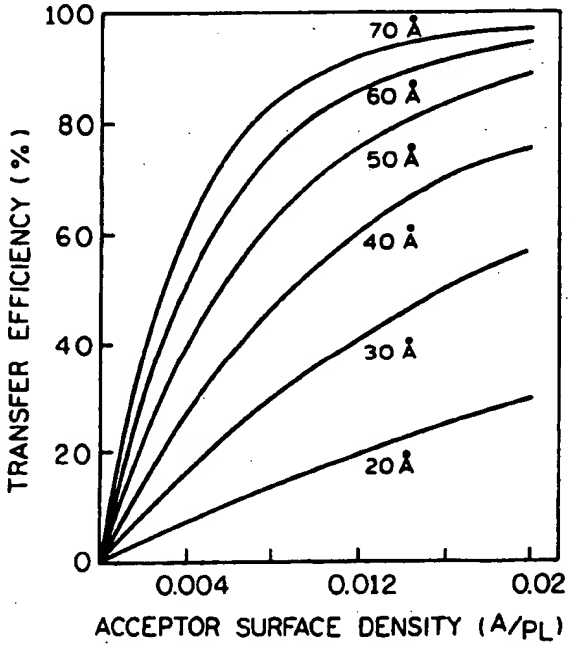

Figure 13.21. Calculated efficiencies of energy transfer for donor–acceptor pairs localized in a membrane. The distances labeled on the curves are the R_0 values for energy transfer, and A/PL is the acceptor-to-phospholipid molar ratio. The area per phospholipid was assumed to be 70 Å^2, so the distance of closest approach was 8.4 Å. Revised from Ref. 5.

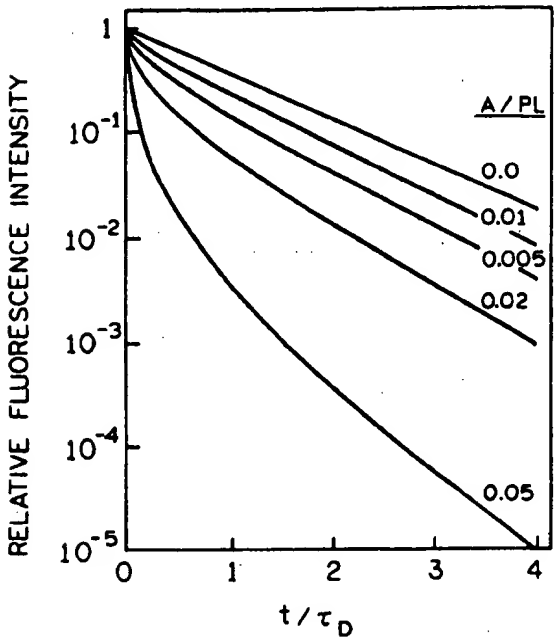

Figure 13.22. Calculated time-resolved decays of donor fluorescence for membrane-bound donors and acceptors. For these calculations R_0 = 40 Å. The values labeled on the curves are the acceptor-to-phospholipid molar ratios (A/PL). Revised from Ref. 5.

tance dependence of energy transfer. At later times, the donors with nearby acceptors have decayed, and the emission results preferentially from donors without nearby acceptors. The decay time of these donors is longer, owing to a slower rate of energy transfer to more distant acceptors.

There is considerable information in these time-resolved decays, and methods to recover this information are described in Chapter 15. In the more general case, the distance between donor and acceptor can vary both as a result of a range of distances and by diffusion. Both factors affect the rates of energy transfer and must be considered in any such analysis.

13.4.A. Lipid Distributions around Gramicidin

Gramicidin is a linear polypeptide antibiotic containing D-and L-amino acids and four tryptophan residues. Its mode of action involves increasing the permeability of membranes to cations and protons. In membranes, this peptide forms a dimer (Figure 13.23)[63] that contains a 4-Å diameter aqueous channel which allows diffusion of cations. The nonpolar amino acids are present on the outside of the helix and are thus expected to be exposed to the acyl side-chain region of the membrane. Hence, gramicidin provides an ideal model with which to examine energy transfer from a membrane-bound protein to membrane-bound acceptors.

It was of interest to determine if membrane-bound gramicidin was surrounded by specific types of phospholipids. This question was addressed by measurement of the transfer efficiencies from the tryptophan donor to dansyl-labeled phosphatidylcholine (PC), 1-acyl-2-[11-[*N*-[5-(dimethylamino)naphthalene-1-sulfonyl]amino]undecanoyl]phosphatidylcholine. The lipid vesicles were composed of PC and phosphatidic acid (PA).[64] Emission spectra of gramicidin bound to PC–PA membranes are

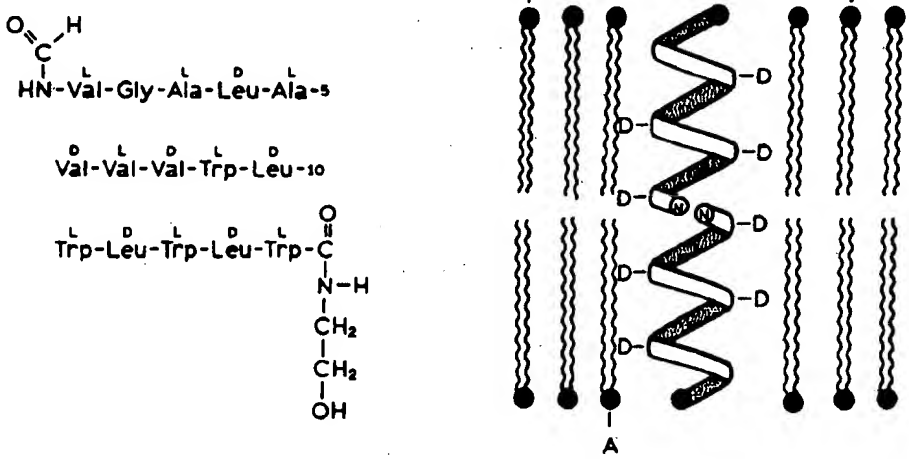

Figure 13.23. Amino acid sequence (*left*) and structure of the membrane-bound dimer (*right*) of gramicidin A. In the amino acid sequence, D and L refer to the optical isomer of the amino acid. Revised from Ref. 63.

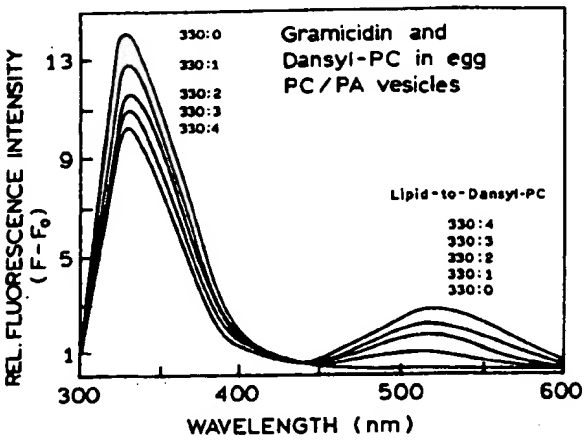

Figure 13.24. Dansyl-PC is 1-acyl-2-[11-[*N*-[5-(dimethylamino)naphthalene-1-sulfonyl]amino]undecanoyl]phosphatidylcholine. Emission spectra of gramicidin and dansyl-PC in vesicles composed of egg PC and egg PA. λ_{ex} = 282 nm. The lipid-to-dansyl-PC ratios are shown on the figure. Revised and reprinted, with permission, from Ref. 64, Copyright © 1988, American Chemical Society.

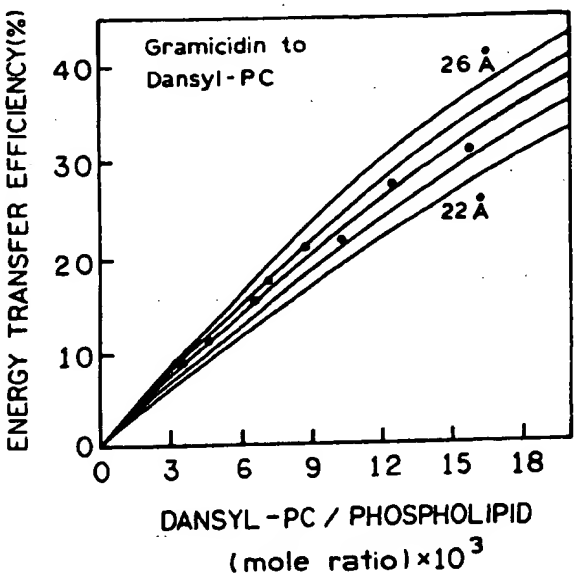

Figure 13.25. Efficiency of energy transfer from gramicidin to dansyl-PC as a function of dansyl-PC/phospholipid ratio. The experimental points (•) were calculated from the tryptophan quenching data, and the solid curves were calculated for a random array of donors and acceptors in two dimensions with R_0 = 22, 23, 24, 25, and 26 Å. A value of R_0 = 24 ± 1 Å gave the best fit to the experimental data. Revised and reprinted with permission from Ref. 64, Copyright © 1988, American Chemical Society.

shown in Figure 13.24. The tryptophan emission is progressively quenched as the dansyl-PC acceptor concentration is increased. The fact that the gramicidin emission is quenched by RET, rather than a collisional process, is supported by the enhanced emission of the dansyl-PC at 520 nm.

The decreasing intensities of the gramicidin emission can be used to determine the tryptophan-to-dansyl-PC transfer efficiencies, as shown in Figure 13.25. The transfer efficiencies are compared with the calculated efficiencies for a random acceptor distribution in two dimensions. These efficiencies were calculated for various values of R_0 using Eqs. [13.26] and [13.28]. The data match the curve calculated for the known R_0 of 24 Å, demonstrating that the distribution of the dansyl-PC acceptors around gramicidin is random. If a particular lipid (PC, PE, or PA) was localized around gramicidin, then RET to the dansyl analog would exceed the calculated values.

13.4.B. Distance of Closest Approach in Membranes

In addition to determining the randomness of lipid distributions, it is also possible to determine the distance of closest approach (r_c) between a membrane-bound protein and an acceptor-labeled lipid. One example is the use of energy transfer to study skeletal protein 4.1.[65] In this case the protein was labeled with IAEDANS, a sulfhydryl-selective dansyl derivative. The acceptor was 3,3′-ditetradecyloxacarbocyanine perchlorate [di-O-C_{14}-(3)], resulting in an R_0 value of 57 Å. Emission spectra are shown in the upper panel of Figure 13.26 for the donor-labeled, acceptor-labeled, and doubly labeled samples as well as the unlabeled sample. The latter spectrum illustrates the need for recording the emission spectra of control samples that do not contain the fluorophores. Depending on the wavelength, the background signal can vary from 20 to nearly 100% of the measured intensity.

In the presence of increasing amounts of acceptor-labeled lipid, the donor-labeled protein is quenched (Figure 13.26, bottom). The fact that the shape of the donor emission spectrum is changing indicates that part of the donor quenching is due to inner filtering by the acceptor absorbance. These data were used to determine the transfer efficiencies to the lipid-bound cyanine dye (Figure 13.27). In this case, the predicted transfer efficiencies were obtained from a simple numerical table[54] which provides a biexponential approximation for various values of r_c/R_0. Use of this table circumvents the need for numerical integration of Eqs. [13.26] and [13.28].

The transfer efficiencies are compared with the calculated curves for various distances of closest approach. As the distance of closest approach becomes larger, the calculated transfer efficiency decreases. The data indicate that the acceptor cannot be closer than 77 Å from the donor-la-

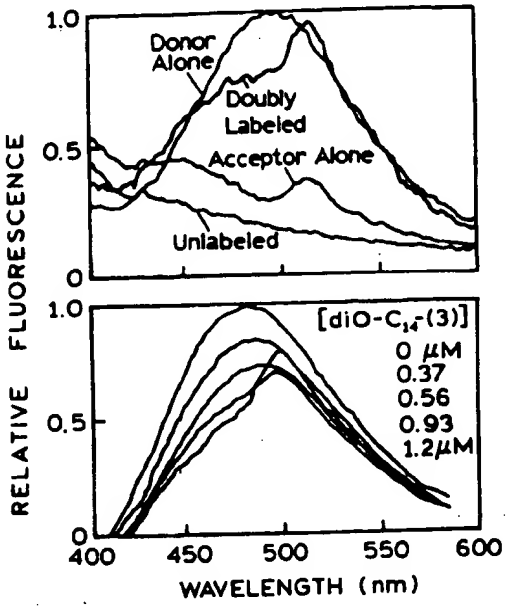

Figure 13.26. *Top:* Emission spectra of skeletal protein 4.1 and of donor-labeled acceptor-labeled, and doubly labeled samples. The donor is IAEDANS and the acceptor is diO-C_{14}-(3). *Bottom:* Emission spectra of IAEDANS-labeled skeletal protein 4.1 in the presence of lipid-bound diO-C_{14}-(3) acceptor. The lipid concentration was 55.4μM, and the acceptor concentrations are shown on the figure. Excitation was at 334 nm. Revised from Ref. 65.

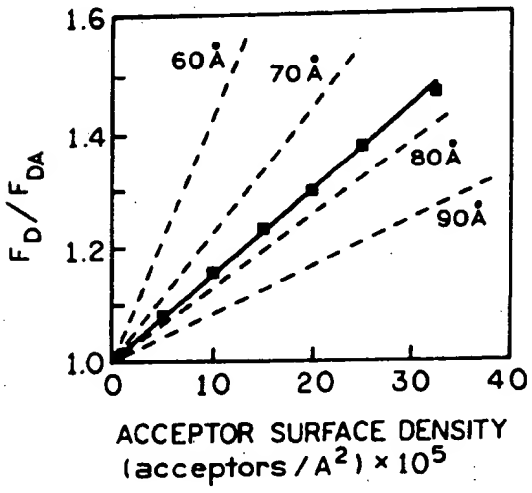

Figure 13.27. RET efficiency from IAEDANS-labeled skeletal protein 4.1 to a lipid-bound cyanine dye. The dashed lines are the predicted transfer efficiencies for various distances of closest approach, calculated according to Ref. 54. Revised from Ref. 65.

beled site and that the donor-labeled site in skeletal protein 4.1 is located deep in the protein. These results suggested that other domains in the protein prevent closer approach of the acceptor.[65] There have been many other reports on energy transfer in membranes, only a few of which can be cited here.[66–69]

13.4.C. Membrane Fusion and Lipid Exchange

Energy transfer has been widely used to study fusion and/or aggregation of membranes. These experiments are shown schematically in Figure 13.28. Suppose that a vesicle contains donor and a surface density of acceptor adequate to quench the donor. As seen from Figure 13.21, the acceptor density does not need to be large. Any process which dilutes the donor and acceptors from the initially labeled vesicles will result in less energy transfer and increased donor emission. For example, if the D–A-labeled residues fuse with an unlabeled vesicle, the acceptor becomes more dilute and the donor intensity increases (Figure 13.28, top). Alternatively, the donor may display a modest water solubility adequate to allow exchange between vesicles (Figure 13.28, left). Then some of the donors will migrate to the acceptor-free vesicles, and again the donor fluorescence will increase. It is also possible to trap a water-soluble fluorophore–quencher pair inside the vesicles. Upon fusion, the quencher can be diluted and/or released. A wide variety of different procedures have been proposed,[70–74] but most rely on these simple proximity considerations.

13.5. ENERGY TRANSFER IN SOLUTION

Energy transfer also occurs for donors and acceptors randomly distributed in three-dimensional solutions. In this case the theory is relatively simple. Following δ-function excitation, the intensity decay of the donor is given by[75–77]

$$I_D(t) = I_D^0 \exp\left[\frac{-t}{\tau_D} - 2\gamma\left(\frac{t}{\tau_D}\right)^{1/2}\right] \qquad [13.29]$$

with $\gamma = A/A_0$, where A is the acceptor concentration. If R_0 is expressed in centimeters, the value of A_0 in moles per liter is given by

$$A_0 = \frac{3000}{2\pi^{3/2} N R_0^3} \qquad [13.30]$$

The relative steady-state quantum yield of the donor is given by

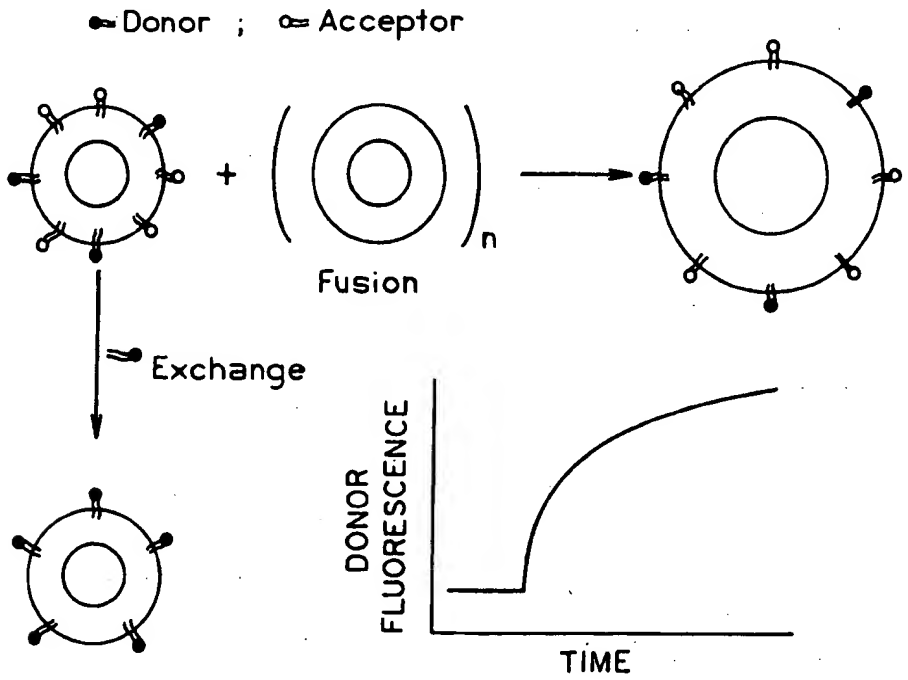

Figure 13.28. Lipid exchange and membrane fusion assays based on energy transfer. Exchange of the donor or acceptor to unlabeled vesicles or fusion of D–A-labeled vesicles with unlabeled vesicles results in dilution of the D–A pairs and increased donor intensities.

$$\frac{F_{DA}}{F_D} = 1 - \sqrt{\pi}\,\gamma \exp(\gamma^2)[1 - \text{erf}(\gamma)] \qquad [13.31]$$

where

$$\text{erf}(\gamma) = \frac{2}{\sqrt{\pi}} \int_0^{\gamma} \exp(-x^2)\,dx \qquad [13.32]$$

These expressions are valid for immobile donors and acceptors for which the orientation factor is randomized by rotational diffusion ($\kappa^2 = \frac{2}{3}$). For randomly distributed acceptors,[3] where rotation is much slower than the donor decay, $\kappa^2 = 0.476$. Still more complex expressions are necessary if the donor and acceptor diffuse during the lifetime of the excited state (Chapters 14 and 15). The complex decay of donor fluorescence reflects the time-dependent population of D–A pairs. Those donors with nearby acceptors decay more rapidly, and donors more distant from acceptors decay more slowly.

The term A_0 is called the critical concentration and represents the acceptor concentration that results in 76% energy transfer. This concentration, in moles per liter (M), can be calculated from Eq. [13.30] or from a simplified expression,[12]

$$A_0 = 447/R_0^3 \qquad [13.33]$$

where R_0 is in units of angstroms. This reveals an important feature of energy transfer between unlinked donors and acceptors, which is that the acceptor concentrations need to be rather high for RET between unlinked donor and acceptors. For instance, if $R_0 = 25$ Å, then $A_0 = 0.029M = 29mM$. This is why we usually ignore energy transfer between donors and acceptors in different linked D–A pairs. However, it is important to consider inner filter effects when one is comparing intensity values. The high acceptor concentrations needed for RET in solution also make such measurements difficult. The high acceptor concentrations result in high optical densities, requiring front-face observation and careful correction for inner filter effects.

13.5.A. Diffusion-Enhanced Energy Transfer

To this point, we have not considered the effects of diffusion on the extent of energy transfer. This is a complex topic, and typically numerical methods are required for simulations and analysis of these effects. However, one simple case is that in which the donor decay times are very long so that diffusive motions of the donors result in their sampling of the entire available space. This is called the rapid-diffusion limit.[78] With fluorophores displaying nanosecond decay times, this limit is not obtainable. However, lanthanides are known to display much longer decay

times—near 0.6–2.5 ms for terbium and europium,[79,80] depending upon the ligands. In relatively fluid solution, the long donor decay times allow the excited donor molecule to diffuse through all available space. The rate of transfer then becomes limited by the distance of closest approach between donors and acceptors. Suppose that an acceptor is buried in a protein or a membrane. One can determine the depth of the acceptor from the extent of energy transfer to the acceptor from terbium or europium chelates in the aqueous phase. Another important feature of energy transfer in the rapid-diffusion limit is that it occurs at much lower acceptor concentrations.[78] For a homogeneous three-dimensional solution, energy transfer is 50% efficient at acceptor concentrations near 1μM, which is 1000-fold lower than for energy transfer without diffusion.[12] This topic is described in detail in Section 15.4.

13.6. REPRESENTATIVE R_0 VALUES

It is often convenient to have an estimate of an R_0 value prior to performing the complex calculation of the overlap integral or labeling of the macromolecule. Unfortunately, there is no general reference for the Förster distances. A larger number of R_0 values are summarized in a book by Berlman,[81] but most of the listed fluorophores are not used in biochemistry. A large number of Förster distances have been summarized in a recent review,[12] and useful examples with spectra are given in a review by Fairclough and Cantor.[82] Some of these R_0 values are summarized in Table 13.3 for a variety of D–A pairs and in Table 13.4 for tryptophan D–A pairs. In the case of lanthanides in environments where the quantum yield is near unity, and for a multichromophore acceptor, R_0 values as large as 90 Å have been calculated.[82] This is the largest Förster distance reported to this time.

Table 13.3. Representative Förster Distances for Various Donor–Acceptor Pairs[a,b]

Donor	Acceptor	R_0 (Å)	Reference
Naphthalene	Dansyl	22	12
Dansyl	FITC	33–41	82
Dansyl	ODR	43	12
ε-A	NBD	38	12
IAF	TMR	37–50	12
Pyrene	Coumarin	39	12
FITC	TMR	49–54	12
IAEDANS	FITC	49	12
IAEDANS	IAF	46–56	12
IAF	EIA	46	12
BODIPY	BODIPY	57	21
BPE	Cy5	72	12
Terbium	Rhodamine	65	23
Europium	Cy5	70	79
Europium	APC	90	83

[a]Values are from Refs. 12, 20, 23, 79, 82, and 83, which should be consulted for further details.

[b]Abbreviations: Dansyl, 5-dimethylamino-1-naphthalenesulfonic acid; ε-A, 1-N^6-ethenoadenosine; IAF, 5-(iodoacetamido)fluorescein; FITC, fluorescein 5-isothiocyanate; IAEDANS, 5-(((2-iodoacetyl)amino)ethyl)amino) naphthalene-1-sulfonic acid; CF, carboxyfluorescein, succinimidyl ester; BODIPY, 4,4-difluoro-4-bora-3a,4a-diaza-s-indacene; BPE, B-phycoerythrin; ODR, octadecylrhodamine; NBD, 7-nitrobenz-2-oxa-1,3-diazol-4-yl; TMR, tetramethylrhodamine; EIA, 5-(iodoacetetamido)eosin; TR, Texas Red; Cy5, carboxymethylindocyanine-*N*-hydroxysuccinimidyl ester; APC, allophycocyanin.

Table 13.4. Förster Distances for Tryptophan–Acceptor Pairs[a]

Acceptor[b]	R_0 (Å)
Nitrobenzoyl	16
Dansyl	21–24
IAEDANS	22
Anthroyloxy	24
TNB	24
Anthroyl	25
Tyr-NO_2	26
Pyrene	28
Heme	29
NBS	30
DNBS	33
DPH	40

[a]From Ref. 12.

[b]Abbreviations: Dansyl, 5-dimethylamino-1-naphthalenesulfonic acid; IAEDANS, 5-(((2-iodoacetyl)amino)ethyl)amino)naphthalene-1-sulfonic acid; TNB, trinitrophenyl; NBS, nitrobenzenesulfenyl; DNBS, dinitrobenzenesulfonyl; DPH, 1,6-diphenyl-1,3,5-hexatriene.

REFERENCES

1. Förster, Th., 1948, Intermolecular energy migration and fluorescence, *Ann. Phys.* 2:55–75. Translated by R. S. Knox, Department of Physics and Astronomy, University of Rochester, Rochester, NY 14627.
2. Stryer, L., 1978, Fluorescence energy transfer as a spectroscopic ruler, *Annu. Rev. Biochem.* 47:819–846.
3. Steinberg, I. Z., 1971, Long-range nonradiative transfer of electronic excitation energy in proteins and polypeptides, *Annu. Rev. Biochem.* 40:83–114.
4. Clegg, R. M., 1996, Fluorescence resonance energy transfer, in *Fluorescence Imaging Spectroscopy and Microscopy*, X. F. Wang and B. Herman (eds.), John Wiley & Sons, New York, pp. 179–252.
5. Fung, B. K. K., and Stryer, L., 1978, Surface density determination in membranes by fluorescence energy transfer, *Biochemistry* 17:5241–5248.

6. Weller, A., 1974, Theodor Förster, *Ber. Bunsen-Ges. Phys. Chem.* **78**:969–971.
7. Gordon, M., and Ware, W. R. (eds.), 1975, *The Exciplex*, Academic Press, New York.
8. Dale, R. E., Eisinger, J., and Blumberg, W. E., 1979, The orientational freedom of molecular probes. The orientation factor in intramolecular energy transfer, *Biophys. J.* **26**:161–194. Erratum **30**:365 (1980).
9. Dale, R. E., and Eisinger, J., 1975, Polarized excitation energy transfer, in *Biochemical Fluorescence, Concepts*, Vol. 1. R. F. Chen and H. Edelhoch (eds.), Marcel Dekker, New York, pp. 115–284.
10. Dale, R. E., and Eisinger, J., 1974, Intramolecular distances determined by energy transfer. Dependence on orientational freedom of donor and acceptor, *Biopolymers* **13**:1573–1605.
11. Cheung, H. C., 1991, Resonance energy transfer, in *Topics in Fluorescence Spectroscopy, Vol. 2, Principles*, J. R. Lakowicz (ed.), Plenum Press, New York, pp. 127–176.
12. Wu, P., and Brand, L., 1994, Review—resonance energy transfer: Methods and applications, *Anal. Biochem.* **218**:1–13.
13. Dos Remedios, C. G., and Moens, P. D. J., 1995, Fluorescence resonance energy transfer spectroscopy is a reliable "ruler" for measuring structural changes in proteins, *J. Struct. Biol.* **115**:175–185.
14. Haas, E., Katchalski-Katzir, E., and Steinberg, I. Z., 1978, Effect of the orientation of donor and acceptor on the probability of energy transfer involving electronic transitions of mixed polarizations, *Biochemistry* **17**:5064–5070.
15. Latt, S. A., Cheung, H. T., and Blout, E. R., 1965, Energy transfer. A system with relatively fixed donor–acceptor separation, *J. Am. Chem. Soc.* **877**:996–1003.
16. Stryer, L., and Haugland, R. P., 1967, Energy transfer: A spectroscopic ruler, *Proc. Natl. Acad. Sci. U.S.A.* **58**:719–726.
17. Gabor, G., 1968, Radiationless energy transfer through a polypeptide chain, *Biopolymers* **6**:809–816.
18. Haugland, R. P., Yguerabide, J., and Stryer, L., 1969, Dependence of the kinetics of singlet–singlet energy transfer on spectral overlap, *Proc. Natl. Acad. Sci. U.S.A.* **63**:23–30.
19. Horrocks, W. DeW., Holmquist, B., and Vallee, B. L., 1975, Energy transfer between terbium(III) and cobalt(II) in thermolysin: A new class of metal–metal distance probes, *Proc. Natl. Acad. Sci. U.S.A.* **72**:4764–4768.
20. Johnson, I. D., Kang, H. C., and Haugland, R. P., 1991, Fluorescent membrane probes incorporating dipyrromethene boron difluoride fluorophores, *Anal. Biochem.* **198**:228–237.
21. Hemmila, I. A. (ed.), 1991, *Applications of Fluorescence in Immunoassays*, John Wiley & Sons, New York. (See p. 113.)
22. Kawski, A., 1983, Excitation energy transfer and its manifestation in isotropic media, *Photochem. Photobiol.* **38**:487–504.
23. Selvin, P. R., 1995, Fluorescence resonance energy transfer, *Methods Enzymol.* **246**:300–334.
24. Lakowicz, J. R., Gryczynski, I., Wiczk, W., Laczko, G., Prendergast, F. C., and Johnson, M. L., 1990, Conformational distributions of melittin in water/methanol mixtures from frequency-domain measurements of nonradiative energy transfer, *Biophys. Chem.* **36**:99–115.
25. Faucon, J. F., Dufourca, J., and Lurson, C., 1979, The self-association of melittin and its binding to lipids, *FEBS Lett.* **102**:187–190.
26. Goto, Y., and Hagihara, Y., 1992, Mechanism of the conformational transition of melittin, *Biochemistry* **31**:732–738.
27. Bazzo, R., Tappin, M. J., Pastore, A., Harvey, T. S., Carver, J. A., and Campbell, I. D., 1988, The structure of melittin: A ^{1}H-NMR study in methanol, *Eur. J. Biochem.* **173**:139–146.
28. Lakowicz, J. R., Gryczynski, I., Cheung, H. C., Wang, C.-K., Johnson, M. L., and Joshi, N., 1988, Distance distributions in proteins recovered by using frequency-domain fluorometry. Applications to troponin I and its complex with troponin C, *Biochemistry* **27**:9149–9160.
29. Cai, K., and Schircht, V., 1996, Structural studies on folding intermediates of serine hydroxymethyltransferase using fluorescence resonance energy transfer, *J. Biol. Chem.* **271**:27311–27320.
30. Chapman, E. R., Alexander, K., Vorherr, T., Carafoli, E., and Storm, D. R., 1992, Fluorescence energy transfer analysis of calmodulin–peptide complexes, *Biochemistry* **31**:12819–12825.
31. Adams, S. R., Bacskai, B. J., Taylor, S. S., and Tsien, R. Y., 1993, Optical probes for cyclic AMP, in *Fluorescent and Luminescent Probes for Biological Activity*, W. T. Mason (ed.), Academic Press, New York, pp. 133–149.
32. Johnson, D. A., Leathers, V. L., Martinez, A.-M., Walsh, D. A., and Fletcher, W. H., 1993, Biomedical example: Use of FRET to measure subunit associations of the regulation (R) and catalytic (C) subunits of a protein kinase, *Biochemistry* **32**:6402–6410.
33. Guptasarma, P., and Raman, B., 1995, Use of tandem cuvettes to determine whether radiative (trivial) energy transfer can contaminate steady-state measurements of fluorescence resonance energy transfer, *Anal. Biochem.* **230**:187–191.
34. Romoser, V. A., Hinkle, P. M., and Persechini, A., 1997, Detection in living cells of Ca^{2+}-dependent changes in the fluorescence emission of an indicator composed of two green fluorescent protein variants linked by a calmodulin-binding sequence, *J. Biol. Chem.* **272**:13270–13274.
35. Miyawaki, A., Llopis, J., Heim, R., McCaffery, J. M., Adams, J. A., Ikura, M., and Tsien, R. Y., 1997, Fluorescent indicators for Ca^{2+} based on green fluorescent proteins and calmodulin, *Nature* **388**:882–887.
36. Cardullo, R. A., Agrawal, S., Flores, C., Zamechnik, P. C., and Wolf, D. E., 1988, Detection of nucleic acid hybridization by nonradiative fluorescence resonance energy transfer, *Proc. Natl. Acad. Sci. U.S.A.* **85**:8790–8794.
37. Parkhurst, K. M., and Parkhurst, L. J., 1996, Detection of point mutations in DNA by fluorescence energy transfer, *J. Biomed. Opt.* **1**:435–441.
38. Morrison, L. E., and Stols, L. M., 1993, Use of FRET to measure association of DNA oligomers, *Biochemistry* **32**:3095–3104.
39. Ghosh, S. S., Eis, P. S., Blumeyer, K., Fearon, K., and Millar, D. P., 1994, Real time kinetics of restriction endonuclease cleavage monitored by fluorescence resonance energy transfer, *Nucleic Acids Res.* **22**:3155–3159.
40. Le Bonniec, B. F., Myles, T., Johnson, T., Knight, C. G., Tapparelli, C., and Stones, S. R., 1996, Characterization of the P'_2 and P'_3 specificities of thrombin using fluorescence-quenched substrates and mapping of the subsites by mutagenesis, *Biochemistry* **35**:7114–7122.
41. Lee, S. P., Censullo, M. L., Kim, H. G., Knutson, J. R., and Han, M. K., 1995, Characterization of endonucleolytic activity of HIV-1 integrase using a fluorogenic substrate, *Anal. Biochem.* **227**:295–301.
42. Mayayoshi, E. D., Wang, G. T., Krafft, G. A., and Erickson, J., 1990, Novel fluorogenic substrates for assaying retroviral proteases by resonance energy transfer, *Science* **247**:954–958.
43. Mitra, R. D., Silva, C. M., and Youvan, D. C., 1996, Fluorescence resonance energy transfer between blue-emitting and red-shifted excitation derivatives of the green fluorescent protein, *Gene* **173**:13–17.

44. Perkins, T. A., Wolf, D. E., and Goodchild, J., 1996, Fluorescence resonance energy transfer analysis of ribozyme kinetics reveals the mode of action of a facilitator oligonucleotide, *Biochemistry* **35**:16370–16377.
45. Lee, P., and Han, M. K., 1997, Fluorescence assays for DNA cleavage, *Methods Enzymol.* **278**:343–361.
46. Bilderback, T., Fulmer, T., Mantulin, W. W., and Glaser, M., 1996, Substrate binding causes movement in the ATP binding domain of *Escherichia coli* adenylate kinase, *Biochemistry* **35**:6100–6106.
47. Epe, B., Steinhauser, K. G., and Woolley, P., 1983, Theory of measurement of Förster-type energy transfer in macromolecules, *Proc. Natl. Acad. Sci. U.S.A.* **80**:2579–2583.
48. Clegg, R. M., 1992, Fluorescence resonance energy transfer and nucleic acids, *Methods Enzymol.* **211**:353–388.
49. Clegg, R. M., Murchie, A. I. H., and Lilley, D. M., 1994, The solution structure of the four-way DNA junction at low-salt conditions: A fluorescence resonance energy transfer analysis, *Biophys. J.* **66**:99–109.
50. Berman, H. A., Yguerabide, J., and Taylor, P., 1980, Fluorescence energy transfer on acetylcholinesterase: Spatial relationships between peripheral site and active center, *Biochemistry* **19**:2226–2235.
51. Pedersen, S., Jorgensen, K., Baekmark, T. R., and Mouritsen, O. G., 1996, Indirect evidence for lipid-domain formation in the transition region of phospholipid bilayers by two-probe fluorescence energy transfer, *Biophys. J.* **71**:554–560.
52. Estep, T. N., and Thomson, T. E., 1979, Energy transfer in lipid bilayers, *Biophys. J.* **26**:195–207.
53. Wolber, P. K., and Hudson, B. S., 1979, An analytical solution to the Förster energy transfer problem in two dimensions, *Biophys. J.* **28**:197–210.
54. Dewey, T. G., and Hammes, G. G., 1980, Calculation of fluorescence resonance energy transfer on surfaces, *Biophys. J.* **32**:1023–1035.
55. Shaklai, N., Yguerabide, J., and Ranney, H. M., 1977, Interaction of hemoglobin with red blood cell membranes as shown by a fluorescent chromophore, *Biochemistry* **16**:5585–5592.
56. Snyder, B., and Freire, E., 1982, Fluorescence energy transfer in two dimensions, *Biophys. J.* **40**:137–148.
57. Bastiaens, P., de Beus, A., Lacker, M., Somerharju, P., Vauhkonen, M., and Eisinger, J., 1990, Resonance energy transfer from a cylindrical distribution of donors to a plane of acceptors, *Biophys. J.* **58**:665–675.
58. Yguerabide, J., 1994, Theory for establishing proximity relations in biological membranes by excitation energy transfer measurements, *Biophys. J.* **66**:683–693.
59. Dewey, T. G., 1991, Fluorescence energy transfer in membrane biochemistry, in *Biophysical and Biochemical Aspects of Fluorescence Spectroscopy*, T. G. Dewey (ed.), Plenum Press, New York, pp. 197–230.
60. Dobretsov, G. E., Kurek, N. K., Machov, V. N., Syrejshchikova, T. I., and Yakimenko, M. N., 1989, Determination of fluorescent probes localization in membranes by nonradiative energy transfer, *J. Biochem. Biophys. Methods* **19**:259–274.
61. Tweet, A. G., Bellamy, W. D., and Gaines, G. L., 1964, Fluorescence quenching and energy transfer in monomolecular films containing chlorophyll, *J. Chem. Phys.* **41**:2068–2077.
62. Loura, L. M. S., Fedorov, A., and Prieto, M., 1996, Resonance energy transfer in a model system of membranes: Application to gel and liquid crystalline phases, *Biophys. J.* **71**:1823–1836.
63. Stryer, L. (ed.), 1995, *Biochemistry*, 4th ed., W. H. Freeman and Company, New York. (See p. 274.)
64. Wang, S., Martin, E., Cimino, J., Omann, G., and Glaser, M., 1988, Distribution of phospholipids around gramicidin and D-β-hydroxybutyrate dehydrogenase as measured by resonance energy transfer, *Biochemistry* **27**:2033–2039.
65. Shahrokh, Z., Verkman, A. S., and Shohet, S. B., 1991, Distance between skeletal protein 4.1 and the erythrocyte membrane bilayer measured by resonance energy transfer, *J. Biol. Chem.* **266**:12082–12089.
66. McCallum, C. D., Su, B., Neuenschwander, P. F., Morrissey, J. H., and Johnson, A. E., 1997, Tissue factor positions and maintains the factor VIIa active site far above the membrane surface even in the absence of the factor VIIa Gla domain, *J. Biol. Chem.* **272**:30160–30166.
67. Davenport, L., Dale, R. E., Bisby, R. H., and Cundall, R. B., 1985, Transverse location of the fluorescent probe 1,6-diphenyl-1,3,5-hexatriene in model lipid bilayer membrane systems by resonance excitation energy transfer, *Biochemistry* **24**:4097–4108.
68. Wolf, D. E., Winiski, A. P., Ting, A. E., Bocian, K. M., and Pagano, R. E., 1992, Determination of the transbilayer distribution of fluorescent lipid analogues by nonradiative fluorescence resonance energy transfer, *Biochemistry* **31**:2865–2873.
69. Isaacs, B. S., Husten, E. J., Esmon, C. T., and Johnson, A. E., 1986, A domain of membrane-bound blood coagulation factor Va is located far from the phospholipid surface. A fluorescence energy transfer measurement, *Biochemistry* **25**:4958–4969.
70. Ladokhin, A. S., Wimley, W. C., Hristova, K., and White, S. H., 1997, Mechanism of leakage of contents of membrane vesicles determined by fluorescence requenching, *Methods Enzymol.* **278**:474–486.
71. Kok, J. W., and Hoekstra, D., 1993, Fluorescent lipid analogues applications in cell and membrane biology, *Fluorescent and Luminescent Probes for Biological Activity*, W. T. Mason (ed.), Academic Press, New York, pp. 101–119.
72. Pyror, C., Bridge, M., and Loew, L. M., 1985, Aggregation, lipid exchange, and metastable phases of dimyristoylphosphatidylethanolamine vesicles, *Biochemistry* **24**:2203–2209.
73. Duzgunes, N., and Bentz, J., 1988, in *Spectroscopic Membrane Probes*, L. D. Loew (ed.), CRC Press, Boca Raton, Florida, pp. 117–159.
74. Silvius, J. R., and Zuckermann, M. J., 1993, Interbilayer transfer of phospholipid-anchored macromolecules via monomer diffusion, *Biochemistry* **32**:3153–3161.
75. Bennett, R. G., 1964, Radiationless intermolecular energy transfer. I. Singlet–singlet transfer, *J. Chem. Phys.* **41**:3037–3041.
76. Eisenthal, K. B., and Siegel, S., 1964, Influence of resonance transfer on luminescence decay, *J. Chem. Phys.* **41**:652–655.
77. Birks, J. B., and Georghiou, S., 1968, Energy transfer in organic systems VII. Effect of diffusion on fluorescence decay, *Proc. R. Soc. (J. Phys. B)* **1**:958–965.
78. Thomas, D. D., Caslsen, W. F., and Stryer, L., 1978, Fluorescence energy transfer in the rapid diffusion limit, *Proc. Natl. Acad. Sci. U.S.A.* **75**:5746–5750.
79. Selvin, P. R., Rana, T. M., and Hearst, J. E., 1994, Luminescence resonance energy transfer, *J. Am. Chem. Soc.* **116**:6029–6030.
80. Li, M., and Selvin, P. R., 1995, Luminescent polyaminocarboxylate chelates of terbium and europium: The effects of chelate structure, *J. Am. Chem. Soc.* **117**:8132–8138.
81. Berlman, I. B., 1973, *Energy Transfer Parameters of Aromatic Compounds*, Academic Press, New York.
82. Fairclough, R. H., and Cantor, C. R., 1978, The use of singlet energy transfer to study macromolecular assemblies, *Methods Enzymol.* **48**:347–379.
83. Mathis, G., 1993, Rare earth cryptates and homogeneous fluoroimmunoassays with human sera, *Clin. Chem.* **39**:1953–1959.

84. Lakowicz, J. R., Johnson, M. L., Wiczk, W., Bhat, A., and Steiner, R. F., 1987, Resolution of a distribution of distances by fluorescence energy transfer and frequency-domain fluorometry, *Chem. Phys. Lett.* 138:587–593.

PROBLEMS

13.1. *Calculation of a Distance from the Transfer Efficiency*: Use the emission spectra in Figure 13.29 to calculate the distance from the indole donor to the dansyl acceptor. Assume that there is a single D–A distance and that diffusion does not occur during the donor excited-state lifetime. The Förster distance $R_0 = 25.9$ Å, and the donor-alone lifetime is 6.8 ns. What is the D–A distance? What is the donor lifetime in the TUD D–A pair?

13.2. *Measurement of RET Efficiencies (E) from Fluorescence Intensities and Lifetimes*: Use Eq. [13.11] to derive the expressions for E based on intensities (Eq. [13.14]) or lifetimes (Eq. [13.13]).

13.3. *Distance Dependence of Energy Transfer*: The theory of Förster states that the rate of energy transfer depends on $1/r^6$, where r is the donor-to-acceptor distance. This prediction was tested experimentally using naphthyl donors and dansyl acceptors linked by rigid polyprolyl spacers (Figure 13.30). Figure 13.31 shows the excitation spectra for this series of D–A pairs. Assume that each polyprolyl spacer contributes 2.83 Å to the spacing and that the D–A distance ranges from 12 Å ($n = 1$) to 46 Å ($n = 12$).

Use the excitation spectra to demonstrate that k_T depends on $1/r^6$. Note that the dansyl acceptor absorbs maximally at 340 nm and the naphthyl donor has an absorption maximum at 290 nm. Excitation spectra were recorded with the emission monochromator centered on the dansyl emission near 450 nm. What is R_0 for this D–A pair?

13.4. *Effect of Spectral Overlap on the Rate of Energy Transfer*: Haugland *et al.*[18] investigated the effect of the magnitude of the spectral overlap integral on the rate of fluorescence energy transfer. For this study, they employed the steroids shown in Figure 13.32. They measured the fluorescence lifetimes of compounds I and II. The indole moiety is the donor which transfers energy to the ketone acceptor. Both the absorption spectrum of the ketone and the emission

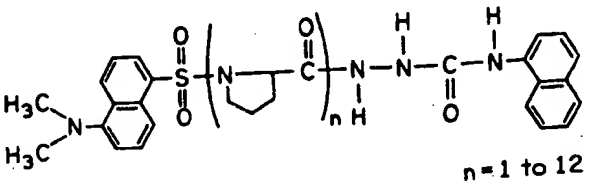

Figure 13.30. Structure of dansyl-(L-prolyl)$_n$-α-naphthyl used for determining the effects of distance on energy transfer. Revised from Ref. 14.

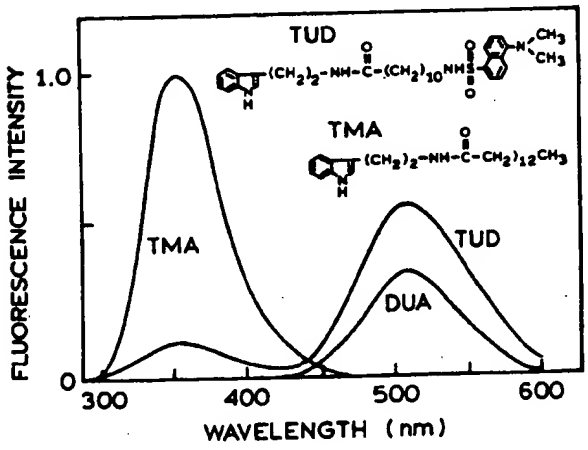

Figure 13.29. Emission spectra of a donor control (TMA) and a donor–acceptor pair (TUD) in propylene glycol at 20 °C. DUA is a dansyl-labeled fatty acid, which is the acceptor-only control sample. Revised from Ref. 84.

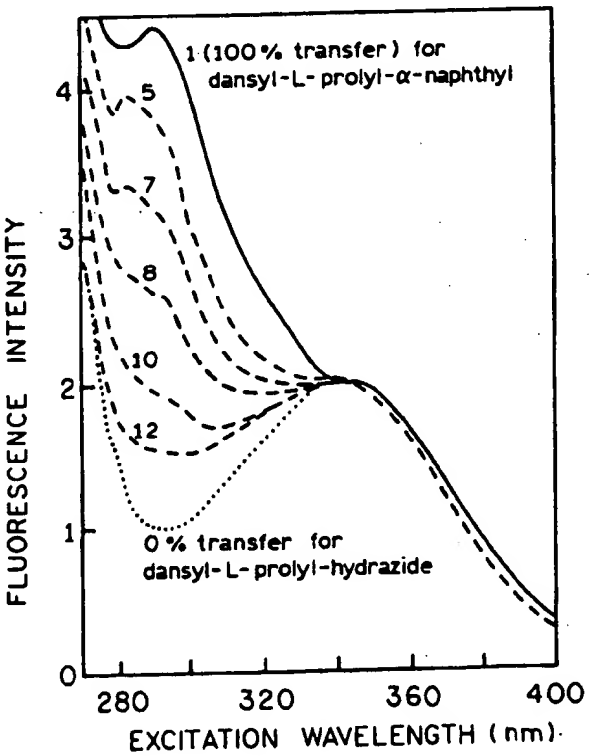

Figure 13.31. Excitation spectra of dansyl-(L-prolyl)$_n$-α-naphthyl molecules. Spectra are shown for dansyl-L-prolyl-hydrazide (···), dansyl-L-prolyl-α-naphthyl (———), and dansyl-(L-prolyl)$_n$-α-naphthyl (— — —), $n = 5$, 7, 8, 10, and 12. Emission was detected at the dansyl emission maximum near 450 nm. Revised from Ref. 16.

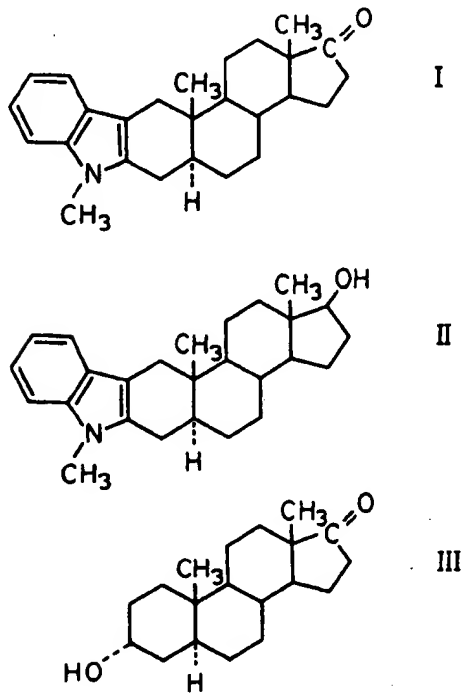

Figure 13.32. Structure of the rigid steroid donor-acceptor pair (I), the steroid containing the donor alone (II), and the steroid containing the acceptor alone (III). Indole is the donor and the carbonyl group is the acceptor. Revised from Ref. 18.

Table 13.5. Fluorescence Spectral Properties of Compounds I and II in a Series of Solvents[a]

Solvent	τ (ns) I	τ (ns) II	n_d	J (cm^6/mmol × 10^{19})
Methanol	5.3	5.6	1.331	1.5
Ethanol	5.6	6.5	1.362	3.0
Dioxane	3.6	5.4	1.423	13.0
Ethyl acetate	3.3	4.7	1.372	12.8
Ethyl ether	2.1	4.5	1.349	30.0
Heptane	1.1	2.8	1.387	60.3

[a]From Ref. 18.

spectrum of the indole are solvent-sensitive. Specifically, the emission spectrum of the indole shifts to shorter wavelengths and the absorption spectrum of the ketone shifts to longer wavelengths as the solvent polarity decreases (Figure 13.33). These shifts result in increasing spectral overlap with decreasing solvent polarity.

Use the data in Table 13.5 to demonstrate that k_T is proportional to the first power of the extent of spectral overlap (J).

13.5. *Calculation of a Förster Distance*: Calculate the Förster distance for the tryptophan-to-dansyl donor–acceptor pair shown in Figure 13.8. The quantum yield of the donor is 0.21.

13.6. *Optical Assay for cAMP*: The effect of cAMP on the donor- and acceptor-labeled protein kinase (Figure 13.15) suggests its use for measuring cAMP. Derive an expres-

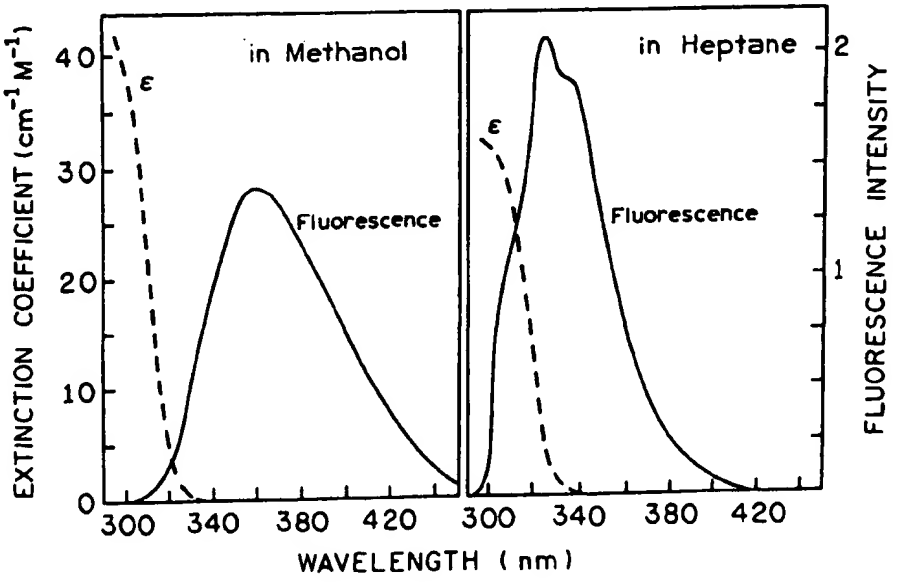

Figure 13.33. Overlap of emission spectrum of the indole donor (II) with the absorption spectrum of the carbonyl acceptor (III). Revised from Ref. 18.

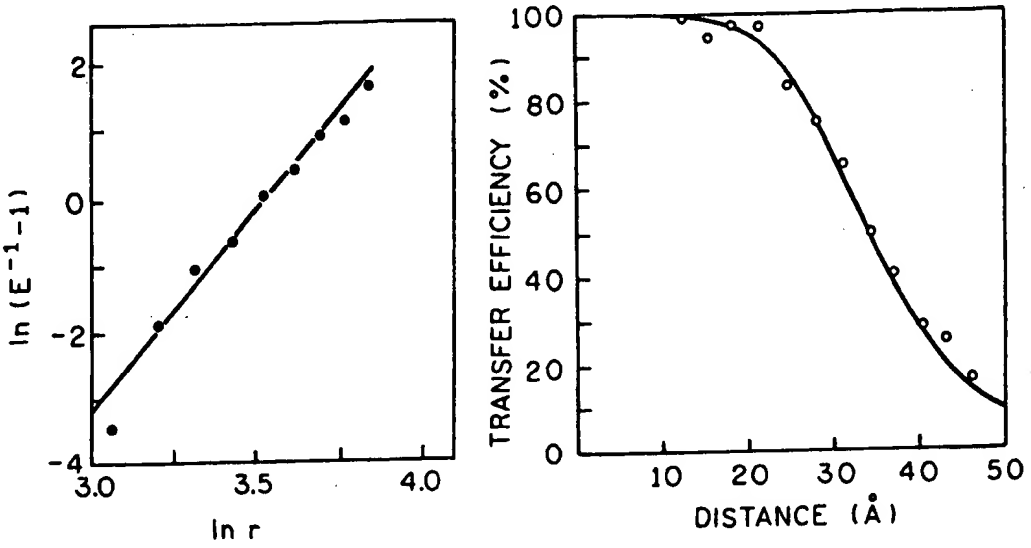

Figure 13.34. Distance dependence of the energy transfer efficiencies in dansyl-(L-propyl)$_n$-α-naphthyl, n = 1–12. Revised from Ref. 16.

sion relating the ratio of donor to acceptor intensities to the protein kinase–cAMP dissociation constant. Assume that the donor and acceptor quantum yields are unchanged upon binding of cAMP, except for the change in energy transfer. Explain any advantages of an assay based on intensity ratios rather than direct intensity measurements.

13.7. *Characteristics of a Closely Spaced D–A Pair.* Assume that you have isolated a protein which contains a single tryptophan residue and binds dinitrophenol (DNP) in the active site. The absorption spectrum of DNP overlaps with the emission spectrum of the tryptophan residue. Assume R_0 = 50 Å and that DNP is not fluorescent. The fluorescence intensities of the tryptophan residue are 20.5 and 4.1 in the absence and presence of DNP, respectively, after correction for the inner filter effects due to the DNP absorption.

A. What is the energy transfer efficiency?
B. Assume that the unquenched lifetime is 5 ns. What is the expected lifetime in the presence of DNP?
C. What is the energy transfer rate?
D. What is the distance between the tryptophan and the DNP?
E. Assume that the solution conditions change so that the distance between the tryptophan and the DNP is 20 Å. What is the expected intensity for the tryptophan fluorescence?
F. For this same solution (r = 20 Å), what would be the effect on the fluorescence intensity of a 1% impurity of a second protein which did not bind DNP? Assume that this second protein has the same lifetime and quantum yield as the protein under investigation.
G. What lifetime would you expect for the sample which contains the impurity? Would this lifetime provide any indication of the presence of an impurity?

13.8. *Effect of* κ^2 *on the Range of Possible Distances:* Suppose you have a donor- and acceptor-labeled protein which displays the following steady-state anisotropies:

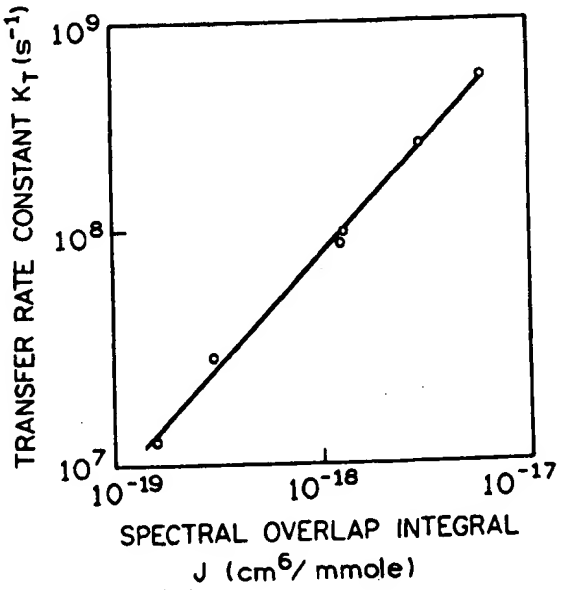

Figure 13.35. Dependence of the rate of energy transfer on the magnitude of the overlap integral. Revised from Ref. 18.

Fluorophore	τ (ns)	r_D or r_A	r_0
Donor-alone control	5	0.1	0.4
Acceptor	15	0.05	0.4

Using an assumed value of $\kappa^2 = \frac{2}{3}$, the D–A distance was calculated to be 25 Å. R_0 is also equal to 25 Å. Assume that the protein displays a rotational correlation time of 5 ns. Use the data provided to calculate the range of distances possible for the D–A pair.

13.9. *Effect of Acceptor Underlabeling on the Calculated Transfer Efficiency*: Suppose that you have a presumed D–A pair. In the absence of acceptor, the donor displays a steady-state intensity $F_D = 1.0$, and in the presence of acceptor, $F_{DA} = 0.5$. Calculate the transfer efficiency assuming that the fractional labeling with acceptor (f_A) is 1.0 or 0.5. How does the change in f_A affect the calculated distance?

13.10. *FRET Efficiency from the Acceptor Intensities*: Derive Eq. [13.25] for the case in which donor labeling is complete; $f_D = 1.0$. Also derive Eq. [13.25] for the case in which donor labeling is incomplete ($f_D < 1$).

13.11. *Correction for Overlapping Donor and Acceptor Emission Spectra*: Equation [13.25] does not consider the possible contribution of the donor emission at the wavelength used to measure acceptor fluorescence (λ_A). Derive an expression for the enhanced acceptor fluorescence when the donor emits at λ_A. Explain how the apparent transfer efficiency, calculated without consideration of the donor contribution, would be related to the true transfer efficiency.

13.12. *Effect of non-RET quenching:* Suppose that you have a protein with a single tryptophan residue. Assume also that the protein noncovalently binds a ligand which serves as a RET acceptor for the tryptophan residue and that the acceptor site is allosterically linked to the donor site such that acceptor binding induces an additional rate of donor quenching, k_q, in addition to k_T.

What is the apparent transfer efficiency upon acceptor binding in terms of τ_D, k_T, and k_q? Is the apparent value (E_D) smaller or larger than the true value (E)?